MEDJ

Volume: 40 Issue: 4 December 2025

MEDENIYET MEDICAL JOURNAL

THE OFFICAL JOURNAL OF ISTANBUL MEDENIYET UNIVERSITY FACULTY OF MEDICINE

Formerly Göztepe Tıp Dergisi

ISSN 2149-2042
E-ISSN 2149-4606

www.medeniyetmedicaljournal.org

ISSN 2149-2042
E-ISSN 2149-4606

MEDENIYET MEDICAL JOURNAL

Formerly Göztepe Tıp Dergisi

Year 2025
Volume 40
Issue 4

www.medeniyetmedicaljournal.org

Printing Date: December 2025

International scientific journal published quarterly.

Medeniyet Medical Journal is the official journal of Istanbul Medeniyet University

It is published four times a year (March, June, September, December).

MEDJ is an open Access, free and peer-reviewed journal

PubMed Abbreviation: Medeni Med J

"Please refer to the journal's webpage (**https://medeniyetmedicaljournal.org/jvis.aspx**) for "Publication Policy", "Instructions to Authors" and "Aims and Scope".

The Medeniyet Medical Journal and/or its editors are members of ICMJE, COPE, WAME, CSE and EASE, and follow their recommendations.

The Medeniyet Medical Journal is indexed in **Emerging Sources Citation Index (Web of Science), PubMed/MEDLINE, PubMed Central, Scopus, EBSCO Academic Search Complete, i-Journals, J-Gate, Türk Medline, Türkiye Atıf Dizini** and **TÜBİTAK ULAKBİM TR Index**.

The journal is printed on an acid-free paper and published electronically.

Owner: ISTANBUL MEDENİYET UNIVERSITY FACULTY OF MEDICINE

Responsible Manager: M. Tayyar KALCIOGLU

www.medeniyetmedicaljournal.org

International Advisory Board

MEDJ

International Advisory Board

Contents

Original Articles

MEDJ

Contents

Contents

DOI: 10.4274/MMJ.galenos.2025.82754
Medeni Med J 2025;40:202-208

Original Article

Sedentary Behavior Worsens the Adverse Impact of E-cigarettes Smoking on Sleep Quality

Hareketsiz Yaşam Tarzı E-sigara İçmenin Uyku Kalitesine Olumsuz Etkisini Artırıyor

Mahmoud Awad ALOMARI[1], Omar Falah KHABOUR[2]

[1]Jordan University of Science and Technology, Department of Rehabilitation Sciences, Irbid, Jordan
[2]Jordan University of Science and Technology, Department of Medical Laboratory Sciences, Irbid, Jordan

ABSTRACT

Objective: Sleep is vital for homeostasis. Smoking negatively affects sleep quality, whereas regular physical activity and reduced sedentary behavior improve sleep quality. However, the combined effect of e-cigarettes, physical activity, and sedentary behavior remains unknown. Therefore, the current study compared sleep quality according to e-cigarette dependence status among adults with high versus low levels of physical activity and sedentary behavior.

Methods: In 644 adults, sleep, e-cigarette dependence, physical activity, and sedentary behavior were assessed using the Pittsburgh Sleep Quality Index (PSQI), the Penn State E-Cigarette Dependence Index, and the International Physical Activity Questionnaire, respectively.

Results: The two-way ANCOVA, after controlling for gender, income, and disease status, revealed main effects of e-cigarette dependence ($p<0.001$) and sedentary behavior ($p<0.03$), and an interaction effect ($p<0.05$) on the PSQI. Post hoc comparisons showed significantly greater PSQI scores among adults with heavy e-cigarette dependence and in the high sedentary behavior group ($p<0.05$). However, the analysis showed no main effect of physical activity on PSQI scores ($p>0.05$).

Conclusions: The results suggest that heavy dependence on e-cigarettes negatively alters sleep quality. These adverse sleep alterations are exacerbated by sedentary behavior. Programs are needed to reduce e-cigarette use and sedentary behavior to enhance sleep quality.

Keywords: Sleep health and quality, physical activity, sedentary behavior, e-cigarettes, tobacco

ÖZ

Amaç: Uyku, homeostaz için hayati öneme sahiptir. Sigara içmek uyku kalitesini olumsuz etkilerken, düzenli fiziksel aktivite ve hareketsiz yaşam tarzının azaltılması uyku kalitesini iyileştirir. Ancak, e-sigara, fiziksel aktivite ve hareketsiz yaşam tarzının birleşik etkisi hala bilinmemektedir. Bu nedenle, mevcut çalışma, yüksek ve düşük düzeyde fiziksel aktivite ve hareketsiz davranış sergileyen yetişkinler arasında e-sigara bağımlılığı durumuna göre uyku kalitesini karşılaştırmıştır.

Yöntem: 644 yetişkinde uyku, e-sigara bağımlılığı, fiziksel aktivite ve hareketsiz davranış sırasıyla Pittsburgh Uyku Kalitesi İndeksi (PSQI), Penn State E-Sigara Bağımlılığı İndeksi ve Uluslararası Fiziksel Aktivite Anketi kullanılarak değerlendirilmiştir.

Bulgular: Cinsiyet, gelir ve hastalık durumu kontrol edildikten sonra yapılan iki yönlü ANCOVA, e-sigara bağımlılığının ($p<0,001$) ve hareketsiz davranışın ($p<0,03$) ana etkilerini ve PSQI üzerinde bir etkileşim etkisini ($p<0,05$) ortaya koymuştur. Post-hoc karşılaştırmalar, ağır e-sigara bağımlılığı olan yetişkinler ve yüksek hareketsiz davranış grubunda ($p<0,05$) önemli ölçüde daha yüksek PSQI puanları olduğunu gösterdi. Ancak, analiz fiziksel aktivitenin PSQI puanları üzerinde ana bir etkisi olmadığını gösterdi ($p>0,05$).

Sonuçlar: Sonuçlar, e-sigaraya yoğun bağımlılığın uyku kalitesini olumsuz yönde değiştirdiğini göstermektedir. Bu olumsuz uyku değişiklikleri, hareketsiz davranışla daha da kötüleşmektedir. Uyku kalitesini artırmak için e-sigara kullanımını ve hareketsiz davranışı azaltmaya yönelik programlara ihtiyaç vardır.

Anahtar kelimeler: Uyku sağlığı ve kalitesi, fiziksel aktivite, hareketsiz davranış, e-sigaralar, tütün

INTRODUCTION

Sleep is crucial for maintaining the homeostasis of multiple vital physiological systems, including cardiovascular, metabolic, immune, neural, and cognitive systems[1]. Conversely, sleep problems are associated with all-cause mortality and an increased risk of cancer, diabetes, obesity, and cardiovascular diseases[2-4]. In recent years, sleep deficiency has become increasingly common.

Address for Correspondence: O.F. Khabour, Jordan University of Science and Technology, Department of Medical Laboratory Sciences, Irbid, Jordan
E-mail: khabour@just.edu.jo **ORCID ID:** orcid.org/0000-0002-3006-3104

Received: 20.07.2025
Accepted: 08.10.2025
Published: 31.12.2025

Cite as: Alomari MA, Khabour OF. Sedentary behavior worsens the adverse impact of e-cigarettes smoking on sleep quality. Medeni Med J. 2025;40:202-208

Inadequate sleep duration, irregular sleep timing, poor sleep quality, and sleep/circadian rhythm disturbances are some indicators of sleep deficiency[5].

Smoking is a risky behavior associated with some of the most devastating disorders[6,7]. In addition, smoking is associated with sleep problems. It can cause sleep-onset latency, frequent nighttime awakenings, sleep bruxism, and breathing difficulties during sleep[3,8]. The use of electronic cigarettes (e-cigarettes) as an alternative smoking-cessation tactic has recently increased, especially among young people[9,10]. It is a battery-operated electronic device that delivers manufactured nicotine as an inhalable aerosol[11]. According to a recent National Center for Health Statistics report on e-cigarette use, 12.6% of adults have tried e-cigarettes, and 3.7% currently use e-cigarettes[12]. The increased prevalence of e-cigarette use is mainly attributed to advertising that presents e-cigarettes to young people as a harmless alternative to combustible cigarettes. However, exposure to e-cigarettes can result in complications such as asthma, chronic obstructive pulmonary disease, and severe lung inflammation[13]. However, studies on the effects of e-cigarette use on sleep quality are still sparse[3,14-17].

Physical activity is any bodily movement that increases energy expenditure. Despite its well-known benefits, many adults do not meet the recommended amounts of physical activity. Physical activity can prevent the most serious diseases, including coronary heart disease, stroke, cancer, type 2 diabetes, hypertension, and osteoporosis[18]. In addition, regular physical activity promotes relaxation, sleep initiation, and sleep maintenance[19], and prevents sleep problems[20,21]. However, evidence regarding the effect of physical activity and sedentary behavior on smoking-induced sleep problems remains scarce[22], especially among e-cigarette smokers.

Therefore, the current study compared sleep quality according to e-cigarette dependence status among individuals with low versus high levels of physical activity and sedentary behavior. Sleep quality is expected to vary according to the e-cigarette dependence score, especially among individuals with low levels of physical activity and high levels of sedentary behavior.

MATERIALS and METHODS

Study Design and Subjects

The study was cross-sectional and comparative, designed to examine the relationship between e-cigarette smoking, physical activity, and sleep quality. E-cigarette smokers of both genders, aged ≥18 years, were invited to participate in the study. Participants were recruited from local community settings (cafes, malls, and universities) across Jordan.

Ethical Approval

The study was conducted in accordance with the Declaration of Helsinki and was approved by the Institutional Review Board of the Jordan University of Science and Technology (protocol no.: JUST-53/149/2022, date: 07.07.2022).

Sample Characteristics

Socioeconomic and demographic data, including age, weight, height, gender, marital status, education, monthly income, and residence, were collected from participants using a structured form. The participants were categorized by household income as low [≤500 Jordanian Dinar (JD)], medium (501-1,199 JD), and high (≥1,200 JD). With respect to education, the participants were divided into three categories: high school or below, diploma or bachelor's degree, and postgraduate degree. Participants were also divided into healthy individuals (free from chronic disease) and those with chronic disease (e.g., diabetes, hypertension, and cardiovascular disease). Informed consent was obtained from study participants as required by the Institutional Review Board.

Sleep Quality

Sleep quality was measured using the Pittsburgh Sleep Quality Index (PSQI). The sleep quality assessment tool comprises 19 items that evaluate seven components of sleep status, each with a separate subscore ranging from 0 to 3. These components are (a) sleep duration; (b) sleep disturbance; (c) sleep latency; (d) daytime dysfunction due to sleepiness; (e) sleep efficiency; (f) overall sleep quality; and (g) use of sleep medications. The seven component scores were summed to yield a global score ranging from 0 to 21; higher scores indicate poorer sleep quality[23]. A total PSQI score ≤5 suggests good sleep quality, whereas a score >5 suggests poor sleep quality[23]. PSQI demonstrated acceptable reliability and validity[24].

Physical Activity

The short Arabic version of the International Physical Activity Questionnaire (IPAQ) was used to measure physical activity and sedentary behavior. The IPAQ is a self-reported questionnaire consisting of seven questions to assess vigorous, moderate, and walking physical activity, as well as sedentary behavior. The IPAQ has been used in people from a variety of socioeconomic statuses and demographic groups and has demonstrated acceptable validity, reliability, and standardization[25,26]. The participants were divided into high and low physical

activity and sedentary behavior levels according to above and below 50th percentile, respectively[27].

E-Cigarette Smoking Status

The Penn State E-Cigarette Dependence Index was used to estimate e-cigarette use among participants. The index includes 10 items, with item scores ranging from 0 to 20. Participants were categorized into dependence groups: none (0-3), light (4-8), intermediate (9-12), and heavy (≥13)[28].

Statistical Analysis

The SPSS software was used for all statistical analyses. Data were reported as mean ± SD and as percentages, and the p-value threshold was set at $p<0.05$. Physical activity and sedentary behavior were classified as low or high according to whether they were below or above the 50th percentile[29]. E-cigarette dependence was categorized into four levels: none, light, intermediate, and heavy[28]. Hierarchical regression was used to examine the associations of physical activity, sedentary behavior, and e-cigarette dependence with the global sleep score. Two-way analysis of covariance (ANCOVA) was used to examine differences in sleep score by physical activity and e-cigarette dependence levels and by sedentary behavior and e-cigarette dependence levels. Confounders for hierarchical regression and ANCOVA were identified using linear regression. Potential confounders entered into the regression model included age, gender, obesity, disease status, marital status, residence, education, and income. Factors found to be significantly related to global sleep scores were considered confounders and adjusted for in the hierarchical regression analysis. In addition to the confounders used in the hierarchical regression, sedentary behavior was included in the physical activity*e-cigarette dependence ANCOVA, whereas physical activity was included in the sedentary behavior*e-cigarette dependence ANCOVA. The data that support the findings of this study are available from the corresponding author upon reasonable request.

RESULTS

As shown in Table 1, 644 individuals agreed to participate in the study, of whom 305 were e-cigarette users. The age, weight, height, and body mass index ranges of the participants were 18-78 years, 33-148 kg, 135-200 cm, and 15.0-45.9 kg/m^2, respectively. The majority of participants were male, had no diseases, lived in rural areas, and held a high school diploma. Table 2 shows that the majority of participants had high physical activity (50.1%), high sedentary behavior (53.1%), and no e-cigarette dependence (55.3%).

According to the linear regression analysis including age, gender, obesity, disease status, marital status, place of residence, education, type of work, and income, only gender ($p<0.03$), income ($p<0.02$), and disease status ($p<0.001$) were related to sleep score. Subsequently, age, disease status, physical activity, and sedentary behavior were considered confounders and adjusted for in hierarchical regression and ANCOVA.

According to hierarchical regression analysis, e-cigarette dependence ($p<0.001$) and sedentary behavior ($p<0.02$), but not physical activity ($p>0.6$), were related to the PSQI score. The two-way ANCOVA shown in Figure 1 revealed a main effect of e-cigarette

Table 1. Participant characteristics (n=644).

Parameter		% or mean (SD)
Age (years), mean (SD)		32.3 (14.2)
Weight (kg), mean (SD)		77.7 (17.4)
Height (cm), mean (SD)		171.2 (0.9)
BMI (kg/m^2), mean (SD)		26.5(5.6)
Income (JD), mean (SD)		690.5 (268.3)
	Low (%)	37.3
	Middle (%)	23.3
	High (%)	39.4
Gender (%)		
	Female	30.9
	Male	69.1
Location (%)		
	Rural	57.0
	Urban	43.0
Smoking status (%)		
	Never smoked	52.6
	Electronic-cigarette smokers	47.4
Disease status (%)		
	Healthy	85.1
	Have chronic disease	14.9
Education (%)		
	High school and less	64.8
	Diploma/bachelor's	26.9
	Postgraduate	8.4
Marital status (%)		
	Single	59.3
	Married	37.6
	Widowed	1.2
	Divorced	0.5
	Engaged	1.4

SD: Standard deviation, BMI: Body mass index, JD: Jordanian Dinar

dependence (p<0.001) but no main effect of physical activity (p=0.14) or interaction effect (p>0.20) on PSQI score after controlling for sedentary behavior. Post-hoc analysis revealed that individuals with heavy e-cigarette dependence had higher PSQI scores than those with no (p<0.001), light (p<0.001), and intermediate (p<0.01) dependence. Another two-way ANCOVA, depicted in Figure 2, revealed main effects of e-cigarette dependence score (p<0.001) and sedentary behavior (p<0.05), and an interaction effect (p<0.05), on PSQI score after controlling for physical activity. Post-hoc analysis revealed that individuals with heavy e-cigarette dependence had higher PSQI scores than those with no (p<0.001), light (p<0.001), and intermediate (p<0.01) dependence. When participants were stratified according to e-cigarette dependence (Table 3), a one-way ANCOVA revealed that PSQI scores were higher among individuals with high sedentary behavior within the light (p<0.02) and heavy (p<0.009) e-cigarette dependence groups. No differences were found between the high and low sedentary levels in the none (p>0.267) and intermediate

Table 2. Participant physical activity and sedentary behavior and e-cigarettes dependency score (n=644).

Parameter		n
Physical activity		
	Low	316
	High	328
Sedentary behavior		
	Low	302
	High	342
E-cigarettes dependence score		
	None	356
	Light	53
	Moderate	77
	Heavy	158

Table 3. PSQI scores in sedentary behavior and according to e-cigarette dependency (n=644).

E-cigarettes dependency	Sedentary activity level	PSQI score	p-value
Non-smokers	Low	6.45±4.0	0.267
	High	6.96±4.0	
Light	Low	4.41±4.2	0.020
	High	6.25±3.0	
Intermediate	Low	6.78±3.6	0.296
	High	5.85±3.3	
Heavy	Low	6.78±4.3	0.009
	High	8.60±4.5	

PSQI: Pittsburgh Sleep Quality Index

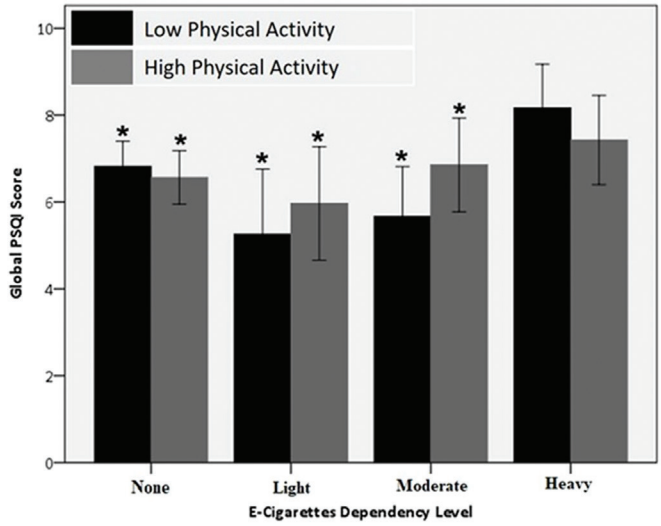

Figure 1. Differences in PSQI score according to e-cigarettes dependency level in the individuals with low versus high physical activity level. Data is presented in mean ± SE. *p<0.05 versus heavy e-cigarettes dependency level.

PSQI: Pittsburgh Sleep Quality Index, SE: Standard error

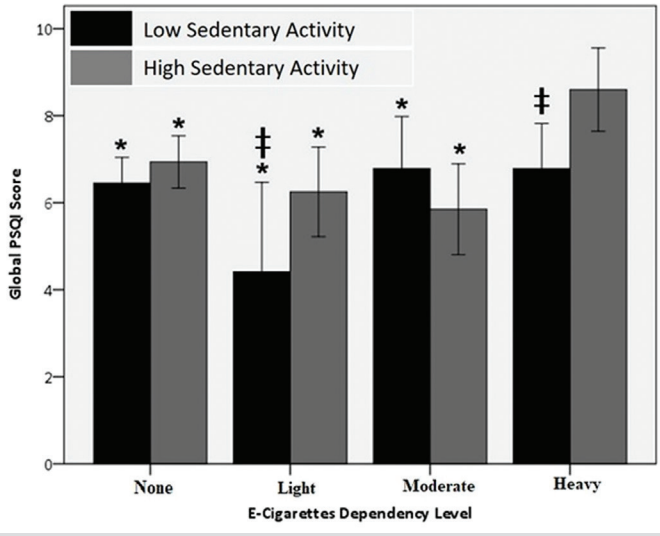

Figure 2. Differences in PSQI score according to e-cigarettes dependency level in the individuals with low versus high sedentary behavior level. Data is presented in mean ± SE. *=p<0.05 versus counterpart with heavy e-cigarettes dependency level. ‡= p<0.05 versus high sedentary behavior level.

PSQI: Pittsburgh Sleep Quality Index, SE: Standard error

(p>0.296) e-cigarette dependence groups. Thus, PSQI scores were higher among individuals with high levels of sedentary behavior.

DISCUSSION

In this study, sleep quality was examined in relation to e-cigarette dependence among individuals with varying levels of physical activity and sedentary behavior. According to the results, e-cigarette dependence and sedentary behavior, but not physical activity, were associated with sleep quality. Additional analyses showed diminished sleep quality among individuals with heavy e-cigarette dependence and increased sedentary behavior after controlling for physical activity. These results are noteworthy, demonstrating that sedentary behavior further worsens the negative impact of e-cigarette use on sleep quality. Therefore, programs to curb the spread of e-cigarettes and to promote alternative strategies for reducing sedentary behavior among adults are needed to improve sleep quality.

The adverse effects of conventional tobacco consumption on sleep quality are well documented. Cigarette smoking alters several sleep parameters, such as sleep depth, sleep duration, sleep latency, sleep stages, nocturnal sleepiness, and daytime awakenings and alertness[30]. However, Fewer, with conflicting results, have examined the combined effect of dual tobacco use (e.g., conventional cigarettes and e-cigarettes) on sleep parameters. For example, Advani et al.[15] found that dual use of tobacco altered sleep latency but not sleep quality, while Kang and Bae[16] reported reduced sleep quality among dual users compared with none or single users of tobacco. Additionally, dual tobacco use was associated with shorter sleep duration, daytime dysfunction due to sleepiness, and increased use of sleeping medications[17]. The current study found changes in sleep quality among exclusive e-cigarette smokers. Only one previous study examined changes in sleep health among exclusive e-cigarette smokers compared with non-smokers and reported more sleep difficulties, greater use of sleep medication, and worse overall sleep health[14].

Current findings indicate that sleep quality is poorer in individuals with greater e-cigarette tobacco dependence. The effects of tobacco dependence on sleep among e-cigarette smokers have not been adequately studied. However, greater tobacco dependence associated with smoking traditional cigarettes has been linked to adverse sleep outcomes. Individuals reporting greater dependence experience diminished sleep quality, sleep insufficiency, sleep disturbances, and frequent nocturnal awakenings[31]. These adverse effects are temporary, but they worsen particularly when smoking occurs near bedtime or during the night[32].

Alterations in sleep architecture associated with e-cigarette smoking have been linked to depression[16] and to narcotic use, and have been attributed to nicotine in e-cigarettes[15]. Nicotine is involved in the regulation of neurotransmitters that are vital for controlling the sleep-wake cycle. These neurotransmitters include acetylcholine, dopamine, serotonin, norepinephrine, and gamma-aminobutyric acid[33]. Additionally, the drop in plasma nicotine, which smokers may experience during nocturnal sleep, can cause withdrawal symptoms, including disturbances in both sleep quality and sleep quantity. Smokers also frequently report sleep problems, including sleep apnea and restless legs syndrome, which may be attributable to smoking-induced respiratory disorders[34].

No previous studies have examined the adverse effect of sedentary behavior on sleep among e-cigarette users or even other tobacco users. Uniquely, the current results suggest that sedentary behavior negatively affects sleep quality and quantity among e-cigarette smokers. The adverse effects of sedentary behavior on sleep are well documented[35-37]. Sedentary behavior has been associated with insomnia, sleep disturbance[36], difficulty falling asleep, frequent nocturnal awakenings, early morning awakenings[38], reduced sleep duration[35], and reduced sleep efficiency[37]. the relationships between sleep quality, subjective sleep quality, sleep latency, sleep disturbance, use of sleeping medication, and daytime dysfunction with sedentary behavior were dose-dependent[39]. Despite the abundant physical and mental benefits of regular physical activity, its effects on sleep remain equivocal. The majority of studies show no relationship between physical activity and sleep architecture[21,40]. Similarly, physical activity in the current study was not associated with sleep, consistent with previous studies. However, some studies have reported that replacing sedentary behavior with physical activity can improve sleep health in older adults[41] and middle-aged adults[42,43]. However, more studies are needed to verify the current findings.

According to the current results, smoking e-cigarettes is associated with poorer sleep quality, particularly among individuals with high levels of sedentary behavior. These results indicate that engaging in sedentary behavior exacerbates the adverse effect of e-cigarette smoking on sleep quality. Given the importance of sleep for homeostasis, programs are needed to educate the public about the health hazards associated with e-cigarette use and sedentary behavior. Subsequently, plans should be initiated to contain e-cigarette use and replace sedentary behaviors with healthier activities.

Study Limitations

The relatively small sample size, recruited from a small Middle Eastern country, and the cross-sectional design limit the generalizability of the findings and the ability to infer causality from the data. Measures of sleep, smoking, physical activity, and sedentary behavior used in the current study are self-reported and thus subject to bias and inaccuracy. Additionally, the discrepancies in recalled time frames for the measured lifestyle behaviors may render these surveys incompatible and prevent them from reflecting one another. Therefore, conducting multi-site longitudinal studies with larger sample sizes that use objective measures is warranted.

CONCLUSIONS

In conclusion, the current study reported altered sleep quality among individuals with heavy e-cigarette dependence. Importantly, sleep architecture alterations associated with e-cigarette smoking are further compromised among individuals with high levels of sedentary behavior, but not among those with high levels of physical activity. These results confirm the adverse health effects of e-cigarette use and sedentary behavior, particularly affecting sleep. Therefore, programs are needed to restrain the spread of e-cigarette use and sedentary behavior, thereby enhancing sleep quality. Additional studies, particularly longitudinal studies, are necessary to confirm the current findings and associated speculations.

Acknowledgments

Authors thank Jordan University of Science and Technology for its support.

Ethics

Ethics Committee Approval: The study was conducted in accordance with the Declaration of Helsinki, and approved by the Institutional Review Board of Jordan University of Science and Technology (protocol no.: JUST-53/149/2022, dated: 07.07.2022).

Informed Consent: Informed consent was obtained from study participants as required by the Institutional Review Board.

Footnotes

Author Contributions

Concept: M.A.A., O.F.K., Design: M.A.A., O.F.K., Data Collection and/or Processing: M.A.A., O.F.K., Analysis or Interpretation: M.A.A., O.F.K., Literature Search: M.A.A., Writing: M.A.A., O.F.K.

Conflict of Interest: The authors have no conflict of interest to declare.

Financial Disclosure: This research was funded by Deanship of Research of Jordan University of Science and Technology, grant number: 488/2022".

REFERENCES

1. Meng S, Li X, Chen Y, Xie J, Yang Y, Guo F. Mechanisms and impact of sleep disturbance in critical illness: a review. J Intensive Care Med. 2025:8850666251359203.
2. Liew SC, Aung T. Sleep deprivation and its association with diseases- a review. Sleep Med. 2021;77:192-204.
3. Wiener RC, Waters C, Bhandari R, Trickett Shockey AK, Alshaarawy O. The Association of Sleep Duration and the Use of Electronic Cigarettes, NHANES, 2015-2016. Sleep Disord. 2020;2020:8010923.
4. Kelters IR, Koop Y, Young ME, Daiber A, van Laake LW. Circadian rhythms in cardiovascular disease. Eur Heart J. 2025;46:3532-45.
5. Grandner MA. Sleep, health, and society. Sleep Med Clin. 2022;17:117-39.
6. Rigotti NA, Kruse GR, Livingstone-Banks J, Hartmann-Boyce J. Treatment of tobacco smoking: a review. JAMA. 2022;327:566-77.
7. Aremu TO, Ogugua FM. Restricting online sales and reclassifying e-cigarettes as prescription-only: a public health policy perspective. Cureus. 2025;17:e86222.
8. Li W, Kalan E, Jebai R, Kondracki AJ, Osibogun O. Is vaping e-cigarettes associated with sleep duration in US young adults? evidence from the 2022 BRFSS. Sleep Breath. 2025;29:248.
9. Al-Sawalha NA, Almomani BA, Mokhemer E, Al-Shatnawi SF, Bdeir R. E-cigarettes use among university students in Jordan: perception and related knowledge. PLoS One. 2021;16:e0262090.
10. Obeidat SR, Malkawi ZA, Khabour OF, AlSa'di AG. Prevalence, knowledge, attitudes, and perceptions about e-cigarette smoking among students in the dental fields in Jordan. Int J Dent. 2025;2025:6521183.
11. Grant JE, Lust K, Fridberg DJ, King AC, Chamberlain SR. E-cigarette use (vaping) is associated with illicit drug use, mental health problems, and impulsivity in university students. Ann Clin Psychiatry. 2019;31:27-35.
12. Schoenborn CA, Gindi RM. Electronic cigarette use among adults: United States, 2014. NCHS Data Brief. 2015:1-8.
13. Banks E, Yazidjoglou A, Brown S, et al. Electronic cigarettes and health outcomes: umbrella and systematic review of the global evidence. Med J Aust. 2023;218:267-75.
14. Brett EI, Miller MB, Leavens ELS, Lopez SV, Wagener TL, Leffingwell TR. Electronic cigarette use and sleep health in young adults. J Sleep Res. 2020;29:e12902.
15. Advani I, Gunge D, Boddu S, et al. Dual use of e-cigarettes with conventional tobacco is associated with increased sleep latency in cross-sectional Study. Sci Rep. 2022;12:2536.
16. Kang SG, Bae SM. The effect of cigarette use and dual-use on depression and sleep quality. Subst Use Misuse. 2021;56:1869-73.
17. So CJ, Meers JM, Alfano CA, Garey L, Zvolensky MJ. Main and interactive effects of nicotine product type on sleep health

among dual combustible and e-cigarette users. Am J Addict. 2021;30:147-55.

18. Warburton DER, Bredin SSD. Health benefits of physical activity: a systematic review of current systematic reviews. Curr Opin Cardiol. 2017;32:541-56.
19. Vanderlinden J, Boen F, van Uffelen JGZ. Effects of physical activity programs on sleep outcomes in older adults: a systematic review. Int J Behav Nutr Phys Act. 2020;17:11.
20. Kredlow MA, Capozzoli MC, Hearon BA, Calkins AW, Otto MW. The effects of physical activity on sleep: a meta-analytic review. J Behav Med. 2015;38:427-49.
21. Kakinami L, O'Loughlin EK, Brunet J, et al. Associations between physical activity and sedentary behavior with sleep quality and quantity in young adults. Sleep Health. 2017;3:56-61.
22. Purani H, Friedrichsen S, Allen AM. Sleep quality in cigarette smokers: associations with smoking-related outcomes and exercise. Addict Behav. 2019;90:71-6.
23. Buysse DJ, Reynolds CF 3rd, Monk TH, Berman SR, Kupfer DJ. The Pittsburgh Sleep Quality Index: a new instrument for psychiatric practice and research. Psychiatry Res. 1989;28:193-213.
24. Farah NM, Saw Yee T, Mohd Rasdi HF. Self-Reported Sleep Quality Using the Malay Version of the Pittsburgh Sleep Quality Index (PSQI-M) In Malaysian Adults. Int J Environ Res Public Health. 2019;16:4750.
25. Helou K, El Helou N, Mahfouz M, Mahfouz Y, Salameh P, Harmouche-Karaki M. Validity and reliability of an adapted arabic version of the long international physical activity questionnaire. BMC Public Health. 2017;18:49.
26. Craig CL, Marshall AL, Sjöström M, et al. International physical activity questionnaire: 12-country reliability and validity. Med Sci Sports Exerc. 2003;35:1381-95.
27. Alomari MA, Keewan EF, Qhatan R, et al. Blood pressure and circulatory relationships with physical activity level in young normotensive individuals: IPAQ validity and reliability considerations. Clin Exp Hypertens. 2011;33:345-53.
28. Saran SK, Salinas KZ, Foulds J, et al. A comparison of vaping behavior, perceptions, and dependence among individuals who vape nicotine, cannabis, or both. Int J Environ Res Public Health. 2022;19:10392.
29. Alomari MA, Khabour OF, Gharaibeh MY, Qhatan RA. Effect of physical activity on levels of homocysteine, folate, and vitamin B12 in the elderly. Phys Sportsmed. 2016;44:68-73.
30. AlRyalat SA, Kussad S, El Khatib O, et al. Assessing the effect of nicotine dose in cigarette smoking on sleep quality. Sleep Breath. 2021;25:1319-24
31. Ozden Sertcelik U, Karalezli A. The association between nicotine dependence and sleep quality in patients referred to a smoking cessation outpatient clinic: a cross-sectional study. Tob Induc Dis. 2024;22.
32. Nuñez A, Rhee JU, Haynes P, et al. Smoke at night and sleep worse? The associations between cigarette smoking with insomnia severity and sleep duration. Sleep Health. 2021;7:177-82.
33. Vanini G, Torterolo P. Sleep-wake neurobiology. Adv Exp Med Biol. 2021;1297:65-82.
34. Jaehne A, Unbehaun T, Feige B, Lutz UC, Batra A, Riemann D. How smoking affects sleep: a polysomnographical analysis. Sleep Med. 2012;13:1286-92.
35. Huang WY, Ho RS, Tremblay MS, Wong SH. Relationships of physical activity and sedentary behaviour with the previous and subsequent nights' sleep in children and youth: a systematic review and meta-analysis. J Sleep Res. 2021;30:e13378.
36. Yang Y, Shin JC, Li D, An R. Sedentary behavior and sleep problems: a systematic review and meta-analysis. Int J Behav Med. 2017;24:481-92.
37. Madden KM, Ashe MC, Lockhart C, Chase JM. Sedentary behavior and sleep efficiency in active community-dwelling older adults. Sleep Sci. 2014;7:82-8.
38. Vancampfort D, Stubbs B, Firth J, et al. Sedentary behaviour and sleep problems among 42,489 community-dwelling adults in six low- and middle-income countries. J Sleep Res. 2018;27:e12714.
39. Jeong SH, Jang BN, Kim SH, Kim GR, Park EC, Jang SI. Association between sedentary time and sleep quality based on the Pittsburgh Sleep Quality Index among South Korean adults. BMC Public Health. 2021;21:2290.
40. Memon AR, Gupta CC, Crowther ME, Ferguson SA, Tuckwell GA, Vincent GE. Sleep and physical activity in university students: a systematic review and meta-analysis. Sleep Med Rev. 2021;58:101482.
41. Seol J, Abe T, Fujii Y, Joho K, Okura T. Effects of sedentary behavior and physical activity on sleep quality in older people: A cross-sectional study. Nurs Health Sci. 2020;22:64-71.
42. Koohsari MJ, Yasunaga A, McCormack GR, et al. Sedentary behaviour and sleep quality. Sci Rep. 2023;13:1180.
43. Vanderlinden J, Biddle GJH, Boen F, van Uffelen JGZ. Are teallocations between sedentary behaviour and physical activity associated with better sleep in adults aged 55+ years? An isotemporal substitution analysis. Int J Environ Res Public Health. 2020;17:9579.

DOI: 10.4274/MMJ.galenos.2025.48323
Medeni Med J 2025;40:209-216

Original Article

Prenatal Exposure to 3.5 GHz Radiofrequency Radiation and Long-Term Skin Histomorphometry: An 18-Month Experimental Rat Study

3.5 GHz Radyofrekans Radyasyonuna Prenatal Maruziyet ve Uzun Dönem Deri Histomorfometrisi: 18 Aylık Deneysel Rat Çalışması

Elif GELENLI DOLANBAY[1], Tugay MERT[1], Reyhan Nur KURTOGLU[2], Unal USLU[1], Suleyman DASDAG[3]

[1]Istanbul Medeniyet University Faculty of Medicine, Department of Histology and Embryology, Istanbul, Türkiye
[2]University of Health Sciences Türkiye, Haydarpasa Numune Training and Research Hospital, Clinic of Family Medicine, Istanbul, Türkiye
[3]Istanbul Medeniyet University Faculty of Medicine, Department of Biophysics, Istanbul, Türkiye

ABSTRACT

Objective: This study aimed to evaluate long-term skin histomorphometry at 18 months postpartum in rats exposed in utero to 3.5 GHz radiofrequency radiation (RFR).

Methods: Pregnant Wistar Hannover rats were exposed to Global System for Mobile Communications-modulated 3.5 GHz RFR for 2 h/day throughout gestation, while the sham group underwent mock exposure. Offspring (n=5 per group) were not exposed to any further RFR until 18 months after birth. Dorsal skin samples were stained with hematoxylin–eosin and Masson's trichrome, and dermal thickness, adipose tissue area, dermal area, adipose/dermis ratio, and fat percentage were quantified. Specific absorption rate (SAR) was calculated using CST Studio Suite. Data were analyzed using the Student's t-test or the Mann-Whitney U test. Statistical significance was defined as $p<0.05$.

Results: The peak spatial SAR (psSAR) values were 0.06622 mW/g (for 1 g) and 0.03825 mW/g (for 10 g). No statistically significant differences were observed between RFR-exposed and sham groups in dermal thickness (655.32±87.46 µm vs 544.42±135.01 µm); fat area percentage (0.73±0.29% vs 0.66±0.22%); dermal area (1.05±0.17 vs 0.88±0.22); adipose/dermis ratio (1.78 ± 0.24 vs 1.54±0.28); or fat percentage (40.04±11.78% vs 42.96±11.60%) (all $p>0.05$).

Conclusions: Prenatal exposure to 3.5 GHz RFR did not cause significant skin histomorphometric alterations in the dermis of aged female rats. The skin's barrier properties, regenerative capacity, and repair mechanisms may mitigate long-term structural effects of such exposures.

Keywords: Radiofrequency radiation, prenatal exposure, skin histomorphometry, 3.5 GHz

ÖZ

Amaç: Bu çalışma, intrauterin dönemde 3,5 GHz radyofrekans radyasyonuna (RFR) maruz kalan ratlarda doğum sonrası 18. ayda uzun dönem deri histomorfometrisini değerlendirmeyi amaçlamaktadır.

Yöntemler: Gebelik süresince Wistar Hannover ratları, deney grubunda günde 2 saat Global System for Mobile Communications modülasyonlu 3.5 GHz RFR'ye maruz bırakılırken, yalancı (sham) gruba simüle maruziyet uygulanmıştır. Doğan yavrular (her grupta n=5), 18 aylık olana kadar ek RFR maruziyeti olmaksızın yetiştirilmiştir. Sırt bölgesinden alınan deri örnekleri hematoksilen–eozin ve Masson trikrom ile boyanmış; dermis kalınlığı, yağ dokusu alanı, dermal alan, yağ/dermis oranı ve yağ yüzdesi nicel olarak değerlendirilmiştir. Spesifik soğurma oranı (SAR) CST Studio Suite kullanılarak hesaplanmıştır. Veriler Student's t-testi veya Mann-Whitney U testi ile analiz edilmiş; istatistiksel anlamlılık $p<0,05$ olarak kabul edilmiştir.

Bulgular: Tepe uzaysal SAR (psSAR) değerleri 1 g için 0,06622 mW/g ve 10 g için 0,03825 mW/g olarak bulunmuştur. RFR'ye maruz kalan ve sham grupları arasında dermis kalınlığı (655,32±87,46 µm vs 544,42±135,01 µm), yağ alanı yüzdesi (0,73±0,29% vs 0,66±0,22%), dermal alan (1,05±0,17 vs 0,88±0,22), yağ/dermis oranı (1,78±0,24 vs 1,54±0,28) veya yağ yüzdesi (40,04±11,78% vs 42,96±11,60%) açısından istatistiksel olarak anlamlı fark saptanmamıştır (tüm $p>0,05$).

Sonuçlar: Prenatal 3.5 GHz RFR maruziyeti, yaşlı dişi sıçanlarda dermiste anlamlı histomorfometrik değişikliklere yol açmamıştır. Derinin bariyer özellikleri, yenilenme kapasitesi ve onarım mekanizmaları, bu tür maruziyetlerin uzun dönem yapısal etkilerine karşı korunma sağlayabilir.

Anahtar kelimeler: Radyofrekans radyasyonu, prenatal maruziyet, deri histomorfometrisi, 3,5 GHz

INTRODUCTION

In recent years, there has been remarkable progress in information and communication technologies, resulting in the widespread integration into daily life of various electronic communication devices and technologies, such as mobile phones and Wi-Fi, which operate via

Address for Correspondence: E. Gelenli Dolanbay, Istanbul Medeniyet University Faculty of Medicine, Department of Histology and Embryology, Istanbul, Türkiye
E-mail: elif.dolanbay@medeniyet.edu.tr **ORCID ID:** orcid.org/0000-0002-7553-5435

Cite as: Gelenli Dolanbay E, Mert T, Kurtoglu RN, Uslu U, Dasdag S. Prenatal exposure to 3.5 GHz radiofrequency radiation and long-term skin histomorphometry: an 18-month experimental rat study. Medeni Med J. 2025;40:209-216

Received: 20.08.2025
Accepted: 23.10.2025
Published: 31.12.2025

electromagnetic fields (EMFs). Radiofrequency radiation (RFRs), defined as electromagnetic radiation in the frequency range 100 kHz to 300 GHz, is predominantly used in communication technologies, particularly in devices such as mobile phones, base stations, laptops, and other wireless systems[1]. 2G, 3G, 4G, and 5G mobile communication technologies utilize radiofrequency (RF) bands such as 900 MHz, 1800 MHz, 2100 MHz, 2400 MHz, 2600 MHz, and 3500 MHz; 5G also employs higher frequencies. 5G technology, which has recently been adopted in numerous countries, primarily operates in the 3.5-GHz frequency band[2].

The biological effects of RF radiation are generally classified as either thermal or non-thermal. Given the low energy levels of RF radiation used in wireless communications, scientific investigations have largely centered on non-thermal effects[3]. Prior studies suggest that non-thermal RF exposure may induce protein conformational alterations and misfolding[4], activate heat shock proteins (HSPs)[5], and cause oxidative stress[6-8].

Fetuses are considered more susceptible than adults to the potential adverse effects of prolonged radiofrequency electromagnetic field (RF-EMF) exposure because rapidly proliferating tissues, such as the central nervous system, endocrine glands, and skin, are sensitive during development. In a study by Sharma et al.[9], prenatal exposure of mice to microwave radiation led to significant alterations in the cytoarchitecture of the hippocampus and cerebellum, including a reduction in Purkinje cell numbers. Similarly, Jensh[10] reported statistically significant growth retardation in rat fetuses exposed to irradiation. Additionally, Odaci et al.[11] demonstrated that 0.9 GHz EMF exposure during development impaired granule cell formation in the dentate gyrus of the rat hippocampus, potentially resulting in cell loss due to disrupted neurogenesis. In contrast, a study by Shirai et al.[12] found that simultaneous exposure to multiple communication-signal EMFs, ranging from 0.8 GHz to 5.2 GHz, had no adverse effects on pregnancy or development in rats.

The skin, as the largest organ of the human body, serves as a crucial barrier against environmental insults. In addition to RF-EMF, other physical environmental agents, most notably ultraviolet radiation (UV-R), are known to affect the skin. While limited exposure to UV-R is beneficial to health by promoting vitamin D synthesis, excessive exposure is closely associated with DNA mutagenesis, apoptosis, and skin cancers such as cutaneous melanoma[13]. Modern wireless communication systems, including 3G, 4G, and Wi-Fi, operate at higher frequencies than earlier GSM 900 MHz systems. As frequency increases, the penetration depth of RF waves into tissues decreases; consequently, the majority of the RF-specific absorption rate (SAR) is concentrated in the skin. Because of its high water content, the skin absorbs more RF or microwave energy than do organs with lower water content[14,15]. However, RF exposure is not ionizing and is therefore not considered to be directly genotoxic on its own[16]. Fetal skin development involves complex processes such as epidermal proliferation, dermal stratification, and connective tissue organization. Any disruption of these processes by external factors can affect the integrity and function of the skin after birth.

Prior studies have reported that RF exposure associated with mobile phone use leads to increased skin temperature[17,18], induces thermally related stress and injury to the skin, and triggers repair processes involving inflammation and tissue matrix remodeling[19]. Furthermore, RF exposure has been linked to a vasodilatory effect on cutaneous blood flow[20].

In the present study, female rats were exposed to RF radiation at a frequency of 3.5 GHz throughout all trimesters of pregnancy. Their offspring were raised to 18 months of age, at which point skin tissue samples were collected and examined histologically and histomorphometrically. The objective was to investigate the long-term effects of prenatal RF radiation exposure on mature skin architecture. It is anticipated that the findings of this study will help to address the current gaps in the literature on the long-term impacts of intrauterine environmental RF exposure on tissue integrity and will enhance our understanding of potential health risks to humans.

MATERIALS AND METHODS

Animal Experiments

The study involved 10 adult female Wistar Hannover rats (18 months old, weighing 300-350 g), comprising groups with and without intrauterine RFR exposure. The reason for selecting 18-month-old rats in our study was to investigate the long-term effects of prenatal exposure to 3.5 GHz RFR that may manifest during the aging process. The number of animals was determined based on an a priori power analysis and in accordance with the 3R principles (Replacement, Reduction, Refinement). All procedures were designed and performed in accordance with the guidelines of the Animal Experiments Local Ethics Committee of Istanbul Bagcilar Training and Research Hospital with decision no: 2024-53, date: 26.11.2024).

The rats were divided into two groups: a sham group and an experimental group. To obtain offspring for the experimental group, pregnant rats were exposed within a Faraday cage to 3.5 GHz RFR for 2 hours per day from the first day of pregnancy until delivery. Rats in the sham group were maintained under the same experimental conditions, except that the signal generator was turned off. Pregnancy was confirmed by vaginal smear cytology and observation of a copulatory plug. Female rats were housed overnight with males, and the presence of spermatozoa in the vaginal smear the following morning or the detection of a copulatory plug was designated as gestation day 0. From each group, five female newborns were randomly selected following parturition, resulting in a total of 10 offspring, which were then monitored under standard laboratory conditions (room temperature 24±1 °C, 12-hour light/12-hour dark cycle, and ad libitum access to water and rodent pellet feed) for 18 months without additional irradiation. To reduce sex-related variability in dermal and adipose tissue parameters and to ensure a more homogeneous sample, only female offspring were included in the study. At the end of the 18-month period, the animals were deeply anesthetized by intraperitoneal injection of ketamine (80 mg/kg) and xylazine (10 mg/kg). Adequate anesthetic depth was verified by loss of pedal reflex. Subsequently, euthanasia was performed via intracardiac administration of a high dose of pentobarbital. Skin tissue samples were collected from the dorsal region of each rat.

Exposure and Field Measurements

In this study, pregnant rats were exposed to 3.5-GHz GSM-modulated RFR generated by a 1-W signal generator (Model 3500 PM10, Everest Comp., Türkiye) for 2 hours per day throughout pregnancy. The power output of the signal generator was maintained at 1 W during the exposure. Exposure was conducted in specially designed, metal-free Plexiglas cages that were placed inside separate Faraday cages. The generator's antenna, similar to a mobile-phone antenna, was positioned 50 cm above the animals at the center of the cage and fitted with a metal reflector above it. Shams were kept under identical conditions with the generator turned off. After birth, female offspring were not exposed to RFR until 18 months of age, thereby ensuring only prenatal exposure. Electric field strengths measured with an EMR 300 device (NARDA, Pfullingen, Germany) ranged from 24 V/m to 27 V/m at the cage corners and were 28 V/m at the center.

SAR Analysis

SAR in the rat uterus was simulated using CST Studio Suite (CST AG, Germany) with a detailed voxel-based rat model derived from CT scans. The simulation replicated the experimental setup, including the antenna, reflector, Plexiglas carousel, and rat positioning. The finite integration technique (FIT) was applied to perform precise electromagnetic and thermal calculations. Electric field strengths, measured with a calibrated EMR-300 device (Narda, Germany) at the four cage corners and at the center, ranged from 24-27 V/m at the corners and 28 V/m at the center, confirming a uniform field distribution. Peak spatial SAR (psSAR) simulations were based on the average 28 V/m field at 3.5 GHz. The exposure plane remained fixed, with no metallic surfaces present, and no body temperature changes were detected during exposure.

Histomorphometric Studies

Skin tissue samples obtained from the dorsal region of the rats were fixed in 10% neutral buffered formalin, processed through routine tissue preparation procedures, and embedded in paraffin. 5-µm sections were cut on a Leica RM2245 microtome and mounted on standard glass slides. For histological evaluation, the slides were stained with hematoxylin and eosin (H&E) to assess dermal thickness, dermal adipose tissue area, and total dermal area (dermis and adipose tissue), and with Masson's trichrome to evaluate the general structural features of the skin and the organization of collagen fibers.

All sections were examined using a light microscope (Olympus BX53) for histological and histomorphometric analyses. A camera and imaging system (Olympus DP21) attached to the microscope was used for measurements and photodocumentation. Dermal thickness was measured in eight fields per section at 10× magnification. Areas of dermal adipose tissue, dermis, and total dermal area were measured at 4× magnification using a guiding line approximately 1.5 mm long. The proportion of dermal adipose tissue was calculated as the adipose tissue area divided by the total dermal area.

Statistical Analysis

SPSS (Statistical Package for Social Sciences) (for Windows, version 22.0) (SPSS Inc., Chicago, IL, USA) software package was used for the statistical analysis of the obtained data. The data distribution was evaluated using the Shapiro-Wilk test. Differences between groups in terms of dermis thickness, dermal adipose tissue area, dermal adipose tissue ratio, and dermis area were evaluated using the Student's t-test. Differences in total dermal area between groups were analyzed using the Mann-Whitney U test. Significant p-values were denoted as $p<0.05$ (*), $p<0.01$ (**), and $p<0.001$ (***). All data were reported as mean ± standard error of the mean.

RESULTS

In this study, the effects of prenatal exposure to RFR during all trimesters on the skin morphology of female rats at 18 months of age were investigated. Histological analyses were performed using H&E staining, and several parameters including dermal thickness, dermis area, dermal adipose tissue area, total dermal area, and dermal adipose tissue ratio were quantitatively measured. Representative histological images illustrating the skin tissue architecture in both groups are shown in Figure 1.

The SAR calculations were conducted using the Institute of Electrical and Electronics Engineers/ International Electrotechnical Commission 62704-1 standard to assess the distribution of SAR values. The PsSAR in the uterus was 0.06622 mW/g for 1 g and 0.03825 mW/g for 10 g.

No statistically significant differences were observed between the sham and RFR-exposed groups in any of the measured parameters. Mean dermal thickness values were 544.42±60.38 µm in the sham group and 655.32±39.11 µm in the RFR-exposed group (p=0.162). Similarly, dermal adipose tissue areas showed no significant difference, with means of 0.66±0.10 in the sham group and 0.73±0.13 in the experimental group (p=0.717).

The dermis area was slightly increased in the RFR group (1.05±0.08) compared with the sham group (0.88±0.10), although this difference was not statistically significant (p=0.198). The total dermal area did not differ significantly between groups (sham: 1.54±0.13; RFR: 1.78±0.11; p=0.175). Finally, dermal adipose tissue ratio did not differ between groups (sham: 42.96±5.19%; RFR: 40.04±5.27%; p=0.704).

These findings suggest that chronic intrauterine exposure to RFR does not cause significant morphological changes in the dermal structure of 18-month-old female rats. The comparative statistical results for dermal

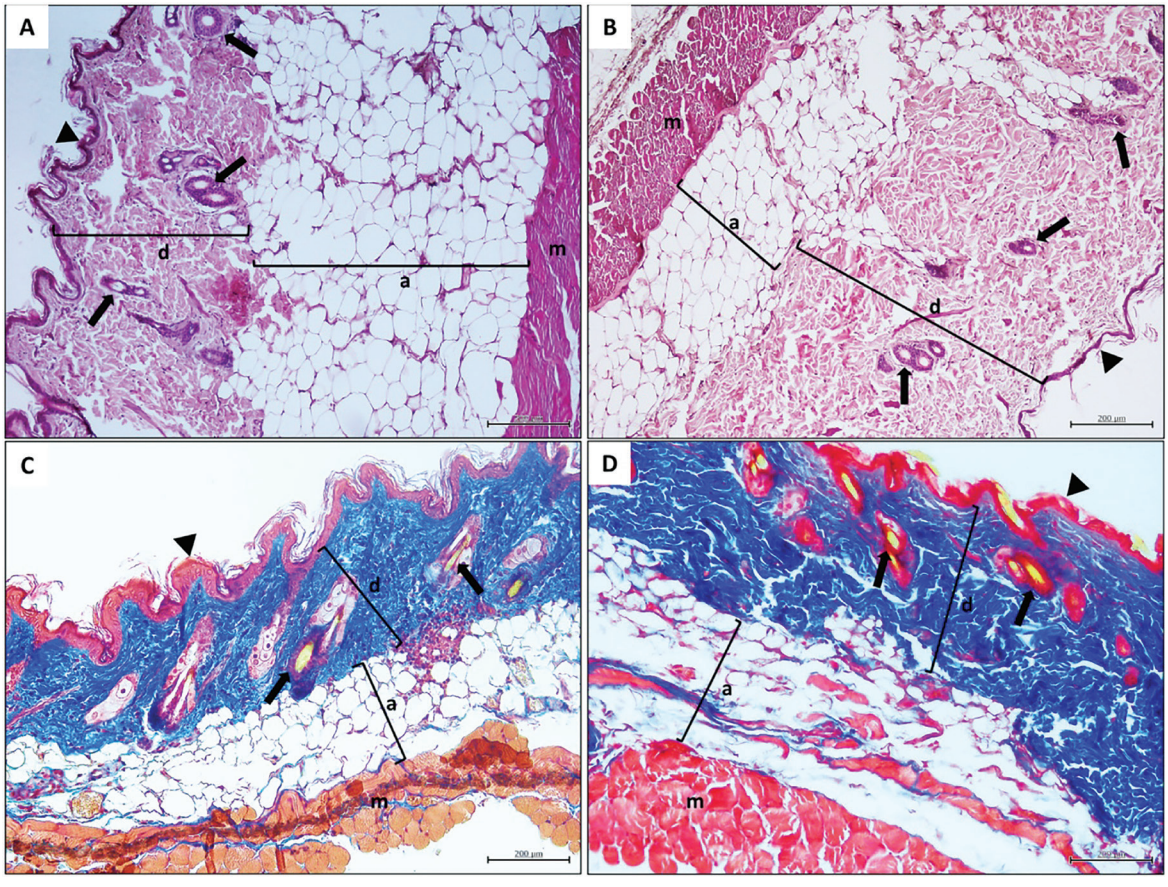

Figure 1. Representative hematoxylin&eosin (H&E) and Masson's Trichrome stained sections of skin tissue from female offspring rats at 18 months of age. Panels A and C: Sham group; Panels B and D: Prenatal RFR exposure group. Arrowheads indicate the epidermal layer; black arrows indicate hair follicles; d = dermis layer; a = adipose tissue layer; m = muscle layer. Scale bars: 200 µm.

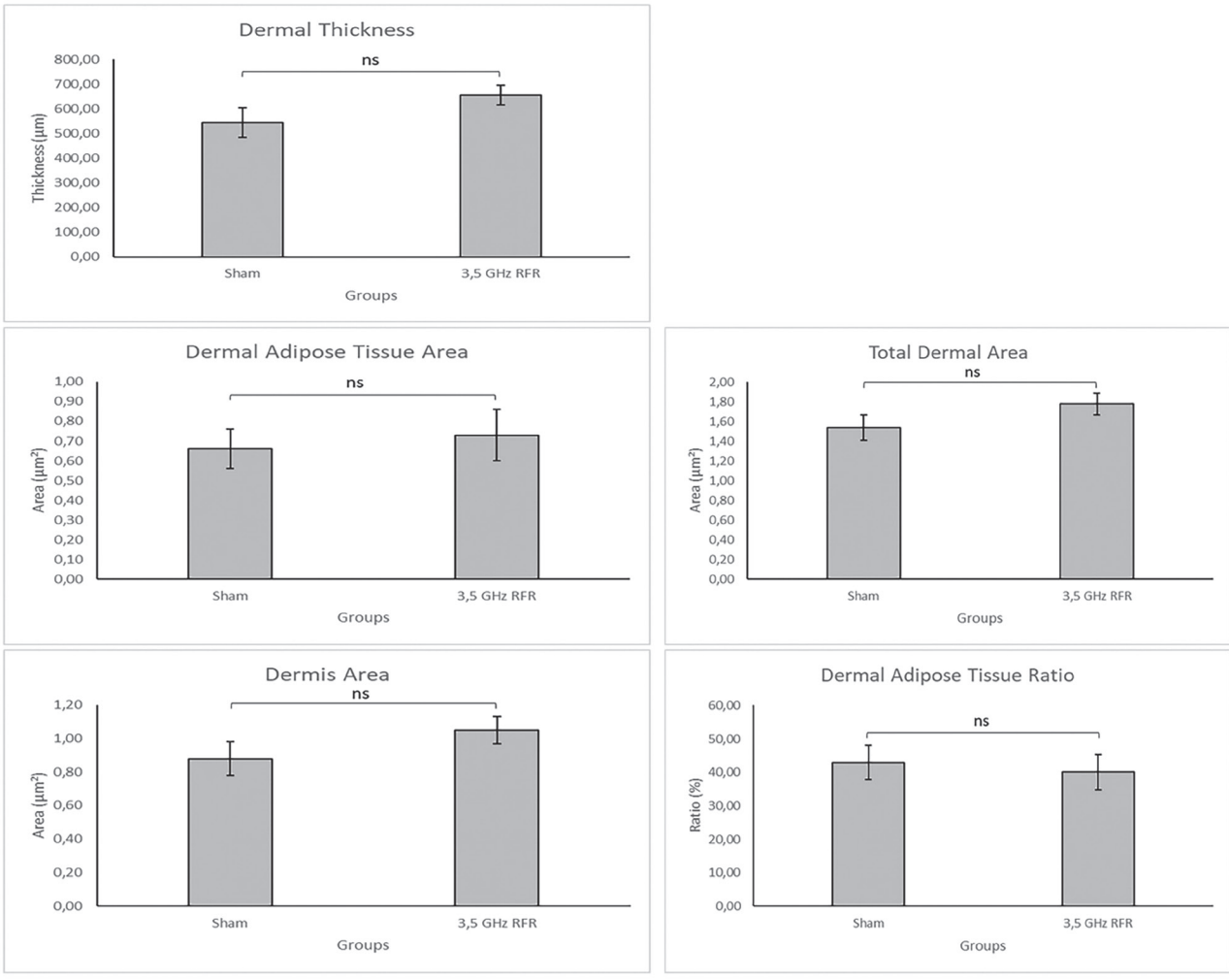

Figure 2. Comparison of histomorphometric parameters in skin tissue of female offspring rats with and without prenatal RFR exposure at 18 months of age. Bar graphs represent mean ± standard error (SE) for dermal thickness, dermal adipose tissue area, dermis area, total dermal area, and dermal adipose tissue ratio. "ns" indicates that the difference between groups was not statistically significant.

RFR: Radiofrequency radiation

thickness, dermis area, dermal adipose tissue area, total dermal area, and dermal adipose tissue ratio are illustrated in Figure 2.

DISCUSSION

In this study, histomorphometric measurements of skin tissue at 18 months of age showed no statistically significant differences between female rats prenatally exposed to RFR throughout all trimesters of the intrauterine period and unexposed shams. Parameters—dermal thickness, dermis area, dermal adipose tissue area, total dermal area, and dermal adipose tissue ratio (p=0.162, 0.717, 0.198, 0.175, and 0.704, respectively). These findings indicate that prenatal RFR exposure produces changes in skin morphology similar to those associated with aging in female rats.

Skin cells, including keratinocytes and fibroblasts, are constantly exposed to various environmental stressors. To counteract these effects, they have evolved numerous protective mechanisms that enable adaptive responses to stimuli such as UV-R, temperature fluctuations, and mechanical stress. Key protective systems include HSPs; antioxidant enzymes, such as superoxide dismutase, catalase, and glutathione peroxidase; and DNA repair

mechanisms[21]. Mild cellular stress caused by low-energy, non-ionizing stimuli such as RFR may not exceed the threshold required to elicit these adaptive responses, or may be rapidly compensated for.

This claim is further substantiated by the findings of Joushomme et al.[22], who conducted a study of the effects of 5G RF-EMF exposure at 3.5 GHz in human fibroblast and keratinocyte cell lines. Their research assessed the activation of stress response pathways, including *HSF1*, RAS, ERK, and *PML*, under both continuous and intermittent exposure conditions. Consistent with our findings, the observed effects were limited and inconsistent: specifically, a reduction in *HSF1* activity and a slight decrease in *PML* SUMOylation were observed in fibroblasts exposed to low SAR levels, but were absent in keratinocytes and not reproducible across different exposure regimens. They concluded that was no convincing evidence that 5G RF-EMF, either alone or in combination with a chemical stressor, induced a significant and consistent cellular stress response[22]. While our study focused on *in vivo* long-term morphological effects, this referenced work explored in vitro short-term exposure and its impact on cellular stress signaling pathways. Together, these complementary approaches suggest that the biological effects of RFR on the skin may be limited at both the molecular and morphological levels.

Similarly, exposure to 1800 MHz RF-EMF at low doses has been shown to cause single- and double-strand breaks in DNA, but it also that, over time, reduce DNA damage below control levels, thereby eliciting a hormesis-like effect[23]. This hormetic response facilitates tissue integrity by activating adaptive mechanisms against low-level environmental stresses. Consequently, chronic and systemic RFR exposure during the prenatal period may activate such adaptation and repair pathways in developing tissues, preventing deterioration of skin morphology later in life.

The skin, particularly the stratum corneum, functions as a robust barrier that limits the penetration of RF-EMF energy into deeper tissues due to its low water content and high keratin density. The absorption of electromagnetic waves depends on the dielectric properties of the tissue; thus, the stratum corneum predominantly reflects or attenuates RFR at the skin surface. Consistent with this, Habauzit et al.[24] (2020) investigated the biological effects of chronic exposure to 94-GHz millimeter waves on skin gene expression in young and adult hairless rats. Their experimental design involved exposure of 3 hours per day, 3 days per week, over 5 months at 10 mW/cm^2—twice the International Commission on Non-Ionizing Radiation Protection occupational exposure limit—without inducing thermal elevation. Using microarray analysis, they found no statistically significant changes in skin gene expression in either age group[24]. The absence of detectable molecular-level alterations supports our morphological findings and suggests that skin tissue may represent a highly resistant target to RF-EMF exposure.

Moreover, the epidermis is a continuously renewing tissue; basal layer cells migrate to the surface and are shed approximately every 28 days. This rapid turnover may prevent the accumulation of sublethal damage induced by RFR. Even under long-term exposure, tissue integrity can be maintained through the elimination of damaged cells[25]. Supporting this, Xu et al.[26] exposed six cell lines to short-term (1 h) and long-term (24 h) intermittent 1800 MHz GSM RF-EMF exposures at a SAR of 3.0 W/kg, assessing DNA damage via γH2AX foci formation. Results showed cell-type-dependent induction of γH2AX foci—a marker of DNA double-strand breaks—with a significant increase in human skin fibroblasts (HSF) and Chinese hamster lung cells. However, the increase in γH2AX in HSF cells did not correspond with sustained functional impairments, as measured by comet assay parameters, Terminal deoxynucleotidyl transferase dUTP Nick End Labeling assay, cell cycle progression, proliferation, or viability. Thus, there was limited evidence that DNA damage translated into cellular dysfunction[26]. Our finding of absent histomorphometric alterations in chronic-phase skin following prenatal RFR exposure supports the hypothesis that potential DNA-level damage does not necessarily lead to functional impairments. Furthermore, it suggests that the epidermis's regenerative capacity during the chronic phase effectively prevents the accumulation of cellular damage over time.

Considering evidence from our study and related *in vitro* and molecular research, it appears that prenatal exposure to RFR under the tested conditions does not significantly impair skin morphology or function over the long term. This resilience likely stems from the skin's robust barrier properties, its dynamic cellular renewal, and effective adaptive and repair mechanisms that mitigate potential damage. Nonetheless, given the variability in exposure parameters and biological responses, further investigations exploring different frequencies, intensities, and combined environmental factors—especially during critical developmental windows—are essential to comprehensively understand the potential risks and safety profile of RFR exposure.

Study Limitations

This study has several limitations that should be acknowledged. First, the investigation was limited to a specific RFR frequency and exposure regimen, which may not represent the full spectrum of environmental exposures. Secondly, only female rats were included, and potential sex-specific differences were not assessed. Thirdly, the focus was restricted to skin morphology without direct in vivo evaluation of functional or molecular endpoints, which could have provided deeper insight into subtle biological effects. Lastly, the sample size may limit the detection of minor effects. Future studies addressing these limitations, including multi-frequency exposures, both sexes, and integrated morphological, molecular, and functional analyses, would strengthen the understanding of RFR's impact on developing tissues.

CONCLUSION

In conclusion, our long-term in vivo study indicated that prenatal 3.5 GHz RFR exposure did not result in significant histomorphometric alterations in the skin of aged (18-month-old) female rats. This lack of morphological change is likely attributable to the skin's inherent protective barriers, efficient cellular repair mechanisms, and continuous regenerative capacity. In conjunction with existing *in vitro* and molecular data, these findings suggest that, under the exposure conditions examined, RFR poses minimal risk to skin structural integrity and function. We believe that further studies in this area will make valuable contributions to the field.

Ethics

Ethics Committee Approval: All procedures were designed and performed in accordance with the guidelines of the Animal Experiments Local Ethics Committee of Istanbul Bagcilar Training and Research Hospital with decision no: 2024-53, and date: 26.11.2024).

Informed Consent: Not appreciable.

Footnotes

Author Contributions

Surgical and Medical Practices: E.G.D., T.M., R.N.K., Concept: E.G.D., U.U., S.D., Design: E.G.D., U.U., S.D., Data Collection and/or Processing: E.G.D., T.M., R.N.K., U.U., Analysis or Interpretation: E.G.D., T.M., S.D., Literature Search: E.G.D., T.M., S.D., Writing: E.G.D., T.M., R.N.K., U.U., S.D.

Conflict of Interest: The authors have no conflict of interest to declare.

Financial Disclosure: The authors declared that this study has received no financial support.

REFERENCES

1. Wang X, Zhou G, Lin J, et al. Effects of radiofrequency field from 5G communication on fecal microbiome and metabolome profiles in mice. Sci Rep. 2024;14:3571.
2. Bektas H, Algul S, Altindag F, Yegin K, Akdag MZ, Dasdag S. Effects of 3.5 GHz radiofrequency radiation on ghrelin, nesfatin-1, and irisin level in diabetic and healthy brains. J Chem Neuroanat. 2022;126:102168.
3. Bektas H, Dasdag S, Altindag F, Akdag MZ, Yegin K, Algul S. Effects of 3.5-GHz radiofrequency radiation on energy-regulatory hormone levels in the blood and adipose tissue. Bioelectromagnetics. 2024;45:209-17.
4. Mancinelli F, Caraglia M, Abbruzzese A, d'Ambrosio G, Massa R, Bismuto E. Non-thermal effects of electromagnetic fields at mobile phone frequency on the refolding of an intracellular protein: myoglobin. J Cell Biochem. 2004;93:188-96.
5. Leszczynski D, Joenväärä S, Reivinen J, Kuokka R. Non-thermal activation of the hsp27/p38MAPK stress pathway by mobile phone radiation in human endothelial cells: molecular mechanism for cancer- and blood-brain barrier-related effects. Differentiation. 2002;70:120-9.
6. Guney M, Ozguner F, Oral B, Karahan N, Mungan T. 900 MHz radiofrequency-induced histopathologic changes and oxidative stress in rat endometrium: protection by vitamins E and C. Toxicol Ind Health. 2007;23:411-20.
7. Luukkonen J, Hakulinen P, Mäki-Paakkanen J, Juutilainen J, Naarala J. Enhancement of chemically induced reactive oxygen species production and DNA damage in human SH-SY5Y neuroblastoma cells by 872 MHz radiofrequency radiation. Mutat Res. 2009;66:54-8.
8. Zeni O, Di Pietro R, d'Ambrosio G, et al. Formation of reactive oxygen species in L929 cells after exposure to 900 MHz RF radiation with and without co-exposure to 3-chloro-4-(dichloromethyl)-5-hydroxy-2(5H)-furanone. Radiat Res. 2007;167:306-11.
9. Sharma A, Kesari KK, Saxena VK, Sisodia R. The influence of prenatal 10 GHz microwave radiation exposure on a developing mice brain. Gen Physiol Biophys. 2017;36:41-51.
10. Jensh RP. Studies of the teratogenic potential of exposure of rats to 6000-MHz microwave radiation. II. Postnatal psychophysiologic evaluations. Radiat Res. 1984;97:282-301.
11. Odaci E, Bas O, Kaplan S. Effects of prenatal exposure to a 900 MHz electromagnetic field on the dentate gyrus of rats: a stereological and histopathological study. Brain Res. 2008;1238:224-9.
12. Shirai T, Wang J, Kawabe M, et al. No adverse effects detected for simultaneous whole-body exposure to multiple-frequency radiofrequency electromagnetic fields for rats in the intrauterine and pre- and post-weaning periods. J Radiat Res. 2017;58:48-58.
13. Kraemer KH. Sunlight and skin cancer: another link revealed. Proc Natl Acad Sci U S A. 1997;94:11-4.
14. Gabriel C, Gabriel S, Corthout E. The dielectric properties of biological tissues: I. Literature survey. Phys Med Biol. 1996;41:2231-49.
15. Roach WP. Radio Frequency Radiation Dosimetry Handbook. Fifth Edition. Texas: Air Force Research Laboratory, 711 Human Performance Wing; 2009. p. 83-125.

16. VIjayalaxmi, Prihoda TJ. Genetic damage in mammalian somatic cells exposed to radiofrequency radiation: a meta-analysis of data from 63 publications (1990-2005). Radiat Res. 2008;169:561-74.
17. Anderson V, Rowley J. Measurements of skin surface temperature during mobile phone use. Bioelectromagnetics. 2007;28:159-62.
18. Straume A, Oftedal G, Johnsson A. Skin temperature increase caused by a mobile phone: a methodological infrared camera study. Bioelectromagnetics. 2005;26:510-9.
19. Millenbaugh NJ, Roth C, Sypniewska R, et al. Gene expression changes in the skin of rats induced by prolonged 35 GHz millimeter-wave exposure. Radiat Res. 2008;169:288-300.
20. Loos N, Thuróczy G, Ghosn R, et al. Is the effect of mobile phone radiofrequency waves on human skin perfusion non-thermal? Microcirculation. 2013;20:629-36.
21. Scieglinska D, Krawczyk Z, Sojka DR, Gogler-Pigłowska A. Heat shock proteins in the physiology and pathophysiology of epidermal keratinocytes. Cell Stress Chaperones. 2019;24:1027-44.
22. Joushomme A, Orlacchio R, Patrignoni L, et al. Effects of 5G-modulated 3.5 GHz radiofrequency field exposures on HSF1, RAS, ERK, and PML activation in live fibroblasts and keratinocytes cells. Sci Rep. 2023;13:8305.
23. Sun C, Wei X, Fei Y, et al. Mobile phone signal exposure triggers a hormesis-like effect in $Atm^{+/+}$ and $Atm^{-/-}$ mouse embryonic fibroblasts. Sci Rep. 2016;6:37423.
24. Habauzit D, Nugue G, Bourbon F, et al. Evaluation of the Effect of chronic 94 GHz exposure on gene expression in the skin of hairless rats *in vivo*. Radiat Res. 2020;193:351-8.
25. Senoo M. Epidermal stem cells in homeostasis and wound repair of the skin. Adv Wound Care (New Rochelle). 2013;2:273-82.
26. Xu S, Chen G, Chen C, et al. Cell type-dependent induction of DNA damage by 1800 MHz radiofrequency electromagnetic fields does not result in significant cellular dysfunctions. PLoS One. 2013;8:e54906.

DOI: 10.4274/MMJ.galenos.2025.59265
Medeni Med J 2025;40:217-225

Original Article

Surgical Success and Predictive Factors for Residual Stones Following Supine Percutaneous Nephrolithotomy in the Galdakao-Modified Valdivia Position

Galdakao-Modifiye Valdivia Pozisyonunda Supin Perkütan Nefrolitotomi Sonrası Cerrahi Başarı ve Rezidüel Taşları Öngören Faktörler

Gunal OZGUR[1], Ersin GOKMEN[1], Yiloren TANIDIR[2], Kamil CAM[3], Tarik Emre SENER[3]

[1]Marmara University Pendik Training and Research Hospital, Department of Urology, Istanbul, Türkiye
[2]Medicana Atasehir Hospital, Clinic of Urology, Istanbul, Türkiye
[3]Marmara University Faculty of Medicine, Department of Urology, Istanbul, Türkiye

ABSTRACT

Objective: Supine percutaneous nephrolithotomy (sPCNL) is widely accepted as a safe and effective treatment for kidney stones. This study aims to assess surgical outcomes and identify predictive factors for residual fragments following sPCNL in the Galdakao-modified Valdivia position (GMV-sPCNL).

Methods: We retrospectively evaluated the clinical data of patients undergoing GMV-sPCNL. The primary outcomes were the stone-free rate (SFR) and the complication rate. Demographic, radiologic, and perioperative parameters were also compared between patients with and without residual stones.

Results: 195 patients [Male:127 (65.1%); Female: 68 (34.9%)] were included. The mean age was 48.6±15.6 years; the mean body mass index (BMI) was 27.4±5 kg/m2. The overall SFR was 83.1%. Residual stones were associated with greater stone burden (number, size, surface area, and volume), longer operative time, and longer hospitalization (p<0.05). Gender, age, BMI, stone laterality, and density were not significantly associated with SFR. The receiver operating characteristic analysis showed that having more than two stones, a stone size ≥26 mm, or a stone volume ≥2639.8 mm3 significantly predicted residual fragments. Stone volume demonstrated the best predictive performance, with sensitivity and specificity of 81.8% and 61.0%, respectively. GMV-sPCNL was associated with a low overall complication rate: 86.2% of patients experienced no or only minor complications, and major complications (Clavien-Dindo ≥3) occurred in just 4.6% of cases.

Conclusions: GMV-sPCNL demonstrates high success rates and an acceptable complication profile. Stone burden parameters such as stone number, stone size, and stone volume are important determinants of surgical success.

Keywords: Galdakao-modified Valdivia position, kidney stones, percutaneous nephrolithotomy, supine position, treatment outcome

ÖZ

Amaç: Supin perkütan nefrolitotomi (sPCNL), böbrek taşlarının tedavisinde güvenli ve etkili bir tedavi yöntemidir. Bu çalışmada, Galdakao-modifiye Valdivia pozisyonunda (GMV-sPCNL) uygulanan sPCNL sonrası cerrahi sonuçların değerlendirilmesi ve rezidüel fragmanları öngören faktörlerin belirlenmesi amaçlanmıştır.

Yöntemler: GMV-sPCNL uygulanan hastalara ait klinik veriler retrospektif olarak incelendi. Çalışmanın birincil sonucu taşsızlık ve komplikasyon oranlarının saptanmasıdır. Rezidü taş varlığına göre hastaların demografik, radyolojik ve perioperatif parametreleri karşılaştırıldı.

Bulgular: Çalışmaya 195 hasta [Erkek: 127 (%65.1)/Kadın: 68 (%34.9)] dahil edildi. Ortalama yaş 48,6 (±15,6) yıl, ortalama beden kitle indeksi (BKİ) 27,4 (±5) kg/m^2 idi. Genel taşsızlık oranı %83,1 olarak saptandı. Rezidü taş varlığı; daha yüksek taş yükü (taş sayısı, boyutu, yüzey alanı ve hacmi), daha uzun operasyon süresi ve uzamış hastanede yatış süresi ile ilişkili bulundu (p<0,05). Cinsiyet, yaş, BKİ, cerrahi tarafı ve taş dansitesi ile taşsızlık arasında anlamlı bir ilişki saptanmadı. Receiver operating characteristic analizinde, taş sayısının 2'den fazla olması, taş boyutunun ≥26 mm ve taş hacminin ≥2639,8 mm^3 olması rezidüel fragmanları anlamlı şekilde öngördü. Taş hacmi, en iyi öngörü performansını göstermiş olup, buna karşılık gelen duyarlılık ve özgüllük değerleri sırasıyla %81,8 ve %61,0 olarak bulunmuştur. GMV-sPCNL hastalarında düşük komplikasyon oranları gözlendi. Hastaların %86,2'sinde hiç komplikasyon görülmedi veya sadece minör olaylar yaşandı. Majör komplikasyon (Clavien-Dindo ≥3) oranı ise %4,6 olarak saptandı.

Sonuçlar: GMV-sPCNL, yüksek taşsızlık ve düşük komplikasyon oranları ile büyük böbrek taşlarında etkili bir tedavi seçeneğidir. Taş yükü parametreleri —taş sayısı, boyutu ve hacmi— cerrahi başarının önemli belirleyicileri olarak saptandı.

Anahtar kelimeler: Galdakao-modifiye Valdivia pozisyonu, böbrek taşları, perkütan nefrolitotomi, supin pozisyon, tedavi sonuçları

Address for Correspondence: T.E. Sener, Marmara University Faculty of Medicine, Department of Urology, Istanbul, Türkiye
E-mail: dr.emresener@gmail.com **ORCID ID:** orcid.org/0000-0003-0085-7680

Cite as: Ozgur G, Gokmen E, Tanidir Y, Cam K, Sener TE. Surgical success and predictive factors for residual stones following supine percutaneous nephrolithotomy in the galdakao-modified valdivia position. 2025;40:209-216

Received: 05.08.2025
Accepted: 19.11.2025
Published: 31.12.2025

INTRODUCTION

Percutaneous nephrolithotomy (PCNL) is widely recognized as the first-line treatment for complex or large kidney stones[1]. The prone position provides adequate access for renal puncture and facilitates effective instrument handling. However, it also poses several disadvantages, including patient discomfort, increased radiation exposure to the surgeon, the need for repositioning in cases of combined retrograde access, and anesthetic challenges—particularly in obese, elderly, or cardiopulmonary-compromised patients[2].

To address these limitations, Valdivia et al. introduced supine PCNL (sPCNL) in 1998, reporting a large series of 557 patients and demonstrating its safety, patient comfort, and low complication rates[3]. Various sPCNL techniques have gained popularity due to their versatility, allowing simultaneous antegrade and retrograde access, improved ergonomics, and airway access for anesthesia[2,4]. The sPCNL were performed in various positions, such as Valdivia, entire supine position, Galdakao-modified Valdivia, flank-free Barts, or Barts-modified[5].

Across studies, sPCNL was associated with shorter operation time (OT), lower infection rates, and fewer visceral injuries[6,7]. However, there is no consensus regarding the optimal supine technique[5]. The Galdakao-modified Valdivia (GMV) position, which was employed in all cases in our study, is a widely accepted and reliably applicable technique[2]. This study aims to assess the clinical efficacy of sPCNL in the Galdakao modified Valdivia position (GMV-sPCNL) over a 5-year period by analyzing stone-free rates (SFR), postoperative complication rates, and clinical and radiological predictors of residual stone formation. Unlike most previous reports, which primarily compared stone-free and complication rates across different PCNL positions, the present study provides quantitative data on stone characteristics from a relatively large cohort of patients treated in the GMV-sPCNL position and evaluates their predictive performance for residual stones using receiver operating characteristic (ROC) analysis.

MATERIALS and METHODS

A retrospective review involving patients who underwent GMV-sPCNL between January 2019 and May 2025 was performed using records from our institutional PCNL database. This study was conducted in accordance with the principles of the Declaration of Helsinki (Recommendations Guiding Physicians in Biomedical Research Involving Human Subjects, first adopted in Helsinki in 1964 and subsequently amended). The study protocol was reviewed and approved by the Institutional Review Board (IRB) of Marmara University (approval no.: 09.2025.25-0626, date: 18.07.2025).

Patients aged above 18 years who underwent GMV-sPCNL for renal stone management in accordance with established clinical guidelines were included[1]. The exclusion criteria included patients undergoing synchronous bilateral endoscopic stone surgery, patients with current UTIs, anatomical or functional urinary tract abnormalities (e.g., ureteropelvic junction obstruction, horseshoe kidney, vesicoureteral reflux), immunocompromised patients, and patients younger than 18 years.

In all cases, surgical indications and stone parameters—including number, size, Hounsfield units (HU), volume, and surface area—were assessed using computed tomography (CT). Stone size was based on the longest axis of the largest stone when multiple stones were present. Stone volume and surface measurements were obtained through 3D reconstruction of axial CT scans using 3D-DOCTOR software (Able Software Corp., Lexington, MA, USA). Postoperative residual fragments that are unlikely to cause renal colic or require further medical or interventional treatment were defined as clinically insignificant residual fragments. In previous studies, stone-free status has most commonly been defined by accepting residual fragments measuring 2-4 mm as clinically insignificant[8-10]. Patients were considered stone-free in our study if follow-up CT imaging at one month postoperatively revealed either no stones or only clinically insignificant residual fragments smaller than 3 mm, a threshold that is commonly used in previous studies[8,9,11].

All GMV-sPCNL procedures were performed by two endourologists with over five years of experience and extensive backgrounds in sPCNL (>200 cases) and flexible ureterorenoscopy (>400 cases). All patients underwent a standardized preoperative and perioperative surgical protocol. Urine cultures were obtained from all patients prior to the procedure. Those with sterile urine cultures received prophylactic ceftriaxone within 30 minutes prior to the operation. Patients with UTIs were managed with appropriate antibiotics for at least seven days and underwent surgery only after sterile urine cultures were obtained. Renal access was achieved using ultrasound, fluoroscopy, or both.

SFR and Clavien-Dindo (CD) complications were evaluated for the entire cohort. Patients were categorised into two groups: those with postoperative residual stones and those without. Demographic data, stone characteristics, and perioperative and postoperative outcomes were compared between the two groups.

Statistical Analysis

No formal a priori power analysis was performed because the study was retrospective in design. However, the sample size of 195 patients is comparable to or larger than those reported in similar studies, and provides sufficient statistical power for the analyses performed[8]. Additionally, a post-hoc power analysis was performed using G*Power 3.1. Within the family of t-tests, the "Means: Wilcoxon-Mann-Whitney test (two groups)" option was selected to perform non-parametric comparisons between the residual-stone and stone-free groups. Effect sizes were calculated from group-specific means and pooled standard deviations. Using a two-sided α=0.05, achieved power (1-β) values were calculated. Statistical analyses were conducted using SPSS (IBM, version 25). The distribution patterns of the variables were explored using visual approaches, such as histograms and probability plots, and through statistical assessments, including the Kolmogorov-Smirnov and Shapiro-Wilk tests. For normally distributed data, values were reported as mean ± standard deviation, and comparisons were carried out using the independent samples t-test. In cases of non-normal distribution, the data were summarized using median and interquartile range, with the Mann-Whitney U test employed for between-group comparisons. Categorical variables were assessed using either the chi-square test or Fisher's exact test, depending on the data structure. For paired samples, the Wilcoxon signed-rank test was utilized. The correlation between variables was determined using Spearman's rank correlation method. To assess the diagnostic performance of different predictors for residual stones, ROC curve analysis was performed. Statistical significance was set at p<0.05.

RESULTS

The cohort of 195 patients who underwent GMV-sPCNL had a mean age of 48.6±15.6 years and a mean body mass index (BMI) of 27.4±5.0 kg/m^2. Most patients were male (65.1%) and had American Society of Anesthesiologists (ASA) scores of 1 or 2. Multiple stones were present in 63.1% of the cohort, with the median diameter of the largest stone and the median volume being 25 (21.8-32) mm and 2927 (1364-7561) mm^3, respectively.

Postoperative evaluation revealed stone-free status in 162 of 195 patients (SFR =83.1%). No statistically significant differences were observed between the groups regarding age (p=0.559), BMI (p=0.729), or the stones' maximum and mean HU (p=0.069 and p=0.110). However, the residual stone group had a significantly higher number of stones (p=0.005), larger stone size (p=0.022), volume (p=0.005), and surface area (p=0.032). Post hoc power analysis demonstrated that the significant differences in stone-related parameters were supported by adequate statistical power, with achieved 1-β (statistical power) values of 0.86 for stone number, 0.84 for maximal stone size, 0.91 for stone volume, and 0.93 for stone surface area. Additionally, the residual stone (+) group had significantly longer OT (p<0.001) and a longer hospital stay (p=0.012) (Table 1).

No statistically significant differences were observed between the groups with respect to gender, ASA score, diabetes mellitus, side of surgery, or pre- and postoperative urinary drainage methods (p>0.05). Residual stones occurred more frequently when multiple stones were present (p=0.014). Postoperative Foley catheter use was more frequent in residual stone-positive patients (p = 0.019) (Table 2).

ROC analysis (Figure 1) revealed that stone number area under the curve [(AUC): 0.647, p=0.008] and largest stone size (AUC: 0.626, p=0.022) were significantly associated with residual stones; cut-off points were identified to aid clinical assessment. Similarly, Figure 2 shows that stone volume (AUC =0.689, p=0.005) and stone surface area (AUC =0.643, p=0.036) are important variables, supported by their respective thresholds. These AUC values indicate a fair discriminatory ability of the evaluated stone parameters to predict residual stones. Additionally, significant positive correlations were observed between stone number and OT (r=0.244, p=0.001), stone size and OT (r=0.222, p=0.002), and OT and hospital stay duration (r=0.162, p=0.023).

In the majority of patients (86.2%) undergoing GMV-sPCNL, no complications occurred; when complications did occur, they were mild (CD grade 1). Only 9 patients (4.6%) experienced CD grade ≥3 complications, whereas 26 patients (13.3%) experienced CD grade ≥2 complications (Table 3). No statistically significant differences in infection rates were observed between the groups (p=0.892). Hemoglobin levels decreased significantly postoperatively, from 14.64±9.11 g/dL to 13.54±8.65 g/dL, and hematocrit levels decreased from 38.99±5.40% to 38.82±5.50% (p<0.001). However, no significant differences were found between the groups (p=0.304 and p=0.108, respectively). Blood transfusions were required in 11 patients (5.6%) because of a drop in hemoglobin levels. Three patients (1.5%) required postoperative intensive care unit (ICU) follow-up. One elderly patient (0.6%) with cardiac and neurological comorbidities developed a postoperative hematoma and sepsis and died during ICU follow-up.

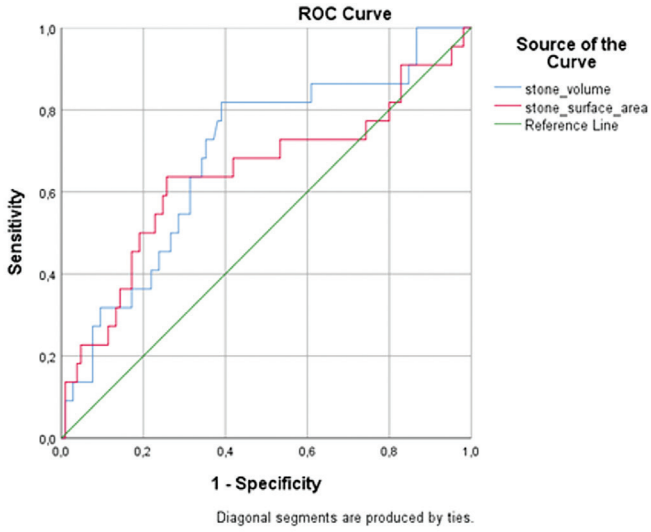

Figure 2. ROC curves for stone volume and stone surface area in predicting residual stone.

Receiver operating characteristic (ROC) analyses were performed for stone volume and stone surface area to evaluate their ability to predict residual stone formation. Stone volume demonstrated an AUC of 0.689 (p=0.005; 95% CI: 0.567-0.811), while stone surface area showed an AUC of 0.643 (p=0.036; 95% CI: 0.497-0.788). The optimal cut-off for stone volume was ≥2639.8 mm^3, corresponding to a sensitivity of 81.8% and specificity of 61.0%. For stone surface area, the optimal cut-off was ≥1250.2 mm^2, with 68.2% sensitivity and 58.1% specificity.

AUC: Area under the curve, CI: Confidence interval

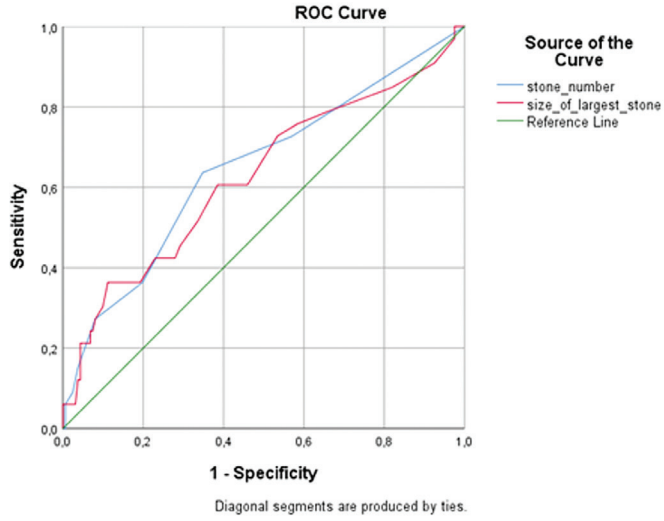

Figure 1. ROC curves for stone number and largest stone size in predicting residual stone.

Receiver operating characteristic (ROC) curves were generated to assess the diagnostic accuracy of stone number and size of the largest stone in predicting the presence of residual stone. The area under the curve (AUC) for stone number was 0.647 (p=0.008; 95% CI: 0.537-0.757), and for the size of the largest stone was 0.626 (p=0.022; 95% CI: 0.513-0.740). The optimal cut-off value for stone number was >2, with a sensitivity of 68.2% and specificity of 66.7%. For the largest stone size, the best cut-off was ≥26 mm, yielding 60.6% sensitivity and 61.5% specificity.

CI: Confidence interval

Table 1. Comparison of continuous parameters by residual stone status.

Variable	Supine PCNL patients N=195	Residual stone (-) n=162 (83.1%)	Residual stone (+) n=33 (16.9%)	p-value
Age (years)	48.6 (±15.6)	48.3 (±16.0)	50.0 (±14.0)	0.559
BMI (kg/m^2)	27.4 (±5.0)	27.4 (±5.1)	27.7 (±4.4)	0.729
Stone number	2 (1-3)	2 (1-3)	3 (1-5)	**0.005**
Size of largest stone (mm)	25 (21.8-32)	25 (21-30.5)	28 (23.5-42)	**0.022**
Stone volume (mm^3)	2927 (1364.3-7561)	2471 (1332.8-6141.6)	5296 (3349.3-12797.6)	**0.005**
Stone surface area (mm^2)	1157.2 (671.2-2671.9)	1121.1 (662-2199.3)	2711.5 (654.5-5448.2)	**0.032**
HU max	1268 (1020.5-1464.5)	1292.5 (1058.5-1491)	1204 (815-1388)	0.069
HU mean	1089.5 (825.8-1207.5)	1100 (846-1216)	980 (635-1124.5)	0.110
Operation time (min)	120 (90-180)	120 (90-150)	180 (122.5-230)	**0.000**
Length of stay (days)	2 (2-5)	2 (2-4.3)	3 (2-7)	**0.012**

Continuous variables are presented as mean (± standard deviation) or median (interquartile range) according to their distribution. The independent samples t-test was used for normally distributed variables, and the Mann-Whitney U test was used for non-normally distributed variables. A p-value of <0.05 was considered statistically significant.

BMI: Body mass index, HU: Hounsfield unit, mm: Millimeter, mm^2: Square millimeter, mm^3: cubic millimeter, min: Minute, IQR: Interquartile range

Table 2. Comparison of categorical parameters by residual stone status.

Variable	Supine PCNL patients n=195	Residual stone (-) n=162 (83.1%)	Residual stone (+) n=33 (16.9%)	p-value
Gender				
Male	127 (65.1%)	101 (62.3%)	26 (78.8%)	0.071
Female	68 (34.9%)	61 (37.7%)	7 (21.2%)	
ASA score				
ASA 1	91(46.7%)	79 (48.8%)	12 (36.4%)	0.086
ASA 2	94 (48.2%)	73 (45.1%)	21 (63.6%)	
ASA 3	10 (5.1%)	10 (6.2%)	0 (0.0%)	
Diabetes mellitus				
No	157 (80.5%)	133 (82.1%)	24 (72.7%)	0.222
Yes	38 (19.5%)	29 (17.9%)	9 (27.3%)	
Multiple stones				
No	72 (36.9%)	66 (40.7%)	6 (18.2%)	**0.014**
Yes	123 (63.1%)	96 (59.3%)	27 (81.8%)	
Surgery side				
Left	108 (55.4%)	86 (53.1%)	22 (66.7%)	0.153
Right	87 (44.6%)	76 (46.9%)	11 (33.3%)	
Amplatz sheath size				
12/16	42 (21.5%)	37 (22.8%)	5 (15.2%)	0.123
16/20	118 (60.5%)	99 (61.1%)	19 (57.6%)	
20/24	29 (14.9%)	23 (14.2%)	6 (18.2%)	
26/30	6 (3.1%)	3 (1.9%)	3 (9.1%)	
Pre-op urinary diversion				
None	159 (81.5%)	134 (82.7%)	25 (75.8%)	0.292
DJ stent	24 (12.3%)	20 (12.3%)	4 (12.1%)	
Nephrostomy	12 (6.2 %)	8 (4.9%)	4 (12.1%)	
Post-op urinary drainage				
None	53 (27.2%)	47 (29.0%)	6 (18.2%)	0.055
Nephrostomy	21 (10.8%)	16 (9.9%)	5 (15.2%)	
DJ stent	102 (52.3%)	87 (53.7%)	15 (45.5%)	
Nephrostomy + DJ stent	19 (9.7%)	12 (7.4%)	7 (21.2%)	
Post-op Foley catheter Use				
No	149 (76.4%)	129 (79.6%)	20 (60.6%)	**0.019**
Yes	46 (23.6%)	33 (20.4%)	13 (39.4%)	

Categorical variables are presented as frequency and percentage. The chi-square test or Fisher's exact test was used for group comparisons, as appropriate. A p-value of <0.05 was considered statistically significant.

ASA: American Society of Anesthesiologists, DJ Stent: Double-J ureteral stent, HU: Hounsfield unit

DISCUSSION

The sPCNL procedure has long been recognized as a safe and effective treatment for complex kidney stones[1, 12]. Various sPCNL techniques are currently used, each offering distinct advantages for surgical access and patient positioning[5]. GMV-sPCNL was highly effective, yielding an SFR of 83.1% in a cohort with a notable stone burden, underscoring the technique's efficacy and potential for clinical success. Additionally, the low complication rates support its safety profile. ROC analyses revealed that patients with more than two stones (>2) or with a largest stone diameter ≥26 mm were at higher risk of residual fragments. Among the evaluated variables, stone

Table 3. Comparison of postoperative outcomes by residual stone status.				
Variable	**Supine PCNL patients n=195**	**Residual stone (-) n=162 (83.1%)**	**Residual stone (+) n=33 (16.9%)**	**p-value**
Urinary tract infection				
No Yes	173 (88.7) 22 (11.3)	144 (88.9%) 18 (11.1%)	29 (87.8%) 4 (12.2%)	0.892
Hemoglobin decrease (g/dl)	0.9 (0.1-1.6)	1 (0.2-1.6)	0.6 (0.1-1.4)	0.304
Hematocrit decrease (%)	2 (0-4.1)	1.9 (0.35-3.9)	1 (0.2-1.6)	0.108
Clavien-Dindo complications				
No CD-1 CD-2 CD-3 CD-4 CD-5	121 (62.1%) 48 (24.6) 17 (8.7%) 5 (2.6%) 3 (1.5%) 1 (0.5%)	102 (63.8%) 41 (24.7%) 14 (8.4%) 3 (1.9%) 1 (0.6%) 1 (0.6%)	19 (57.5%) 7 (21.2%) 3 (9.1%) 2 (6.1%) 2 (6.1%) 0 (0.0%)	0.140
Intensive Care Unit Admission				
No Yes	192 (98.5%) 3 (1.5%)	161 (99.4%) 1 (0.6%)	31 (93.9%) 2 (6.1%)	0.075

Data are presented as frequency (percentage) for each group. Differences between groups were evaluated using Pearson's chi-square test or Fisher's exact test, as appropriate. A p-value<0.05 was considered statistically significant.

CD: Clavien-Dindo classification, PCNL: Percutaneous nephrolithotomy

volume with a cut-off value of ≥2639.8 mm^3 predicted residual stone formation with a sensitivity of 81.8% and a specificity of 61.0%.

SPCNL has been shown to achieve favorable SFR across different patient positioning techniques. In a study using Giusti's position, a modification of GMV-sPCNL, Batratanakij et al.[6] reported an SFR of 86.2% among patients with a mean stone size of 31.8 (±11.7) mm. Similarly, Babaoff et al.[13] documented an SFR of 81.4%. Ahmed et al.[9] observed a 75.4% SFR in cases with a mean stone size of 28.34 (±10.02) mm using the split-leg modified lateral supine position. Using GMV-sPCNL, Kannan et al.[14] reported an 86.7% success rate in patients with stones averaging 24±4 mm. In another study, Jones et al.[15] achieved a 70% SFR in patients treated with the modified supine approach; the average stone size was 22.9 (±13.5) mm.

Melo et al.[10] compared complete supine, Valdivia, and GMV-sPCNL and reported SFRs ranging from 49% to 58%, without significant differences among positions. Studies in sPCNL patients have also reported success rates exceeding 90%[12,16]. In a meta-analysis, Li et al.[7] achieved an SFR of 78.1% for all sPCNL patients, regardless of position. Similarly, Lachkar et al.[8] reported, across 45 studies, a pooled SFR of 71.85% for sPCNL in patients with a mean stone size of approximately 2 cm. Consistent with previous reports, this study demonstrated a notable SFR of 83.1% among patients with a median stone size of 25 mm (range, 21.8-32 mm) who underwent GMV-sPCNL.

It is also important to note that the definition used for stone-free status can significantly influence the reported SFR values across studies. There is no universally accepted definition of "stone-free status" in endourological stone management[17]. Although the complete absence of residual fragments is the most objective indicator of success, such an approach would require consideration of clinically insignificant fragments that are unlikely to cause symptoms or require further intervention. Previous studies have used various size thresholds (e.g., ≤2 mm to ≤4 mm) to define stone-free status[7,9,10]. Because of the heterogeneity and lack of standardization in defining stone-free status across studies, including meta-analyses, it is not possible to draw definitive conclusions regarding the clinical significance of different cut-off values reported in studies[7,8]. Therefore, in the present study, we adopted the widely accepted threshold of ≤3 mm to define clinically insignificant residual fragments and compared our findings with those of other studies.

Stone burden remains the most influential factor in determining stone-free outcomes after PCNL. Higher

stone number, size, and complexity are consistently associated with lower success rates[18-20]. Specifically, patients with multiple stones or greater stone burden exhibit significantly reduced SFR (74% vs. 45% and 69% vs. 47%, respectively; p<0.001)[21]. Several studies have identified stone size, stone number, volume, and surface-area as predictors of SFR[19, 20, 22]. In the present study, ROC analysis showed that patients with multiple stones (>2) or with a maximum stone diameter ≥26 mm were less likely to be stone-free; a stone volume ≥2639.8 mm^3 predicted residual stone formation with high sensitivity (81.8%). Additionally, increased stone size was correlated with longer OT, reflecting greater surgical complexity[19]. Conversely, factors such as gender, age, BMI, laterality, and stone density did not appear to influence surgical success in our cohort[19, 21].

A significant difference in OT was observed between the two positions, favoring sPCNL with 103.9 (±42.6) minutes over the prone approach with 116.3 (±38.9) minutes (p=0.016), mainly because patient repositioning was not required[6]. However, notable variations exist in the reported OT across different sPCNL studies. These discrepancies can partly be attributed to differences in how OT is defined. Some studies begin timing at anesthesia induction, patient positioning or initiation of PCNL, and end at completion of PCNL or placement of a double-J catheter or nephrostomy[13, 23, 24]. In an sPCNL meta-analysis, the mean OT was reported as 80.76 minutes[8]. Another meta-analysis reported a wide range of OT, from 43 to 114 minutes across different studies[7]. In our study, OT was measured from induction of anesthesia to recovery from anesthesia, yielding a median duration of 120 minutes (range, 90-180 minutes), which is slightly longer than previously reported but remains within an acceptable clinical range. This difference may be attributed to the higher stone burden and complexity of our cohort (median stone volume 2927 (1364.3-7561) mm^3 and multiple stones in 63.1% of patients), to differences in time-measurement methodology, or to a combination of the two. Notably, patients with residual stones had significantly longer OT than stone-free patients, consistent with their higher stone burden and increased surgical complexity.

In patients with a high stone burden and complex renal stones, multi-tract access during PCNL is considered an effective and safe option[25]. Previous studies have reported that patients undergoing multi-tract PCNL generally present with a higher stone burden and may experience a slightly higher rate of minor complications[26]. In our study, multi-tract access was performed in only 7 patients (3.7%), all of whom had large or multiple stones. Stone-free status was achieved in four of these cases. However, the limited number of patients who underwent multi-tract PCNL precluded meaningful statistical comparisons of SFR, stone burden, OT, or complication rates. Because our data were collected retrospectively, we cannot draw definitive conclusions for our cohort; nevertheless, prospective studies based on predefined criteria—such as stone number and total stone volume—would provide more robust evidence to guide decision-making in this area.

In addition to high success rates, sPCNL has been associated with low complication rates. Kiss et al.[27] documented an overall complication rate of 9.55% and noted that there were no CD grade 4 or 5 complications. Hoznek et al.[4] observed complication rates for CD grades 1 and 2 of 10.6% and 8.5%, respectively. Abu-Ghanem reported a complication rate of 21.7%[19]. Lachkar et al.[8] reported an overall complication rate of 15.58%, while the rate of major complications was only 4.04%. In a meta-analysis by Li et al.[7], the overall complication rate was 16.1% 7. Jones et al.[15] reported an 8% complication rate and a 2.6% requirement for blood transfusion. Liu et al.[12] calculated a mean intraoperative hemoglobin decrease of 1.04 g/dL without the need for transfusion, whereas Ahmed et al.[9] recorded a transfusion rate of 14.7% due to bleeding. Babaoff et al.[13] found a postoperative hemoglobin drop of 1.7 (±1.5 g/dL and a transfusion rate of 7.1%. In a meta-analysis by Lachkar et al.[8], the mean decrease in hemoglobin was 1.68 g/dL, with a transfusion rate of 4.92%. In patients who underwent GMV-sPCNL, the rates of minor complications (CD grade 1-2) and major complications (CD grade ≥3) were 19.5% and 7.3%, respectively[28]. In the present study, the rate of major complications (CD grade ≥3) was 4.6%. Hemoglobin decreased by approximately 1.1 g/dL and erythrocyte transfusion was required in 5.6% of patients, which aligns with the findings in current literature and confirms an acceptable safety profile for GMV-sPCNL.

A randomized study of patients undergoing flexible ureteroscopy found no association between postoperative Foley catheterization and complications or fever; to our knowledge, no comparable data exist for sPCNL[29]. In our routine practice, urethral Foley catheters are generally not used after sPCNL; however, in complex or prolonged cases, surgeons may prefer to place a catheter to ensure adequate drainage and to minimize postoperative discomfort and complications. Therefore, the higher catheterization rate observed among patients with residual stones in our series likely reflects their greater stone burden, greater surgical complexity, and longer OT.

Reported Infectious complications, such as fever and UTI, vary among studies of sPCNL. Postoperative fever occurred in 10% of patients in Liu et al.[12]'s study, compared with 33% in the cohort described by Batratanakij et al.[6], who also reported a UTI rate of 11.5%. In our study, the UTI rate was 11.3%, which is comparable to findings from previous studies.

Hospital stays in sPCNL patients are generally short, although reported values vary across studies. Hoznek et al.[4] and Jones et al.[15] reported average hospital stays of 3.4±1.9 days and 2.0±2.1 days, respectively. Lachkar et al.[8], in a meta-analysis, reported a mean hospitalization duration of 4 days, whereas Li et al.[7] found a range from 1.43 to 8.4 days. Median hospital stay was 2 days (2-4.3) in the stone-free group and 3 days (2-7) in patients with residual fragments. These findings suggest that sPCNL generally allows for a short hospitalization period, even in patients with higher stone complexity.

Study Limitations

This study has some limitations. The retrospective design and single-center setting may restrict the applicability of the results to broader populations. Furthermore, the study focused primarily on perioperative parameters affecting surgical success; therefore, long-term outcomes such as the need for secondary interventions were not assessed. In addition, the lack of data on short- and long-term postoperative changes in renal function represents a limitation of the present study. Prospective, multicenter studies with long-term follow-up are needed to confirm and extend these findings.

CONCLUSION

sPCNL performed in the GMV achieves high SFR, even in patients with a significant stone burden. It is a safe and effective technique with acceptable complication rates. Patients with residual stones were observed to have a higher number of stones and increased stone size, volume, and surface area. Preoperative assessment of these parameters helps classify patients at higher risk for residual stones. In such patients, surgical strategies such as multiple access tracts or adjunctive procedures may be considered to optimize stone clearance and minimize the need for re-intervention.

Ethics

Ethics Committee Approval: The study protocol was reviewed and approved by the Institutional Review Board (IRB) of Marmara University, School of Medicine (approval no.: 09.2025.25-0626, date: 18.07.2025).

Informed Consent: This study was conducted retrospectively using previously collected and anonymized data from the PCNL Database; therefore, obtaining written informed consent from participants was not required.

Footnotes

Author Contributions

Surgical and Medical Practices: G.O., E.G., Y.T., T.E.S., Concept: G.O., K.C., T.E.S., Design: G.O., K.C., T.E.S., Data Collection and/or Processing: G.O., E.G., Y.T., Analysis or Interpretation: G.O., K.C., Literature Search: G.O., Writing: G.O., T.E.S.

Conflict of Interest: The authors have no conflict of interest to declare.

Financial Disclosure: The authors declared that this study has received no financial support.

REFERENCES

1. Skolarikos A, Geraghty R, Somani B, et al. European Association of Urology Guidelines on the Diagnosis and Treatment of Urolithiasis. Eur Urol. 2025;88:64-75.
2. Ibarluzea G, Scoffone CM, Cracco CM, et al. Supine Valdivia and modified lithotomy position for simultaneous anterograde and retrograde endourological access. BJU Int. 2007;100:233-6.
3. Valdivia Uría JG, Valle Gerhold J, López López JA, et al. Technique and complications of percutaneous nephroscopy: experience with 557 patients in the supine position. J Urol. 1998;160:1975-8.
4. Hoznek A, Rode J, Ouzaid I, et al. Modified supine percutaneous nephrolithotomy for large kidney and ureteral stones: technique and results. Eur Urol. 2012;61:164-70.
5. Kumar P, Bach C, Kachrilas S, Papatsoris AG, Buchholz N, Masood J. Supine percutaneous nephrolithotomy (PCNL): 'in vogue' but in which position? BJU Int. 2012;110:E1018-21.
6. Batratanakij N, Liwrotsap C, Tangpaitoon T. A Comparison of postoperative urological infection rates between supine and prone positions during percutaneous nephrolithotomy. Urol Res Pract. 2025;51:22-6.
7. Li J, Gao L, Li Q, Zhang Y, Jiang Q. Supine versus prone position for percutaneous nephrolithotripsy: a meta-analysis of randomized controlled trials. Int J Surg. 2019;66:62-71.
8. Lachkar S, Boualaoui I, Ibrahimi A, El Sayegh H, Nouini Y. Supine or prone position in percutaneous nephrolithotomy: a systematic review and meta-analysis of 11,774 cases. Fr J Urol. 2025;35:102882.
9. Ahmed AF, Gomaa A, Daoud A, et al. Split-leg modified lateral versus prone position in percutaneous nephrolithotomy: a prospective, randomized trial. World J Urol. 2021;39:1247-1256.
10. Melo PAS, Vicentini FC, Perrella R, Murta CB, Claro JFA. Comparative study of percutaneous nephrolithotomy performed in the traditional prone position and in three different supine positions. Int Braz J Urol. 2019;45:108-17.
11. Miçooğulları U, Kamacı D, Yıldızhan M, et al. Prone versus Barts "flank-free" modified supine percutaneous nephrolithotomy: a match-pair analysis. Turk J Med Sci. 2021;51:1373-9.

12. Liu YY, Chen YT, Luo HL, et al. Totally x-ray-free ultrasound-guided mini-percutaneous nephrolithotomy in Galdakao-modified supine Valdivia position: a novel combined surgery. J Clin Med. 2022;11:6644.
13. Babaoff R, Creiderman G, Darawsha AE, Ehrlich Y, Somani B, Lifshitz DA. Propensity score-matched analysis of perioperative outcomes of supine versus prone percutaneous nephrolithotomy. J Clin Med. 2024;13:2492.
14. Kannan D, Quadri M, Sekaran PG, Paul R, Panneerselvam A, Jain N. Supine versus prone percutaneous nephrolithotomy (PCNL): a single surgeon's experience. Cureus. 2023;15:e41944.
15. Jones MN, Ranasinghe W, Cetti R, et al. Modified supine versus prone percutaneous nephrolithotomy: Surgical outcomes from a tertiary teaching hospital. Investig Clin Urol. 2016;57:268-73.
16. Pak Y, Kalyagina N, Yagudaev D. Percutaneous nephrolithotomy and laparoscopic surgery efficacy and renal function outcomes for large and complex renal calculi. Curr Urol. 2024;18:268-72.
17. Panthier F, Gauhar V, Ventimiglia E, Kwok JL, Keller EX, Traxer O. Rethinking stone-free rates and surgical outcomes in endourology: a point of view from PEARLS members. Eur Urol. 2024;86:198-9.
18. Desai M, De Lisa A, Turna B, et al. The clinical research office of the endourological society percutaneous nephrolithotomy global study: staghorn versus nonstaghorn stones. J Endourol. 2011;25:1263-8.
19. Abu-Ghanem Y, Forster L, Khetrapal P, et al. Factors predicting outcomes of supine percutaneous nephrolithotomy: large single-centre experience. J Pers Med. 2022;12:1956.
20. Atalay HA, Canat L, Bayraktarlı R, Alkan I, Can O, Altunrende F. Evaluation of stone volume distribution in renal collecting system as a predictor of stone-free rate after percutaneous nephrolithotomy: a retrospective single-center study. Urolithiasis. 2018;46:303-9.
21. el-Nahas AR, Eraky I, Shokeir AA, et al. Factors affecting stone-free rate and complications of percutaneous nephrolithotomy for treatment of staghorn stone. Urology. 2012;79:1236-41.
22. Kuroda S, Ito H, Sakamaki K, et al. Development and internal validation of a classification system for predicting success rates after endoscopic combined intrarenal surgery in the modified valdivia position for large renal stones. Urology. 2015;86:697-702.
23. Zanaty F, Mousa A, Elgharabawy M, Elshazly M, Sultan S. A prospective, randomized comparison of standard prone position versus flank-free modified supine position in percutaneous nephrolithotomy: a single-center initial experience. Urol Ann. 2022;14:172-6.
24. Radfar MH, Nasiri M, Shemshaki H, Sarhangnejad R, Dadpour M. A study on comparative outcomes of totally ultrasonography-guided percutaneous nephrolithotomy in prone versus flank position: a randomized clinical trial. World J Urol. 2021;39:4241-6.
25. Balaji S, Ganpule A, Herrmann T, Sabnis R, Desai M. Contemporary role of multi-tract percutaneous nephrolithotomy in the treatment of complex renal calculi. Asian J Urol. 2020;7:102-9.
26. Muntahi-Reza AF, Hossain AK, Karmaker U, et al. Comparative study of complications of single-tract versus multi-tract percutaneous nephrolithotomy using the modified clavien system. Mymensingh Med J. 2025;34:1207-15.
27. Kiss Z, Drabik G, Murányi M, Nagy A, Goumas IK, Flaskó T. Tubeless percutaneous nephrolithotomy in the barts 'flank-free' modified supine position with 24-hour discharge: a single-center experience. Medicina (Kaunas). 2025;61:748.
28. Curry D, Srinivasan R, Kucheria R, et al. Supine percutaneous nephrolithotomy in the galdako-modified valdivia position: a high-volume single center experience. J Endourol. 2017;31:1001-6.
29. Sener TE, Ozgur G, Cetin M, et al. Foley catheter after ureteroscopy and JJ stent placement: a randomised prospective European Association of Urology Section of Urolithiasis-Young Academic Urologists (EULIS-YAU) endourology study. BJU Int. 2025;135:95-102.

DOI: 10.4274/MMJ.galenos.2025.48830
Medeni Med J 2025;40:226-234

Original Article

Serum Interleukin-40 and Soluble CD40 Ligand as Complementary Biomarkers for Disease Activity in Multiple Sclerosis Patients

Multipl Skleroz Hastalarında Hastalık Aktivitesinin Tamamlayıcı Biyobelirteçleri Olarak Serum

Mustafa Ziyad NEAMAH[1], Inas K SHARQUIE[1], Gheyath AL GAWWAM[2]

[1]University of Baghdad College of Medicine Department of Microbiology and Immunology, Baghdad, Iraq
[2]University of Baghdad College of Medicine, Department of Medicine, Baghdad, Iraq

ABSTRACT

Objectives: Multiple sclerosis (MS) is a complex autoimmune disease of the central nervous system for which reliable biomarkers of disease activity remain an unmet need. Interleukin-40 (IL-40) and soluble CD40 ligand (sCD40L) have been proposed to play roles in the pathogenesis of autoimmune diseases. This study aimed to evaluate serum levels of IL-40 and sCD40L as biomarkers of disease activity in MS patients, and to compare their diagnostic and monitoring performance between MS patients and healthy controls.

Methods: One hundred twenty MS patients were recruited from the Department of MS at the Baghdad Teaching Hospital and divided into two groups based on disease status: active (n=60) and inactive (n=60). Additionally, 57 matched healthy individuals were included as controls. A sandwich enzyme-linked immunosorbent assay was used to measure the serum levels of IL-40 and sCD40L in blood samples from each participant.

Results: Both active and inactive patient cohorts showed significantly higher serum levels of IL-40 (44.25±8.57 ng/mL and 38.98±11.31 ng/mL, respectively) compared with their control group (20.82±14.27 ng/mL) (p=0.005). Likewise, sCD40L concentrations were elevated in both active (2155.59±587.02 pg/mL) and inactive (1885.23±851.32 pg/mL) patients compared with controls (849.79±341.87 pg/mL; p=0.0006). IL-40 correlated positively with sCD40L (r=0.399, p=0.005). The receiver operating characteristic analysis showed high diagnostic performance for IL-40 (area under the curve =0.873; sensitivity 87.5%; specificity 76.7%) and sCD40L (area under the curve =0.901; sensitivity 92.5%; specificity 81.7%).

Conclusions: Both IL-40 and sCD40L are significantly elevated in MS and exhibit promising diagnostic validity. These biomarkers may serve as complementary tools for monitoring MS disease activity and progression, offering potential value in clinical practice and therapeutic decision-making.

Keywords: Multiple sclerosis, interleukin-40, soluble CD40 ligand, biomarker, disease activity

ÖZ

Amaç: Multipl skleroz (MS), merkezi sinir sisteminin karmaşık bir otoimmün hastalığıdır ve hastalık aktivitesinin güvenilir biyobelirteçleri hala karşılanmamış bir ihtiyaçtır. Interlökin-40 (IL-40) ve çözünür CD40 ligandının (sCD40L) otoimmün hastalıkların patogenezinde rol oynadığı öne sürülmüştür. Bu çalışma, MS hastalarında hastalık aktivitesinin biyobelirteçleri olarak IL-40 ve sCD40L serum düzeylerini değerlendirmek ve MS hastaları ile sağlıklı kontrol grubu arasında bu belirteçlerin tanı ve izleme performansını karşılaştırmak amacıyla yapılmıştır.

Yöntemler: Bağdat Eğitim Hastanesi MS Bölümünden 120 MS hastası seçildi ve hastalık durumuna göre aktif (n=60) ve inaktif (n=60) olmak üzere iki gruba ayrıldı. Ayrıca, 57 eşleştirilmiş sağlıklı birey kontrol grubu olarak dahil edildi. Her katılımcının kan örneklerinde IL-40 ve sCD40L serum düzeylerini ölçmek için sandviç enzim bağlı immünosorbent testi kullanıldı.

Bulgular: Hem aktif hem de inaktif hasta kohortları, kontrol grubuna (20,82±14,27 ng/mL) kıyasla (p=0,005) anlamlı olarak daha yüksek IL-40 serum düzeyleri (sırasıyla 44,25±8,57 ng/mL ve 38,98±11,31 ng/mL) gösterdi. Benzer şekilde, sCD40L konsantrasyonları, aktif (2155,59±587,02 pg/mL) ve inaktif (1885,23±851,32 pg/mL) hastalarda kontrol grubuna (849,79±341,87 pg/mL; p=0,0006) kıyasla yükselmiştir. IL-40, sCD40L ile pozitif korelasyon gösterdi (r=0,399, p=0,005). Alıcı işletim karakteristiği analizi, IL-40 (eğri altındaki alan =0,873; duyarlılık %87,5; özgüllük %76,7) ve sCD40L (eğri altındaki alan =0,901; duyarlılık %92,5; özgüllük %81,7) için yüksek tanısal performans gösterdi.

Sonuçlar: Hem IL-40 hem de sCD40L, MS'te önemli ölçüde yükselmiştir ve umut verici tanısal geçerlilik sergilemektedir. Bu biyobelirteçler, MS hastalığının etkinliğini ve ilerlemesini izlemek için tamamlayıcı araçlar olarak hizmet edebilir ve klinik uygulamada ve tedavi kararlarında potansiyel değer sunabilir.

Anahtar kelimeler: Multipl skleroz, interlökin-40, Çözünür CD40 ligand, biyobelirteçler, hastalık etkinliği

Address for Correspondence: I.K.Sharquie, University of Baghdad College of Medicine Department of Microbiology and Immunology, Baghdad, Iraq
E-mail: iksharquie@yahoo.com, inasksharquie@comed.uobaghdad.edu.iq **ORCID ID:** orcid.org/0000-0002-4953-7365

Received: 22.09.2025
Accepted: 19.11.2025
Published: 31.12.2025

Cite as: Neamah MZ, Sharquie IK, Al Gawwam G. Serum interleukin-40 and soluble CD40 ligand as complementary biomarkers for disease activity in multiple sclerosis patients. Medeni Med J. 2025;40:226-234

INTRODUCTION

Multiple sclerosis (MS) is a chronic disorder of the central nervous system (CNS) that involves immune-mediated attack on CNS tissues, leading to inflammation, demyelination, and nerve damage[1,2]. The most common type is relapsing-remitting multiple sclerosis (RRMS), which affects both adults and children[3]. This form is characterized by periods of worsening neurological symptoms followed by partial or full recovery[1]. Since the disease can progress in variable and unpredictable ways, researchers are developing more accurate diagnostic and predictive tests for MS.

Research advances in the field of immunology have led to a significant reshaping of the understanding of the pathophysiology of MS[4], which is thought to encompass genetic susceptibility, environmental triggers, and dysregulation of immune responses leading to CNS tissue damage[5]. A central focus of research in this area has been the identification of biomarkers that aid in the diagnosis[6] and prognosis[7] of the disease, and that guide possible therapeutic approaches[8]. Neurofilament light chain (NfL) and glial fibrillary acidic protein (GFAP) have been linked to axonal injury[9] and astrocyte injury[10]. However, their ability to distinguish between the activity phases of MS is limited[11]. Cytokines and chemokines have been identified as potentially useful biomarkers for MS due to their roles in immune cell activation, trafficking, and communication[12]. Early studies have linked chemokine ligand 13, interleukin-6 [(IL)-6], and IL-17 to inflammation and disease progression[13], but their specificity in MS remains uncertain. Despite research into biomarkers for MS, including serum glutamate[14] and GFAP[15] as potential predictors of disease activity, there is a lack of consensus on any single biomarker with sufficient sensitivity and specificity to be used routinely in clinical practice to diagnose and monitor disease progression in patients with MS[16].

B cell biology is a pivotal component of the immunopathology of MS[17], and B cell-depleting therapies are therapeutically effective[18]. Advances in B cell research have led to studies on associated molecules, including IL-40, which is known to be involved in the maturation of B cells and in immune regulation[19, 20], and soluble CD40 ligand (sCD40L), which is a co-stimulatory molecule known to mediate crosstalk between T and B cells[21]. Research in these areas may increase understanding of inflammatory activity and immune dysregulation in MS. Evaluating IL-40 and sCD40L within the clinical context could therefore further elucidate biomarkers in MS and improve disease monitoring, risk stratification, and risk mitigation in MS patients.

IL-40 has been identified as a potential biomarker in autoimmune diseases, including rheumatoid arthritis[22] and systemic lupus erythematosus[23], suggesting a pro-inflammatory role for IL-40, given its association with increased disease activity. Elevated levels of sCD40L have been reported in inflammatory and autoimmune diseases[24] and correlate with immune activation and disease severity. In MS patients, the CD40-CD40L pathway has been reported to contribute to T-cell priming and the amplification of CNS-directed autoimmunity[25], suggesting that sCD40L is a potentially reliable marker of immune activation during MS relapses[26].

MS has long been considered primarily driven by T cells. However, recent advances in immunology and pathology have uncovered novel insights into the pathogenesis of MS, shedding light on the role of B cells. Given that IL-40 is mainly secreted by activated B cells and sCD40L is a co-stimulatory molecule that enhances B cell activation and antibody production, studying these markers may provide complementary insights into B cell-related immune dysregulation in MS and improve the accuracy of assessing disease activity.

To the best of our knowledge, this is the first study to simultaneously investigate IL-40 and sCD40L as complementary biomarkers for MS activity assessment. This study aims to examine the association between IL-40, sCD40L, and disease activity in MS patients. Evaluating these potential biomarkers could improve understanding of the immunopathology of MS and provide additional means to assess disease activity and progression, particularly in patients with atypical disease progression.

MATERIALS and METHODS

This cross-sectional study involved 177 participants (both males and females), aged 18-63 years, recruited from Baghdad Teaching Hospital between October 2024 and March 2025. In this cohort, 120 patients were diagnosed with MS according to the McDonald criteria 2017[27].

Patients were divided into two subgroups based on their disease activity according to No Evidence of Disease Activity-3 (NEDA-3) criteria (28): active (n=60) and inactive (n=60). The remaining 57 subjects constituted the control group of apparently healthy individuals age- and sex-matched to the study participants. All inactive MS patients were in remission period without any clinical relapses or new magnetic resonance imaging (MRI) lesions for at least 12 months.

Active MS patients (n=60) were defined according to NEDA-3 criteria as those showing at least one of the following: (a) clinical relapse confirmed by a neurologist, (b) new or enlarging T2 lesions on MRI, or (c) disability progression. Among active patients were newly diagnosed patients presenting with recent attacks and previously diagnosed patients who experienced relapses and/or MRI activity. Exclusion criteria included other autoimmune or inflammatory diseases, pregnancy or lactation, and lack of voluntary patient consent to participate in the study.

The demographic data for all participants and the clinical data for patients (last relapse, Expanded Disability Status Scale (EDSS), disease type, disease duration, and family history) were recorded. Written informed consent was obtained from all participants. The study was approved by the Scientific Committee of Ethics at the College of Medicine, University of Baghdad (approval number: 0254, date: 21.09.2025).

Body mass index (BMI) was recorded for all participants to evaluate any potential association between body composition and serum cytokine concentrations, given that adipose tissue is known to produce inflammatory mediators that may influence immune responses in autoimmune conditions.

A 5-mL venous blood sample was obtained from each participant. Serum was separated and stored at -20 °C until the time of analysis. Human sandwich IL-40 and sCD40L enzyme-linked immunosorbent assay (ELISA) kits were used according to the manufacturer's instructions. ELISA plates pre-coated with antibodies specific to either IL-40 or sCD40L were employed. Samples and standards were added to the predetermined wells and incubated for 80 minutes at 37 °C. Any unbound substances were removed by washing three times with an automatic plate washer. Biotinylated antibodies specific to either IL-40 or sCD40L were added and incubated for 50 minutes at 37 °C. After incubation and washing, streptavidin-HRP was added, and the mixture was incubated for 50 minutes at 37 °C. Plates were washed an additional five times before adding the tetramethylbenzidine substrate solution. The reaction was stopped by adding the stop solution, and the absorbance was measured at 450 nm using a microplate reader. All samples and standards were run in duplicate to ensure assay reliability. The ELISA kits (catalogue numbers ELK0969 for IL-40 and ELK9196 for sCD40L) were obtained from ELK Biotechnology (China).

Statistical Analysis

The Statistical Package for the Social Sciences (version 26, IBM, Armonk, NY, USA) was used for the statistical analysis. Microsoft Office Excel 2010 (Microsoft Corporation, Redmond, WA, USA) was used to produce all figures except for the receiver operating characteristic (ROC) curve.

Normality testing was performed before applying the parametric tests [analysis of variance (ANOVA) and t-test] using the Kolmogorov-Smirnov test. Normally distributed data are expressed as mean ± standard deviation (SD). Independent-samples Student's t-test, ANOVA, and least significant difference (S) tests were performed to compare quantitative variables among study groups (age, years), BMI, disease duration, EDSS, serum IL-40 (ng/mL), and sCD40L (pg/mL). The Pearson chi-square test (χ^2) was applied only to categorical variables such as sex, smoking status, MS type, and family history.

Test validity was estimated using ROC curve analysis, the cut-off value, the area under the curve (AUC), sensitivity (%), specificity (%), positive predictive value (PPV), negative predictive value (NPV), and accuracy. The statistical significance threshold (p-value) was defined as follows: $p>0.05$ for a non-S, $p<0.05$ for a S, and $p<0.01$ for a highly significant difference (HS).

RESULTS

Table 1 summarizes the demographic data. One hundred twenty patients with MS (active =60; inactive =60) were aged 18–63 years, and the mean age of active MS patients was slightly higher than that of inactive MS patients and controls. The remaining participants (n=57) were apparently healthy controls, aged 19-58 years (mean age 32.77±10.43 years). Across all cohorts studied, female participants outnumbered male participants [female MS group: n=78 (65%); female control group: n=34 (59.6%)]. Statistical analysis revealed no Ss in age (p=0.673) or sex (p=0.516) among the studied groups (i.e., the healthy controls were age- and sex-matched).

Age was categorized into four groups: 18-30, 31-40, 41-50, and 51-63 years. Nearly half of the patients (n=50, 41.6%) and more than one-third of the controls (n=21, 36.8%) were aged 18-30 years. Similar to age, the BMI was categorized as normal weight, overweight, or obese using the standard BMI classification (normal: 18.50-24.9, overweight: 25.0-29.9, obese: 6gt; ≥30). The frequencies of overweight among active MS patients (n=27, 45%) and healthy controls (n=25, 43.9%) were elevated. However, nearly half of the inactive patients (n=27, 45%) fall into the normal-weight category. No statistically S was observed (p=0.495). The mean BMI of active MS patients (27.05±4.64 kg/m^2), inactive MS patients (26.20±4.50 kg/m^2), and the control group (26.57±4.16 kg/m^2) did not differ significantly (p=0.575).

Table 1. Distribution of demographic and other data among study groups.

Parameters		Activity			p-value
		Control (C) n=57	Inactive (I) n=60	Active (A) n=60	
Smoking	Smokers	12 (21.1%)	13 (21.7%)	14 (23.3%)	p=0.911
	Non-smokers	45 (78.9%)	47 (78.3%)	46 (76.7%)	
Sex	Male	23 (40.4%)	20 (33.3%)	22 (36.7%)	p=0.516
	Female	34 (59.6%)	40 (66.7%)	38 (63.3%)	
Age groups /year	18-30	21 (36.8%)	27 (45%)	23 (38.3%)	p=0.673
	31-40	18 (31.6%)	19 (31.7%)	18 (30%)	
	41-50	14 (24.6%)	10 (16.7%)	17 (28.3%)	
	51-63	4 (7%)	4 (6.7%)	2 (3.3%)	
BMI Groups	Normal weight	21 (36.8%)	27 (45%)	19 (31.7%)	p=0.495
	Overweight	25 (43.9%)	23 (38.3%)	27 (45%)	
	Obese	11 (19.3%)	10 (16.7%)	14 (23.3%)	
Age / year	Mean	32.77	33.83	34.71	C-I- p=0.563
	Standard deviation	10.427	10.484	9.323	C-A - p=0.295
	Standard error	1.346	1.353	1.204	I-A - p=0.639
	ANOVA test (p-value): p=0.578				
BMI /kg/m^2	Mean	26.5667	26.2001	27.0517	C-I - p=0.651
	SD	4.15939	4.50326	4.63829	C-A - p=0.551
	Standard error	0.53698	0.58137	0.5988	I-A - p=0.296
	ANOVA test (p-value): p=0.575				

p>0.05: Non-significant difference, BMI:Body mass index, SD: Standard deviation, ANOVA: Analysis of variance.

Non-smokers predominated among active MS patients (n=46, 76.7%), inactive MS patients (n=47, 78.3%), and controls (n=45, 78.9%); no S was observed (p=0.911).

Table 2 presents the clinical data for MS patients. In the active group, 39 patients (65%) were newly diagnosed following recent relapses, while 21 patients (35%) had an MS diagnosis established at least 1 year ago and presented with either a relapse or MRI activity. None of the inactive patients were newly diagnosed; all had been diagnosed with MS for at least 1 year, and a HS was observed (p=0.004). The majority of patients (49 active and 52 inactive) were diagnosed with RRMS, followed by primary progressive multiple sclerosis (PPMS) and secondary progressive multiple sclerosis (SPMS); there was no statistically S between the active and inactive groups (p=0.253). A limited number of patients (5 active and 7 inactive) had a family history of MS, but this difference was not statistically significant (p=0.543).

There was a statistically S in disease duration (p=0.008), with inactive patients having longer disease duration than active patients.

Lastly, the mean EDSS scores of the two patient cohorts are similar, with no statistically observed (p=0.291).

Table 3 summarizes the mean serum biomarker levels across all study groups. Both active and inactive MS patients showed higher serum IL-40 concentrations than healthy controls, with a statistically S (p=0.005). The active group had slightly but statistically significantly higher serum concentrations of IL-40 than the inactive group (p=0.014).

Likewise, the mean serum concentrations of sCD40L of active MS patients were higher than inactive, and control groups (p=0.0006).

There was no S (p=0.236) in the serum levels of the study markers among the three types of MS (Table 4). Serum levels of IL-40 in patients diagnosed with SPMS are lower than those in patients diagnosed with RRMS and PPMS. Similarly, serum sCD40L levels in patients with SPMS are lower than those in patients with RRMS and PPMS (p=0.434).

In this study, the vast majority of patients were taking medications for MS. No Ss was observed in

Table 2. Clinical characteristics of MS patients according to disease activity.				
Parameters		**Activity**		**p-value**
		Inactive N=60	**Active N=60**	
Newly diagnosed	Yes	0 (0%)	39 (65%)	**p=0.004**
	No	60 (100%)	21 (35%)	
Family history	Yes	7 (11.7%)	5 (8.3%)	p=0.543
	No	53 (88.3%)	55 (91.7%)	
Type of MS	SPMS	3 (5%)	1 (1.7%)	p=0.253
	RRMS	52 (86.7%)	49 (81.7%)	
	PPMS	5 (8.3%)	10 (16.7%)	
Duration/ Year	Mean	7.6	3.57	**p=0.008**
	SD	4.85	4.82	
	Standard error	0.63	0.62	
EDSS	Mean	1.86	1.52	p=0.291
	Standard deviation	2.07	1.39	
	Standard error	0.27	0.18	

p>0.05: Non-significant difference, p<0.01: Highly significant difference, MS: Multiple sclerosis, EDSS: Expanded disability status scale, SD: Standard deviation, SPMS: Secondary progressive multiple sclerosis, RRMS: Relapsing-remitting multiple sclerosis, PPMS: Primary progressive multiple sclerosis, ANOVA: Analysis of variance.

Table 3.Mean distributions of serum IL-40 and sCD40L among study groups according to the activity of MS.						
Activity of MS		**Mean**	**Standard deviation**	**Standard error**	**p-value**	
IL-40 (ng/mL)	Control (C)	20.82	14.27	1.84	C-I	**p=0.003**
	Inactive (I)	38.98	11.31	1.46	C-A	**p=0.001**
	Active (A)	44.25	8.57	1.11	I-A	**p=0.014**
	ANOVA test (p-value): **p=0.005**					
sCD40L (pg/mL)	Control (C)	849.79	341.88	44.14	C-I	**p=0.005**
	Inactive (I)	1885.23	851.32	109.91	C-A	**p=0.0002**
	Active (A)	2155.59	587.02	75.78	I-A	**p=0.021**
	ANOVA test (p-value): **p=0.0006**					

p<0.05: Significant difference, p<0.01: Highly significant difference, MS: Multiple sclerosis, IL-40: Interleukin-40, sCD40L: Soluble cluster of differentiation 40 ligand, ANOVA: Analysis of variance.

serum levels of IL-40 and sCD40L in most comparisons between MS patients receiving treatment and those not receiving treatment; mean ± standard deviation values were similar. However, there are exceptions for those taking Natalizumab (p=0.044), Avonex (p=0.047), and Fingolimod (p=0.009). Correlation analyses of patient parameters also revealed a positive, statistically significant association between serum IL-40 and sCD40L levels in patients with MS (r=0.399, p=0.005). In contrast, all other correlations were weak, either positive or negative, and not statistically significant (p>0.05) (Table 5).

Sensitivity and Specificity Analysis

ROC curves show that IL-40 demonstrates good diagnostic validity at a cut-off value of 28.5 ng/mL, with an AUC of 0.873 [95% confidence interval (CI), 0.81-0.92] and high sensitivity (87.5%), specificity (76.7%), PPV (88.2%), NPV (75.4%), and accuracy (83.89%) (p=0.0005) (Figure 1).

Additionally, sCD40L demonstrated excellent validity for the diagnosis and follow-up of MS patients of, with an AUC of 0.901 (95% CI, 0.85-0.94), high sensitivity (92.5%), good specificity (81.7%), PPV (91%), NPV (84.5%), and accuracy (88.89%) (p<0.0002) (Figure 2).

Table 4. Mean distributions of serum IL-40 and sCD40L in MS patients according to the type of MS.						
Assays	**Type of MS**	**N**	**Mean**	**Standard deviation**	**Standard error**	**p-value**
IL-40 (ng/mL)	SPMS	4	32.1	6.94	3.47	p=0.236
	RRMS	101	41.86	10.62	1.06	
	PPMS	15	42.28	8.41	2.17	
	Total	120				
sCD40L (pg/mL)	SPMS	4	1753.13	935.58	467.79	p=0.434
	RRMS	101	2001.23	746.08	74.24	
	PPMS	15	2220.67	658.49	170.02	
	Total	120				

p>0.05: Non-significant difference, MS: Multiple sclerosis, IL-40: Interleukin-40, sCD40L: Soluble cluster of differentiation 40 ligand, SPMS: Secondary progressive multiple sclerosis, RRMS:Relapsing-remitting multiple sclerosis, PPMS: Primary progressive multiple sclerosis.

Table 5. Correlation study between the parameters of MS patients.			
Pearson Correlation (MS patients)		**IL-40 (ng/mL)**	**sCD40L (pg/mL)**
sCD40L (pg/mL)	r	0.399	
	p-value	0.005	
	Sign.	HS	
Age/year	r	0.031	0.146
	p-value	0.737	0.111
	Sign.	NS	NS
BMI (Kg/m^2)	r	-0.027	0.102
	p-value	0.772	0.266
	Sign.	NS	NS
Duration / Year	r	0.148	0.025
	p-value	0.107	0.785
	Sign.	NS	NS
EDSS	r	-0.026	0.051
	p-value	0.776	0.578
	Sign.	NS	NS

p>0.05: Non-significant difference (NS), p<0.01: Highly significant difference (HS), MS: Multiple sclerosis, IL-40: Interleukin 40, sCD40L: Soluble cluster of differentiation 40 ligand, BMI: Body mass index, EDSS: Expanded disability status scale, Sign: Significance, r:correlation coefficient.

DISCUSSION

This study has shown that both IL-40 and sCD40L are significantly elevated in patients with MS compared to healthy controls. Patients with active disease had particularly high concentrations of both IL-40 and sCD40L. These two biomarkers were positively correlated, with both showing robust diagnostic validity in ROC analyses, and with sensitivities and specificities comparable to those of established candidate biomarkers. This suggests that IL-40 and sCD40L could be useful biomarkers for the clinical evaluation of MS activity and disease progression.

The positive correlation observed between IL-40 and sCD40L in this study may reflect their complementary roles in immune regulation. IL-40 is known to be a B cell–associated cytokine involved in the production of immunoglobulins as well as the modulation of humoral responses. sCD40L is biologically active and can engage CD40 expressed on B cells. Their concurrent elevation in active MS suggests a possible contributing role in immune activation and subsequent disease activity[19,25].

Elevated serum concentrations of IL-40 may reflect enhanced B cell activation, whereas higher levels of sCD40L may indicate an ongoing T cell-mediated immune response. Therefore, their combined profiling could serve as a helpful tool for assessing disease progression risk and monitoring therapeutic response, specifically sCD40L, which has been reported to decrease after treatment[26,29,30]. However, further longitudinal studies are required to validate their predictive utility in clinical practice.

The results of this study are consistent with previous research implicating the CD40-CD40L axis in MS pathogenesis[25]. Elevated levels of sCD40L have been reported in SPMS and have been linked to immune activation through B cell and T cell interactions[31]. Studies in animal models of experimental autoimmune encephalomyelitis have shown that blocking the CD40-CD40L pathway leads to attenuation of CNS inflammation and demyelination[32], indicating the mechanistic relevance of this pathway to immune activation. The study adds to these observations by demonstrating that sCD40L levels are elevated in progressive MS and in actively relapsing patients, suggesting that they are a dynamic marker of immune activity.

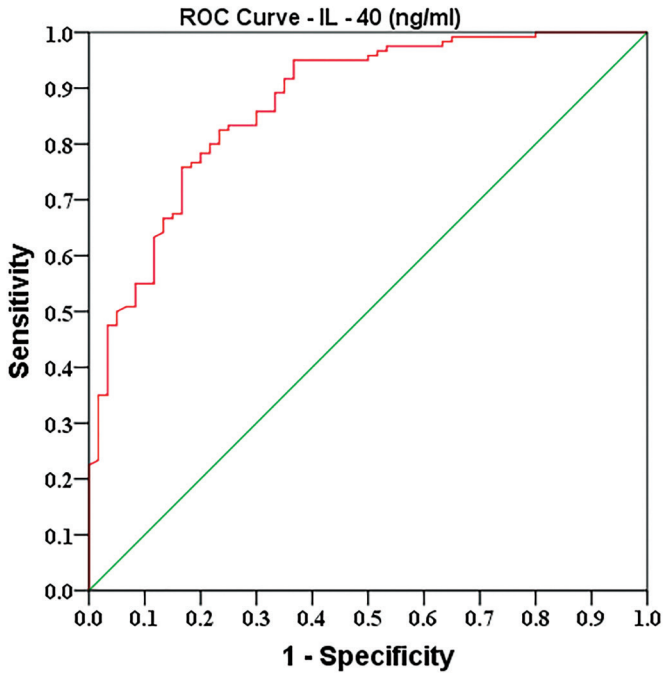

Figure 1. Validity tests of IL-40 by using ROC test in sera of MS patients and controls.

MS: Multiple, ROC: receiver operating characteristic, IL-40: Interleukin-40

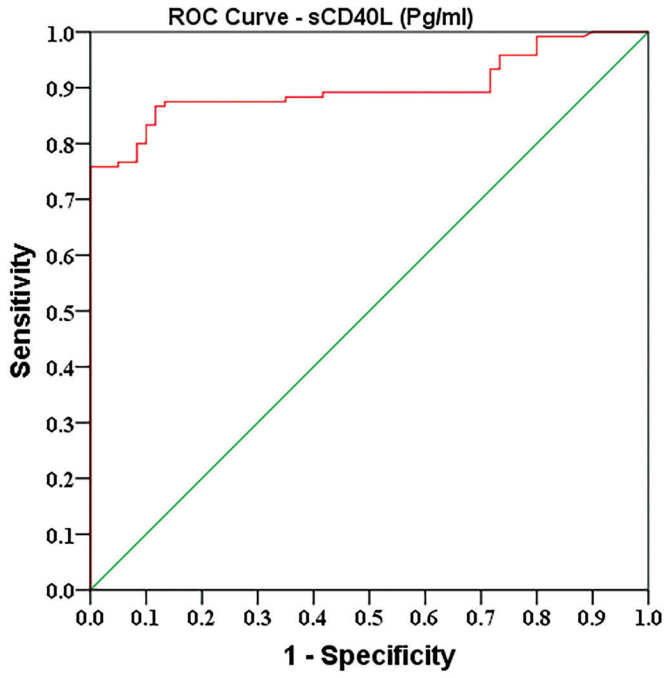

Figure 2. Validity tests of sCD40L by using ROC test in sera of MS patients and controls.

ROC: receiver operating characteristic, sCD40L: Soluble cluster of differentiation 40 ligand, MS: Multiple

IL-40 is a biomarker associated with immunoglobulin production and mucosal immunity through B cell homeostasis[33]. Subsequent research has reported elevated IL-40 levels in rheumatoid arthritis[34] and systemic lupus erythematosus[23], with IL-40 levels correlating with disease activity. The results of this study, showing higher IL-40 concentrations in active versus inactive MS patients, support the assertion that IL-40 may be an activity-related biomarker that complements markers of axonal damage, such as NfL.

The high sensitivity and specificity observed for IL-40 and sCD40L in distinguishing MS patients from healthy controls are clinically relevant findings. Currently, no single biomarker is recommended for the diagnosis of MS; diagnosis remains based on clinical and MRI-based assessments. Biomarkers with strong diagnostic validity could offer adjunctive value, especially in atypical presentations of MS or in settings where advanced neuroimaging is not widely available. Beyond diagnosis, the identified differential expression of IL-40 and sCD40L could signify impending relapses or subclinical inflammatory activity, thereby guiding decisions about therapeutic interventions and monitoring frequency for such patients.

The results from the subgroup analysis presented in this study suggest that disease-modifying therapies, such as Natalizumab, Avonex, and Fingolimod, can all influence biomarker levels. Notably, patients receiving Fingolimod exhibited reduced sCD40L levels, reinforcing its role as a modulator of lymphocyte trafficking[26]. This finding suggests that IL-40 and sCD40L could be useful in evaluating treatment response, allowing the stratification of patients who are likely to benefit from specific therapeutic approaches.

The novelty of this study lies in its combined evaluation of IL-40 and sCD40L; although both biomarkers have been investigated separately in the context of autoimmune diseases, limited research has examined their interplay in MS. The positive correlation between these two biomarkers observed in this study suggests that they may have a shared or complementary role in disease activity. This approach, using two biomarkers, may therefore be more beneficial than single biomarkers for understanding MS heterogeneity and disease progression.

The results of the present study can lay the foundation for future longitudinal research tracking IL-

40 and sCD40L concentrations in MS patients across different disease phases. Accordingly, researchers might determine whether changes in IL-40 and sCD40L levels precede relapses or the onset of new MRI-detected inflammation. This will reflect the interplay of B and T cells that perpetuates CNS inflammation[35,36]. Future studies combining cytokine-level measurements with brain imaging and treatment-response data could help clarify how IL-40 and sCD40L affect MS, thereby facilitating more personalized care.

Study Limitations

This study has several limitations. First, the study used a cross-sectional design and did not undertake longitudinal monitoring, which may have limited the study's ability to determine whether IL-40 and sCD40L levels fluctuate predictably prior to clinical relapses. Additionally, the potentially confounding effects of disease-modifying therapies on biomarker levels cannot be excluded in this study. Despite these limitations, our study provides important preliminary evidence supporting IL-40 and sCD40L as complementary biomarkers in MS, warranting validation in larger, longitudinal, and multi-center investigations.

CONCLUSION

The current study reports significantly elevated levels of IL-40 and sCD40L in MS patients compared with controls, indicating their potential utility as diagnostic biomarkers, and higher levels in patients with active MS than in those with inactive MS, indicating their potential utility in disease monitoring. Positive ROC results indicate promising clinical utility. However, multi-center and longitudinal studies are needed to validate these findings and to explore the predictive value of IL-40 and sCD40L for monitoring disease relapse and progression before integrating these biomarkers into multi-biomarker panels to deliver precision medicine to MS patients.

Ethics

Ethics Committee Approval: The study was approved by the Scientific Committee of Ethics at the College of Medicine, University of Baghdad (approval number: 0254, date: 21.09.2025).

Informed Consent: Written informed consent was obtained from all participants.

Footnotes

Author Contributions

Surgical and Medical Practices: G.A.G., Concept: M.Z.N., I.K.S., G.A.G., Design: M.Z.N., I.K.S., G.A.G., Data Collection and/or Processing: M.Z.N., G.A.G., Analysis or Interpretation: M.Z.N., I.K.S., G.A.G., Literature Search: M.Z.N., I.K.S., G.A.G., Writing: M.Z.N., I.K.S.,

Conflict of Interest: The authors have no conflict of interest to declare.

Financial Disclosure: The authors declared that this study has received no financial support.

References

1. Papiri G, D'Andreamatteo G, Cacchiò G, et al. Multiple sclerosis: inflammatory and neuroglial aspects. Curr Issues Mol Biol. 2023;45:1443-70.
2. Aljawadi ZA, Al-Derzi AR, Abdul-Majeed BA, Almahdawi AM. MicroRNAs (20a, 146a, 155, and 145) expressions in a sample of Iraqi patients with multiple sclerosis. J Fac Med Baghdad. 2016;58:371-7.
3. Saadi nw, Fahad QA. Paediatric multiple sclerosis: a case report of missed and dismissed diagnosis. J Fac Med Baghdad. 2021;63:36-9.
4. Afzali AM, Korn T. The role of the adaptive immune system in the initiation and persistence of multiple sclerosis. Semin Immunol. 2025;78:101947.
5. Rida Zainab S, Zeb Khan J, Khalid Tipu M, Jahan F, Irshad N. A review on multiple sclerosis: unravelling the complexities of pathogenesis, progression, mechanisms and therapeutic innovations. Neuroscience. 2025;567:133-49.
6. Paul A, Comabella M, Gandhi R. Biomarkers in multiple sclerosis. Cold Spring Harb Perspect Med. 2019;9:a029058.
7. Ciubotaru A, Smihor MI, Grosu C, et al. Neurodegenerative biomarkers in multiple sclerosis: at the interface between research and clinical practice. Diagnostics (Basel). 2025;15:1178.
8. Khan B, Sartaj R, Rahiyab M, et al. Systematic identification of molecular biomarkers and drug candidates targeting MAPK3 in multiple sclerosis. Hum Gene (Amst). 2025;45:201436.
9. Aburashed R, Eghzawi A, Long D, Pace R, Madha A, Cote J. Neurofilament light chain and multiple sclerosis: building a neurofoundational model ofbBiomarkers and diagnosis. Neurol Int. 2025;17:56.
10. Saraste M, Bezukladova S, Matilainen M, et al. Increased serum glial fibrillary acidic protein associates with microstructural white matter damage in multiple sclerosis: GFAP and DTI. Mult Scler Relat Disord. 2021;50:102810.
11. Fung WH, Wessels MHJ, Coerver EME, et al. Reliability of serum neurofilament light and glial fibrillary acidic protein for detecting disease activity upon discontinuation of first-line disease-modifying therapy in stable multiple sclerosis (DOT-MS). J Neurol. 2025;272:530.
12. Liu R, Du S, Zhao L, et al. Autoreactive lymphocytes in multiple sclerosis: pathogenesis and treatment target. Front Immunol. 2022;13:996469.
13. Fissolo N, Pappolla A, Rio J, et al. Serum levels of CXCL13 are associated with teriflunomide response in patients with multiple sclerosis. Neurol Neuroimmunol Neuroinflamm. 2022;10:e200050.
14. Al Gawwam G, Sharquie IK. Serum glutamate Is a predictor for the diagnosis of multiple sclerosis. ScientificWorldJournal. 2017;2017:9320802.

15. Sharquie IK, Gawwam GA, Abdullah SF. Serum glial fibrillary acidic protein: a surrogate marker of the activity of multiple sclerosis. Medeni Med J. 2020;35:212-8.
16. Maroto-García J, Martínez-Escribano A, Delgado-Gil V, et al. Biochemical biomarkers for multiple sclerosis. Clin Chim Acta. 2023;548:117471.
17. Gharibi T, Babaloo Z, Hosseini A, et al. The role of B cells in the immunopathogenesis of multiple sclerosis. Immunology. 2020;160:325-35.
18. Miyazaki Y, Niino M. B-cell depletion therapy for multiple sclerosis. Immunol Med. 2022;45:54-62.
19. Dabbagh-Gorjani F. A Comprehensive review on the role of interleukin-40 as a biomarker for diagnosing inflammatory diseases. Autoimmune Dis. 2024;2024:3968767.
20. Catalan-Dibene J, Vazquez MI, Luu VP, et al. Identification of IL-40, a Novel B Cell-Associated Cytokine. J Immunol. 2017;199:3326-35.
21. Mabrouk M, Wahnou H, Merhi Y, Abou-Saleh H, Guessous F, Zaid Y. The role of soluble CD40L in autoimmune diseases. J Transl Autoimmun. 2025;10:100288.
22. Ag Al Ghuraibawi Z, Sharquie IK, Gorial FI. Diagnostic potential of interleukin-40 (IL-40) in rheumatoid arthritis patients. Egypt Rheumatol. 2022;44:377-80.
23. Al Rubaye AM, Sharquie IK, Gorial FI. Serum interleukin 40: an innovative diagnostic biomarker for patients with systemic lupus erythematosus. Med J Malaysia. 2023;78:609-15.
24. Tian S, Wang Y, Wan J, Yang M, Fu Z. Co-stimulators CD40-CD40L, a potential immune-therapy target for atherosclerosis: A review. Medicine (Baltimore). 2024;103:e37718.
25. Aarts SABM, Seijkens TTP, van Dorst KJF, Dijkstra CD, Kooij G, Lutgens E. The CD40-CD40L Dyad in Experimental Autoimmune Encephalomyelitis and Multiple Sclerosis. Front Immunol. 2017;8:1791.
26. Wu Q, Wang Q, Yang J, et al. Elevated sCD40L in Secondary progressive multiple sclerosis in comparison to non-progressive benign and relapsing remitting multiple sclerosis. J Cent Nerv Syst Dis. 2021;13:11795735211050712.
27. Thompson AJ, Banwell BL, Barkhof F, et al. Diagnosis of multiple sclerosis: 2017 revisions of the McDonald criteria. Lancet Neurol. 2018;17:162-73.
28. Simonsen CS, Flemmen HØ, Broch L, et al. Rebaseline no evidence of disease activity (NEDA-3) as a predictor of long-term disease course in a Norwegian multiple sclerosis population. Front Neurol. 2022;13:1034056.
29. Pastor Bandeira I, de Almeida Franzoi AE, Murillo Wollmann G, et al. Interleukin-31 and soluble CD40L: new candidate serum biomarkers that predict therapeutic response in multiple sclerosis. Neurol Sci. 2022;43:6271-8.
30. Vermersch P, Granziera C, Mao-Draayer Y, et al. Inhibition of CD40L with Frexalimab in Multiple Sclerosis. N Engl J Med. 2024;390:589-600.
31. Zhong X, Wang H, Ye Z, et al. Serum concentration of CD40L is elevated in inflammatory demyelinating diseases. J Neuroimmunol. 2016;299:66-9.
32. Zhong C, Chen Z, Xia Y, et al. Treatment of experimental autoimmune encephalomyelitis using AAV gene therapy by blocking T cell costimulatory pathways. Mol Ther Methods Clin Dev. 2022;25:461-75.
33. Navrátilová A, Oreská S, Wünsch H, et al. Serum IL-40 is elevated in systemic sclerosis and is linked to disease activity, gastrointestinal involvement, immune regulation and fibrotic processes. Arthritis Res Ther. 2025;27:119.
34. Navrátilová A, Andrés Cerezo L, Hulejová H, et al. IL-40: A New B Cell-Associated Cytokine Up-Regulated in Rheumatoid Arthritis Decreases Following the Rituximab Therapy and Correlates With Disease Activity, Autoantibodies, and NETosis. Front Immunol. 2021;12:745523.
35. Ots HD, Tracz JA, Vinokuroff KE, Musto AE. CD40-CD40L in Neurological Disease. Int J Mol Sci. 2022;23:4115.
36. Touil H, Li R, Zuroff L, et al. Cross-talk between B cells, microglia and macrophages, and implications to central nervous system compartmentalized inflammation and progressive multiple sclerosis. EBioMedicine. 2023;96:104789.

DOI: 10.4274/MMJ.galenos.2025.95690
Medeni Med J 2025;40:235-240

Original Article

Machine Learning-Based Analysis of Serum Interleukin-39 and Interleukin-40 Levels for Differentiating Rheumatoid Arthritis and Systemic Lupus Erythematosus

Romatoid Artrit ve Sistemik Lupus Eritematozusun Ayırt Edilmesi için Serum İnterlökin-39 ve İnterlökin-40 Düzeylerinin Makine Öğrenimi Temelli Analizi

Inas K. SHARQUIE[1], Faiq Isho GORIAL[2], Zahraa Adnan AL-GHURAIBAWI[3], Amal Mahdi AL RUBAYE[4]

[1]University of Baghdad Faculty of Medicine, Department of Microbiology and Immunology, Baghdad, Iraq
[2]University of Baghdad Faculty of Medicine, Department of Medicine, Baghdad, Iraq
[3]Iraqi National Cancer Research Center, University of Baghdad, Baghdad, Iraq
[4]Diyala Health Directorate, Baqubah General Hospital, Educational Laboratories, Baqubah, Iraq

ABSTRACT

Objective: Rheumatoid arthritis (RA) and systemic lupus erythematosus (SLE) are both severe autoimmune diseases characterised by immune dysregulation and systemic inflammation. Despite advances in diagnostic tools, distinguishing RA from SLE remains challenging due to overlapping clinical manifestations. Emerging evidence highlights the potential roles of novel cytokines, such as interleukin-39 [(IL)-39] and IL-40, in autoimmune pathogenesis. This study aimed to evaluate the diagnostic utility of serum levels of IL-39 and IL-40 for differentiating RA from SLE using several machine learning (ML) algorithms.

Methods: Data from 66 patients with RA and 66 patients with SLE were analysed using previously published serum IL-39 and IL-40 datasets. ML algorithms, namely logistic regression, random forest, decision tree, and support vector machine, were applied. Model performance was evaluated using sensitivity, accuracy, specificity, and area under the receiver operating characteristic curve.

Results: SLE patients exhibited significantly higher serum IL-39 and IL-40 levels than those of RA patients ($p<0.001$). The random forest model achieved an accuracy of 92.4% and an AUC of 0.95. Feature importance analysis revealed that IL-39 and IL-40 contributed 58% and 42%, respectively to the classification performance.

Conclusions: ML models based on IL-39 and IL-40 serum levels can effectively differentiate RA from SLE. The findings suggest that integrating artificial intelligence-based analytical approaches with novel cytokine biomarkers may enhance diagnostic precision and support differential diagnosis in autoimmune diseases.

Keywords: Rheumatoid arthritis, systemic lupus erythematosus, interleukin-39, interleukin-40, machine learning, biomarkers

ÖZ

Amaç: Romatoid artrit (RA) ve sistemik lupus eritematozus (SLE), bağışıklık düzensizliği ve sistemik enflamasyon ile karakterize edilen ciddi otoimmün hastalıklardır. Tanı araçlarındaki gelişmelere rağmen klinik belirtilerin birbiriyle örtüşmesi nedeniyle RA'yı SLE'den ayırt etmek hala zordur. Ortaya çıkan kanıtlar, interlökin-39 [(IL)-39] ve IL-40 gibi yeni sitokinlerin otoimmün patogenezdeki potansiyel rollerini vurgulamaktadır. Bu çalışma, çeşitli makine öğrenimi (ML) algoritmaları kullanarak RA ile SLE'yi ayırt etmek için serum IL-39 ve IL-40 düzeylerinin tanısal yararını değerlendirmeyi amaçlamıştır.

Yöntemler: RA'lı 66 hasta ve SLE'li 66 hastadan elde edilen veriler, daha önce yayınlanmış serum IL-39 ve IL-40 veri setleri kullanılarak analiz edilmiştir. Lojistik regresyon, rastgele orman, karar ağacı ve destek vektör makinesi gibi ML algoritmaları uygulandı. Model performansı, duyarlılık, doğruluk, özgüllük ve alıcı işletim karakteristik eğrisi altındaki alan kullanılarak değerlendirildi.

Bulgular: SLE hastaları, RA hastalarına göre anlamlı olarak daha yüksek serum IL-39 ve IL-40 düzeyleri sergiledi ($p<0,001$). Rastgele orman modeli %92,4 doğruluk ve 0,95 AUC elde etti. Özellik önem analizi, IL-39 ve IL-40'ın sınıflandırma performansına sırasıyla %58 ve %42 katkıda bulunduğunu ortaya koydu.

Sonuçlar: IL-39 ve IL-40 serum düzeylerine dayalı ML modelleri, RA'yı SLE'den etkili bir şekilde ayırt edebilir. Bulgular, yapay zeka tabanlı analitik yaklaşımların yeni sitokin biyobelirteçleriyle entegre edilmesinin, otoimmün hastalıklarda tanı doğruluğunu artırabileceğini ve ayırıcı tanıyı destekleyebileceğini göstermektedir.

Anahtar kelimeler: Romatoid artrit, sistemik lupus eritematozus, interlökin-39, interlökin-40, makine öğrenimi, biyobelirteçler

Address for Correspondence: I.K. Sharquie, University of Baghdad Faculty of Medicine, Department of Microbiology and Immunology, Baghdad, Iraq
E-mail: iksharquie@yahoo.com **ORCID ID:** orcid.org/0000-0002-4953-7365

Received: 25.07.2025
Accepted: 19.11.2025
Published: 31.12.2025

Cite as: Sharquie IK, Gorial FI, Al-Ghuraibawi ZA, Al Rubaye AM. Machine learning-based analysis of serum interleukin-39 and interleukin-40 levels for differentiating rheumatoid arthritis and systemic lupus erythematosus. Medeni Med J. 2025;40:235-240

INTRODUCTION

Autoimmune diseases, dysregulated immune responses directed against self-antigens, can lead to chronic inflammation and tissue damage. Two prevalent and commonly studied autoimmune diseases are rheumatoid arthritis (RA) and systemic lupus erythematosus (SLE). RA predominantly affects synovial joints, leading to progressive joint destruction. By contrast, SLE is a systemic disease that affects multiple organs, including the skin, kidneys, lungs, and central nervous system[1]. Despite distinct pathological mechanisms, RA and SLE frequently present with overlapping clinical features—including joint pain, fatigue, and systemic inflammation—especially in early stages[2]. Being able to distinguish between RA and SLE is crucial, as therapeutic approaches and prognoses can vary significantly. Although traditional diagnostic biomarkers are reported to have limitations in sensitivity and specificity[3,4], they remain valuable in clinical settings. Commonly tested biomarkers include rheumatoid factor, antinuclear antibodies, anti-cyclic citrullinated peptide antibodies, and anti-double-stranded DNA antibodies.

Recent advances in immunology have identified several novel cytokines linked to autoimmune diseases[5,6]. Notably, interleukin-39 [(IL)-39] and (IL-40) are promising biomarkers. IL-39, a heterodimer composed of the IL-23p19 and *Epstein-Barr virus-induced gene 3* subunits, promotes neutrophil activation and production of inflammatory cytokines, particularly in lupus models[7]. IL-40, primarily secreted by activated B cells, helps regulate immunoglobulin production; its levels are markedly elevated in individuals with RA and SLE[8-10]. Alongside advances in biomarker discovery, artificial intelligence (AI) and machine learning (ML) have revolutionised data analysis, particularly in medical research. ML algorithms can effectively process large, complex datasets and identify patterns that may be overlooked by conventional statistical methods[11]. The use of AI in rheumatology is growing exponentially, with ML models used for classifying diseases, informing prognoses, and predicting therapeutic responses[12]. However, few studies have used multiple cytokines to train ML models to diagnose RA and SLE. Combining biomarker profiling with the power of AI may enhance the accuracy and reliability of current diagnostic approaches.

Given the urgent need for improved diagnostic accuracy in autoimmune diseases and increasing reports about the likelihood that IL-39 and IL-40 are suitable biomarkers for RA and SLE, this study investigated the combined diagnostic utility of IL-39 and IL-40 using an ML approach. We applied a random forest classifier to distinguish RA from SLE based on patients' serum levels of IL-39 and IL-40. We hypothesised that this integrated approach would enable enhanced diagnostic performance compared with conventional biomarker analysis, inform therapeutic choices, and ultimately improve patient outcomes.

MATERIALS and METHODS

Study Design and Participants

This retrospective analytical study utilised previously collected serum cytokine data from 132 patients: 66 with RA and 66 with SLE. Patient data were initially collected at the Rheumatology Unit, Baghdad Teaching Hospital, University of Baghdad. All patients diagnosed with RA met the 2010 American College of Rheumatology/European League Against Rheumatism (ACR/EULAR) classification criteria[13], whereas patients diagnosed with SLE fulfilled the 2019 EULAR/ACR classification criteria[14].

Sample Collection and Cytokine Measurement

No new biological samples were collected for the present study, as our previously published data sets of serum levels of IL-39 and IL-40 were used[9,10,15,16]. Following standardised protocols, cytokine levels were measured using enzyme-linked immunosorbent assay kits (SunLong Biotech Co., Ltd, China). The present work reanalyses these validated cytokine datasets using ML models.

Data Preprocessing

The analysed dataset included two input features per patient: serum IL-39 concentration (pg/mL) and serum IL-40 concentration (pg/mL). The target variable was the diagnostic group (RA or SLE). All datasets were complete with no missing values.

ML Model Development

Supervised ML models were developed using the following algorithms: decision tree classifier, logistic regression, random forest classifier, and support vector machine (SVM). Data were randomly split into a training set (comprising 70% of the data) and a testing set (the remaining 30%). Model hyperparameters were optimised using grid search with five-fold cross-validation. Model performance was assessed using accuracy (overall proportion of correctly classified cases), sensitivity (true positive rate), specificity (true negative rate), and the area under the receiver operating characteristic (ROC) area under the curve (AUC).

Ethical Considerations

The original data collection procedures were approved by the Scientific Ethical Committee of the College of Medicine, University of Baghdad. Informed consent was obtained from all patients at the time of the original studies with ethical approval no.: 0252, date: 29.07.2025.

Statistical Analysis

Continuous variables (the IL-39 and IL-40 levels) were expressed as mean ± SD. Independent samples t-tests were used to compare biomarker levels between RA and SLE groups. ROC curve analysis was performed to assess model discrimination.

All analyses and ML modelling were conducted using Python version 3.9, the Scikit-learn library version 1.0.2, and SPSS version 25. The random forest classifier demonstrated the best performance and was selected for further analysis of the ROC curve and the confusion matrix. AUC values were interpreted according to the following standard: an AUC >0.9 was considered excellent, 0.8-0.9 was considered good, 0.7-0.8 was considered fair, and <0.7 was considered poor discrimination. A two-tailed p-value <0.05 was considered statistically significant.

RESULTS

Demographic Characteristics

The demographic characteristics of the patients are summarised in Table 1. There were no statistically significant differences between RA and SLE patients regarding age, sex, or disease duration (p>0.05). Since there were no significant demographic differences between the two groups, potential confounding effects were deemed to be minimal.

Serum IL-39 and IL-40 Levels

The serum concentrations of IL-39 and IL-40 differed significantly between patients with RA and SLE (both p<0.001), as shown in Table 2; SLE patients had significantly higher concentrations of IL-39 and IL-40 than RA patients, suggesting that these cytokines may play a role in SLE pathogenesis.

ML Model Performance

The application of ML algorithms revealed strong discriminatory power to distinguish RA from SLE using only serum IL-39 and IL-40. Among the tested models, the random forest classifier achieved the highest diagnostic accuracy and area under the ROC curve, indicating its potential as a reliable AI-based diagnostic tool. These findings emphasize the clinical utility of ML systems in differentiating autoimmune diseases with overlapping manifestations, such as RA and SLE.

The performance of four ML models—logistic regression, decision tree, random forest, and SVM—is summarised in Table 3. The random forest classifier outperformed other models, confirming its robustness and high discriminative capacity when integrating IL-39 and IL-40 levels.

Table 1. Demographic characteristics of the study population.

Variable	RA patients (n=66)	SLE patients (n=66)	p-value
Age (years, mean ± SD)	45.8±12.4	44.6±11.7	0.38
Female sex (n)	54	58	0.45
Disease duration (years)	6.8±3.1	6.1±2.9	0.27

SD: Standard deviation, RA: Rheumatoid arthritis, SLE: Systemic lupus erythematosus

Table 2. Serum IL-39 and IL-40 levels in RA and SLE patients.

Cytokine	RA patients (Mean ± SD)	SLE patients (Mean ± SD)	p-value
IL-39 (pg/mL)	4.95±1.10	13.70±0.35	<0.001
IL-40 (pg/mL)	9.1±1.3	12.54±3.006	<0.001

RA: Rheumatoid arthritis, SLE: Systemic lupus erythematosus, IL: Interleukin, SD: Standard deviation

Table 3. Performance metrics of machine learning models for classifying RA and SLE.

Model	Accuracy (%)	Sensitivity (%)	Specificity (%)	AUC
Logistic regression	81.8	80	83	0.87
Decision tree	79.5	77	82	0.84
Random forest	92.4	93.9	91.0	0.95
Support vector machine	85.6	84	87	0.89

RA: Rheumatoid arthritis, SLE: Systemic lupus erythematosus, AUC: Area under the curve

ROC Curve Analysis

An overview of the ROC curve analysis for the random forest model is shown in Table 4. The model demonstrated very high accuracy in classifying RA versus SLE.

Confusion Matrix Analysis

The confusion matrix results for the random forest model are presented in Table 5. The model demonstrated excellent classification performance with minimal misclassification.

Feature Importance Analysis

Feature importance scores derived from the random forest model are shown in Table 6. IL-39 contributed more to model prediction than IL-40.

Overall, these results highlight that integrating ML techniques with novel cytokine biomarkers such as IL-39 and IL-40 can enhance diagnostic precision in complex autoimmune disorders.

Table 4. Receiver operating characteristic (ROC) parameters for the random forest classifier.

Parameter	Value
Area under curve	0.95
95% confidence interval	0.91-0.97
Optimal diagnostic threshold	0.50 (SLE >0.50; RA ≤0.50

SLE: Systemic lupus erythematosus

Table 5. Confusion matrix for random forest model.

	Predicted RA	Predicted SLE
Actual RA	61	5
Actual SLE	2	64

RA: Rheumatoid arthritis, SLE: Systemic lupus erythematosus

Table 6. Feature importance score derived from the random forest model.

Feature	Importance (%)
IL-39	58%
IL-40	42%

This table presents the percentage contribution of IL-39 and IL-40 in differentiating RA and SLE using the random forest classifier.

RA: Rheumatoid arthritis, SLE: Systemic lupus erythematosus, IL: Interleukin

DISCUSSION

Using ML models, this study investigated the potential of serum IL-39 and IL-40 levels to differentiate between cases of RA and SLE. The findings demonstrated that both cytokines are valuable biomarkers and that assessing their serum levels enables accurate distinction between these diseases. Among the models evaluated—logistic regression, decision tree, random forest, and SVM—the random forest classifiers consistently outperformed the others across all metrics. Its superior performance highlights the strength of the ensemble learning strategy, which aggregates multiple decision trees to reduce overfitting and improve generalisation.

The significantly higher IL-39 levels observed in SLE patients than in RA patients are consistent with findings reported by Wang et al.[17], who described the pro-inflammatory role of IL-39 in neutrophil activation and systemic immune responses in lupus models. The authors suggested that IL-39 contributes significantly to the pathogenesis of SLE. Similarly, Lv et al.[18] demonstrated that IL-39 increased disease severity in murine models of experimental lupus, further supporting its relevance in human SLE pathophysiology. However, relatively low IL-39 levels in the data from patients with RA assessed in this study show that RA pathogenesis is predominantly T-cell-driven rather than neutrophil-based mechanisms.

Although IL-40 levels were high in both RA and SLE patients, they were slightly higher in the SLE group. This observation is consistent with prior research indicating that IL-40 is produced by activated B cells and contributes to local inflammation and immunoglobulin regulation. Navrátilová et al.[19] found that IL-40 plays a significant role in humoral immunity, particularly in autoimmune conditions. Moreover, IL-40 levels have previously been linked to markers of disease activity in autoimmune diseases, highlighting its broad relevance[8]. Higher IL-40 levels identified in this study among cases of SLE may reflect the intense B cell hyperactivity and extensive autoantibody production typically seen in SLE. Feature importance analysis further reinforced these biological roles, revealing that IL-39 and IL-40 contributed 58% and 42%, respectively to model predictions. The significantly higher levels of IL-39 observed in patients with SLE, which are also elevated in RA, reflect B cell hyperactivity and intense autoantibody production.

Among the ML models evaluated in this study—logistic regression, decision tree, random forest, and SVM—all demonstrated reasonable performance. However, the random forest classifier consistently outperformed the others across all evaluated metrics. The ensemble learning strategy, a crucial component of the random forest approach, aggregates multiple decision trees to reduce overfitting and improve generalisation[20], and likely contributes to its superior performance. This finding aligns with the growing body of literature supporting the application of ML methods, particularly ensemble techniques, in biomedical classification tasks[20,21]. Moreover, our results are consistent with the work of Shi et al.[22], who emphasised the significant role of ML models in enhancing diagnostic accuracy, disease classification, and management of autoimmune diseases—particularly RA. Their study demonstrated that ensemble methods, such as random forests, can effectively identify complex disease patterns and improve clinical decision-making. The strong performance of the random forest model in our study of IL-39 and IL-40 levels, even when limited to these two biomarkers, underscores the power of ML to extract meaningful diagnostic insights from minimal but highly informative data.

Strengths of this study include the novel combination of IL-39 and IL-40 in an AI-driven diagnostic model, robust cross-validation methods, and consistent performance across multiple ML algorithms. The ability to achieve high diagnostic accuracy with such a limited biomarker set is particularly promising and highlights the potential for simplifying future diagnostic workflows. Additionally, using multiple ML approaches, cross-validation, and performance comparisons enhances the robustness of the findings. Despite the promising results, some limitations must be acknowledged. First, the data used in this study were reconstructed from published mean ± SD values rather than from individual patient measurements. Although the simulated datasets approximate real-world distributions, they may not capture the full variability seen in clinical practice. Second, only two biomarkers (IL-39 and IL-40) were analysed. Although these markers demonstrated significant diagnostic utility, evaluating additional cytokines, genetic markers, and clinical features may improve model performance and increase generalisability. Third, external validation on prospective, multicentre datasets remains necessary to confirm the reproducibility of our findings.

Future research should prioritise prospective, large-scale, real-world clinical data collection across diverse patient populations. Additionally, integrating multi-omics data (e.g., transcriptomic, proteomic, and metabolomic profiles) with ML frameworks could further enhance diagnostic precision. Exploring more advanced deep-learning models may also uncover complex patterns not captured by traditional ensemble approaches. Finally, longitudinal studies evaluating the prognostic value of IL-39 and IL-40 in relation to disease activity, treatment response, and long-term outcomes would also advance this field.

Study Limitations

The present study addresses only two biomarkers, IL-39 and IL-40, and does not include additional clinical, serological, and imaging parameters that may enhance diagnostic accuracy. Furthermore, the lack of external validation using independent or multicenter datasets limits the generalisability of the findings across broader patient populations. The retrospective nature of the analysis also restricts the ability to draw causal inferences. Future research should focus on these aspects by integrating diverse biomarkers and prospective designs, and validating findings across different clinical settings.

CONCLUSION

This study demonstrates that using a random forest ML model to combine serum IL-39 and IL-40 levels achieves high accuracy in distinguishing patients with RA from those with SLE. Our results highlight that integrating novel cytokine biomarkers with AI-based approaches holds significant promise for advancing precision diagnostics in autoimmune diseases, leading to improvements in clinical decision-making and patient outcomes.

Ethics

Ethics Committee Approval: The original data collection procedures were approved by the Scientific Ethical Committee of the College of Medicine, University of Baghdad. Informed consent was obtained from all patients at the time of the original studies with ethical approval no.:0252, date: 29.07.2025.

Informed Consent: This is a retrospective study.

Footnotes

Author Contributions

Surgical and Medical Practices: F.I.G., Concept: I.K.S., F.I.G., Design: I.K.S., F.I.G., Data Collection and/or Processing: I.K.S., Z.A.A.G., A.M.AR., Analysis or Interpretation: I.K.S., F.I.G., Literature Search: I.K.S., Z.A.A.G., A.M.AR., Writing: I.K.S., F.I.G., Z.A.A.G., A.M.AR.

Conflict of Interest: The authors have no conflict of interest to declare.

Financial Disclosure: The authors declared that this study has received no financial support.

REFERENCES

1. Firestein GS, McInnes IB. Immunopathogenesis of rheumatoid arthritis. Immunity. 2017;46:183-96.
2. Tsokos GC. Systemic lupus erythematosus. N Engl J Med. 2011;365:2110-21.
3. van Boekel MA, Vossenaar ER, van den Hoogen FH, van Venrooij WJ. Autoantibody systems in rheumatoid arthritis: specificity, sensitivity and diagnostic value. Arthritis Res. 2002;4:87-93.
4. Pisetsky DS. Antinuclear antibodies in rheumatic disease: a proposal for a function-based classification. Scand J Immunol. 2012;76:223-8.
5. Chasov V, Zmievskaya E, Ganeeva I, et al. Immunotherapy strategy for systemic autoimmune diseases: betting on CAR-T cells and antibodies. Antibodies (Basel). 2024;13:10.
6. Ugolkov Y, Nikitich A, Leon C, et al. Mathematical modeling in autoimmune diseases: from theory to clinical application. Front Immunol. 2024;15:1371620.
7. Wang X, Wei Y, Xiao H, et al. A novel IL-23p19/Ebi3 (IL-39) cytokine mediates inflammation in lupus-like mice. Eur J Immunol. 2016;46:1343-50.
8. Dabbagh-Gorjani F. A comprehensive review on the role of interleukin-40 as a biomarker for diagnosing inflammatory diseases. Autoimmune Dis. 2024;2024:3968767.
9. Ag Al Ghuraibawi Z, Sharquie IK, Gorial FI. Diagnostic potential of interleukin-40 (IL-40) in rheumatoid arthritis patients. The Egyptian Rheumatologist. 2022;44:377-80.
10. Al Rubaye AM, Sharquie IK, Gorial FI. Serum interleukin 40: an innovative diagnostic biomarker for patients with systemic lupus erythematosus. Med J Malaysia. 2023;78:609-15.
11. Al-Qudimat AR, Fares ZE, Elaarag M, Osman M, Al-Zoubi RM, Aboumarzouk OM. Advancing medical research through artificial intelligence: progressive and transformative strategies: a literature review. Health Sci Rep. 2025;8:e70200.
12. Yang Y, Liu Y, Chen Y, Luo D, Xu K, Zhang L. Artificial intelligence for predicting treatment responses in autoimmune rheumatic diseases: advancements, challenges, and future perspectives. Front Immunol. 2024;15:1477130.
13. Aletaha D, Neogi T, Silman AJ, et al. 2010 Rheumatoid arthritis classification criteria: an American College of Rheumatology/ European League Against Rheumatism collaborative initiative. Arthritis Rheum. 2010;62:2569-81.
14. Aringer M, Costenbader K, Daikh D, et al. 2019 European League Against Rheumatism/American College of Rheumatology Classification Criteria for Systemic Lupus Erythematosus. Arthritis Rheumatol. 2019;71:1400-12.
15. Al Ghuraibawi ZAG, Sharquie IK, Gorial FI. A novel link of serum IL-39 levels in patients with rheumatoid arthritis. Iraqi Journal of Science. 2023:1651-6.
16. Al Rubaye AM, Sharquie IK, Gorial FI. Novel insights into the role of serum interleukin-39 in patients with systemic lupus erythematosus. Iraqi Journal of Science. 2024;65:5518-31.
17. Wang T, Kuley R, Hermanson P, et al. Immune complexes-mediated activation of neutrophils in systemic lupus erythematosus is dependent on RNA recognition by toll-like receptor 8. Front Immunol. 2024;15:1515469.
18. Lv K, Hu B, Xu M, et al. IL-39 promotes chronic graft-versus-host disease by increasing T and B Cell pathogenicity. Exp Hematol Oncol. 2022;11:34.
19. Navrátilová A, Andrés Cerezo L, Hulejová H, et al. IL-40: a new B cell-associated cytokine up-regulated in rheumatoid arthritis decreases following the rituximab therapy and correlates with disease activity, autoantibodies, and NETosis. Front Immunol. 2021;12:745523.
20. Breiman L. Random forests. Machine Learning. 2001;45:5-32.
21. LeCun Y, Bengio Y, Hinton G. Deep learning. Nature. 2015;521:436-44.
22. Shi Y, Zhou M, Chang C, et al. Advancing precision rheumatology: applications of machine learning for rheumatoid arthritis management. Front Immunol. 2024;15:1409555.

DOI: 10.4274/MMJ.galenos.2025.47041
Medeni Med J 2025;40:241-249

Original Article

Evaluation of the Combined Effects of Rosmarinic Acid and Cisplatin in Gastric Cancer Cells

Mide Kanseri Hücrelerinde Rosmarinik Asit ve Sisplatinin Kombine Etkilerinin Değerlendirilmesi

Ceren SARI[1], Ceren SUMER[1], Saniye KOC ADA[2], Burcu YUCEL[3]

[1]Türkiye Cancer Institute, Health Institutes of Türkiye, Ankara, Türkiye
[2]Istanbul Medeniyet University Faculty of Medicine, Department of Medical Biochemistry, Istanbul,Türkiye
[3]Istanbul Medeniyet University Faculty of Medicine, Department of Medical Biology, Istanbul, Türkiye

ABSTRACT

Objective: Gastric cancer remains a significant global health concern, necessitating investigation into more effective treatment approaches. This study investigates the combined effects of rosmarinic acid, a polyphenolic compound with known anticancer properties, and cisplatin, a conventional chemotherapeutic agent, on human gastric carcinoma (HGC-27) cells.

Methods: Cell viability was evaluated at different concentrations for rosmarinic acid and cisplatin, and inhibitory concentration (IC)50, IC30, and IC10 values were subsequently determined. IC30 and IC10 doses were selected for combination experiments. Thiazolyl Blue Tetrazolium Bromide assay, colony formation assay, *in vitro* scratch assay, and 3D tumor spheroid growth assay were performed to evaluate the effects of individual and combined treatments.

Results: Rosmarinic acid and cisplatin individually reduced cell viability in a dose-dependent manner. Both the IC10 and IC30 dose combinations of the two agents demonstrated significant inhibitory effects on colony formation and cell motility, indicating an additive interaction compared with the control and the individual treatments. The combined treatment also inhibited spheroid growth, although the extent of the reduction was similar to that observed with the individual agents.

Conclusions: This study provides initial insights into the potential efficacy of the rosmarinic acid-cisplatin combination. The combination of these agents reduced cell viability, colony formation, and cell motility. The increased cytotoxicity observed in 2D models was not evident in 3D spheroid models, highlighting the importance of 3D systems that more accurately mimic the complex structure of tumors. This finding suggests that differences in drug sensitivity between 2D and 3D models should be considered when evaluating combination therapies.

Keywords: Cisplatin, drug combinations, multicellular spheroid, rosmarinic acid, stomach neoplasms

ÖZ

Amaç: Mide kanseri, dünya çapında önemli bir sağlık sorunu olmaya devam etmektedir ve bu durum daha etkili tedavi yaklaşımlarına olan ihtiyacı artırmaktadır. Bu çalışmada, bilinen anti-kanser özelliklere sahip polifenolik bir bileşik olan rosmarinik asit ile geleneksel bir kemoterapötik ajan olan sisplatinin insan mide kanseri (HGC-27) hücreleri üzerindeki kombine etkileri araştırılmıştır.

Yöntemler: Hücre canlılığı, her iki ajanın farklı konsantrasyonları için değerlendirildi ve inhibitör konsantrasyon (IC)50, IC30 ve IC10 değerleri belirlendi. Kombinasyon deneylerinde IC30 ve IC10 dozları kullanıldı. Tekli ve kombine tedavilerin etkilerini değerlendirmek için Thiazolyl Blue Tetrazolium Bromide, koloni oluşumu, *in vitro* çizik deneyi ve 3D tümör sferoid büyüme deneyleri gerçekleştirildi.

Bulgular: Rosmarinik asit ve sisplatin, tekli kullanımlarında hücre canlılığını doza bağlı olarak azalttı. Her iki ajanın IC10 dozlarının ve IC30 dozlarının kombinasyonu, koloni oluşumu ve hücre hareketliliği üzerinde önemli bir inhibitör etki göstererek, kontrol grubu ve tekli ajan uygulamalarına kıyasla ek bir etkileşim olduğunu düşündürdü. Kombine uygulama sferoid oluşumunu da etkiledi, ancak bu etki tekli ajan uygulanan gruplardaki etkiyle benzerlik gösterdi.

Sonuçlar: Bu çalışma, rosmarinik asit ve sisplatin kombinasyonunun potansiyel etkisine yönelik ön bulgular sunmaktadır. Bu ajanların kombinasyonu, hücre canlılığını, koloni oluşumunu ve hücre hareketliliğini sınırlamıştır. 3D sferoid modellerde, 2D modellerde gözlenen artmış sitotoksik etkinin ortaya çıkmaması, tümörlerin karmaşık yapısını daha iyi taklit eden 3D sistemlerin önemini vurgulamaktadır. Bu sonuç, kombinasyon tedavilerinin değerlendirilmesinde 2D ve 3D modeller arasındaki ilaç duyarlılığı farklarının dikkate alınması gerektiğini göstermektedir.

Anahtar kelimeler: Sisplatin, ilaç kombinasyonları, multiselüler sferoid, rosmarinik asit, mide neoplazmaları

Address for Correspondence: B. Yucel, Istanbul Medeniyet University Faculty of Medicine, Department of Medical Biology, Istanbul, Türkiye
E-mail: burcu_yucel@msn.com **ORCID ID:** orcid.org/0000-0002-6599-4558

Received: 09.08.2025
Accepted: 24.11.2025
Published: 31.12.2025

Cite as: Sarı C, Sumer C, Koc Ada S, Yucel B. Evaluation of the combined effects of rosmarinic acid and cisplatin in gastric cancer cells. Medeni Med J. 2025;40:241-249

INTRODUCTION

Gastric carcinoma poses a significant public health challenge, as it is one of the leading causes of cancer-related mortality worldwide[1]. The etiology of gastric cancer is associated with multiple factors, such as genetic predisposition, *Helicobacter pylori* infection, dietary behaviors, and environmental factors[2]. Since gastric cancer is often diagnosed at an advanced stage, chemotherapy is a critical component of treatment. Cisplatin (CP), a platinum-based chemotherapeutic drug, is among the most widely used antineoplastic agents in treating gastric cancer[3].

The mechanism of action of CP involves the inhibition of cell division through the formation of covalent bonds with genomic or mitochondrial DNA, which leads to DNA damage, mitochondrial dysfunction, and eventual death of tumor cells[4]. However, clinical use is significantly restricted by drug resistance and systemic toxicity. Thus, there is increasing interest in novel combination therapies to improve CP's therapeutic efficacy and mitigate its toxicity.

Combination therapies in oncology have gained considerable attention in recent years because of their potential for improved efficacy compared to monotherapies. Combining diverse agents can enhance treatment efficacy and reduce the likelihood of cancer cells developing resistance[5]. It may also lower systemic toxicity by allowing the use of reduced amounts of chemotherapy drugs. The use of natural compounds in combination with cytotoxic drugs is considered a promising strategy because it can improve treatment outcomes while minimizing side effects[6,7].

Currently, natural compounds are being studied to enhance the efficacy of chemotherapeutic agents and mitigate adverse effects in anticancer treatments. Rosmarinic acid (RA) is a polyphenolic compound present in several aromatic plants, notably Rosmarinus officinalis. Because of its strong antioxidant, anti-inflammatory, and antiproliferative effects, RA is being investigated as a potential anticancer agent, with emphasis on its cytotoxic effects in a variety of cancers[8-11]. RA is proposed to exhibit synergistic potential in chemotherapy due to its impact on oxidative stress reduction, regulation of apoptotic pathways, and modulation of the cell cycle[12-15].

The purpose of this study is to enhance scientific understanding of the development of alternative and complementary therapeutic strategies by investigating the effects of RA in combination with CP on human gastric carcinoma (HGC)-27 gastric cancer cells.

MATERIALS and METHODS

Reagents

Thiazolyl blue tetrazolium bromide (MTT) reagent was purchased commercially (AppliChem, Darmstadt, Germany, A2231-0001, Lot: 3103285). MTT solution was prepared using Dulbecco's phosphate-buffered saline (DPBS; Sigma-Aldrich, St. Louis, MO, USA). RA was purchased from its commercial supplier. (Sigma-Aldrich, St. Louis, MO, USA). The stock solution of RA was prepared using dimethyl sulfoxide as the solvent and stored at -20 °C until use. CP was used as a ready-to-use solution and stored at room temperature. Drug solutions were diluted in culture media to obtain the final doses.

Ethics Statement

Since this study does not involve human participants, human data, or animal experiments, ethical approval is not required.

Cell Culture

HGC-27 is a human gastric cancer cell line obtained from a metastatic lesion in an adult patient with undifferentiated gastric carcinoma. This cell line demonstrates a strong capacity for proliferation and maintains the morphological and molecular characteristics typical of poorly differentiated gastric cancer. HGC-27 cells are commonly used as an in vitro model to investigate the biological properties of aggressive gastric cancer and to assess the cytotoxicity of chemotherapeutic drugs or natural substances[16-18]. HGC-27 gastric carcinoma cells were grown in Dulbecco's Modified Eagle Medium (DMEM, Gibco-Thermo Scientific, Waltham, MA, U.S.) supplemented with 10% (v/v) fetal bovine serum (FBS, Gibco-Thermo Scientific, Waltham, MA, U.S.) and 1% (v/v) penicillin-streptomycin (Pen/Strep, Gibco-Thermo Scientific, Waltham, MA, U.S.). Cells were maintained at 37 °C within a humidified incubator that contained 5% CO_2. Cells were subcultured when culture flasks reached approximately 80% confluency.

Cell Viability Assay

Cells were seeded at a density of 5×10^3 cells per well and incubated overnight at 37 °C in a humidified incubator with 5% CO_2. After incubation, cells were treated with different concentrations of RA (25, 50, 100, 200, 400, 800 µM) or CP (2.5, 5, 10, 20, 40, 80 µM) for 48 hours. At the end of the incubation period, MTT dye was added, and the cells were incubated for an additional 3 hours. Spectrophotometric analysis was performed at 570 nm using a microplate reader (Varioskan Lux, Thermo Fisher Scientific).

Colony Formation Assay

Cells cultured in 6-well plates were treated for 48 hours with IC10 and IC30 doses of RA and CP, and with combined doses (IC10 of RA together with IC10 of CP, or IC30 of RA together with IC30 of CP). After trypsinization, cells were harvested, seeded at a density of 8×10^2 cells/well in 6-well plates, and maintained at 37°C with 5% CO_2 for 10 days. Upon completion of the incubation, cells were washed with phosphate-buffered saline (PBS) and fixed in methanol:acetic acid:water (1:1:8 v/v). Following fixation, cells were stained with crystal violet for 20 minutes and then rinsed with distilled water to remove residual dye. Spots with more than 50 cells were considered colonies and were analyzed[19]. Treated cell groups were normalized to the untreated control groups. The colony formation rate was determined using the formula (number of colonies / number of seeded cells) ×100%.

In Vitro Scratch Assay (Wound Healing)

Wound healing was evaluated using 24-well plates seeded with 1×10^5 cells per well and incubated overnight at 37 °C in a 5% CO_2 incubator. Following incubation, cells were serum starved in fresh medium containing 0.5% FBS for 19 hours. Cell monolayers were carefully scratched the next day using sterile 200-µl pipette tips, and cellular debris was removed by washing with PBS. Cells were grown in serum-reduced medium (containing 0.5% FBS) with or without RA, CP, or their combination for 48 h. Imaging was performed at 0 and 48 h. The distribution of cells in the scratch area was evaluated via microscopic imaging (Labscope software, Primovert, Zeiss). ImageJ, with the MRI Wound Healing Tool (RRID:SCR_025260), enables quantitative measurement of wound closure.

Tumor Spheroid Growth Assay

Spheroids were formed by seeding HGC-27 cells at a density of 5 × 10^3 cells in 200 µl of DMEM into 96-well U-bottom spheroid plates (Nunclon Sphera, Thermo Scientific, Waltham, MA, U.S.). Spheroids were formed by incubating cells at 37°C in 5% CO_2 for 72 hours. Spheroids were exposed to RA, CP, or their combination at doses of IC10 and IC30. Images were acquired on days 0, 1, 2, and 3 using a Zeiss Primovert microscope (4x objective) with Labscope and Zen software. The spheroid core area was measured using ImageJ software.

Statistical Analysis

Statistical analysis was performed using GraphPad Prism 10 software. Student's t-test with Welch correction was applied to compare two groups. All analyses were conducted using three replicates from independent experiments. The error bars show the mean ± SEM of at least three independent experiments. Treated cell groups in all experiments were normalized to the untreated control groups.

RESULTS

RA and CP Reduced Cell Viability in HGC-27 Cells

The MTT assay was employed to assess the cytotoxicity of RA and CP in HGC-27 cells. Cell viability decreased in RA- and CP-treated cell groups in a dose-dependent manner (Figure 1A-B). The IC50, IC30, and IC10 values were determined from the cell viability analysis. The IC50, IC30, and IC10 values for RA were found to be 52 µM, 27 µM, and 9 µM, respectively. Furthermore, CP exhibited IC50, IC30, and IC10 values of 11 µM, 5 µM, and 2 µM, respectively.

The anticipated increase in cytotoxic effect of the combined treatment was assessed by administering combinations of the determined IC10, IC30, and IC50 doses. Therefore, the combinations of IC10, IC30, and IC50 doses of RA and CP were analyzed separately. Compared with single treatments, IC10, IC30, and IC50 combinations showed greater cytotoxicity (Figure 1C). The combined IC10 doses showed efficacy comparable to the single IC30 doses, and the combined IC30 doses closely replicated the effects observed with IC50 doses. Thus, IC10 and IC30 doses were selected for combined use in subsequent experiments.

Combination Therapy Decreased The Formation of Cancer Cell Colonies

A colony formation assay was performed to examine the combined effects of RA and CP on continuous cell growth and colony formation. When tested alone, RA significantly reduced colony formation at IC10 and IC30 concentrations (18% and 40%, respectively). However, CP showed a much stronger inhibitory effect at its IC10 and IC30 concentrations (82% and 89%, respectively). Nevertheless, the cell groups treated with the combination doses exhibited significantly decreased colony formation compared to the groups treated with the individual drugs (Figure 2). Specifically, the combination of IC10 concentrations led to a 94% decrease in colony formation, while the combination of IC30 concentrations resulted in a 99% decrease in colony formation.

Combination Therapy Decreased Cell Movement

The effects of a combination of RA and CP on cell motility were evaluated using an in vitro scratch assay. Following a 48-hour incubation, the untreated cell group

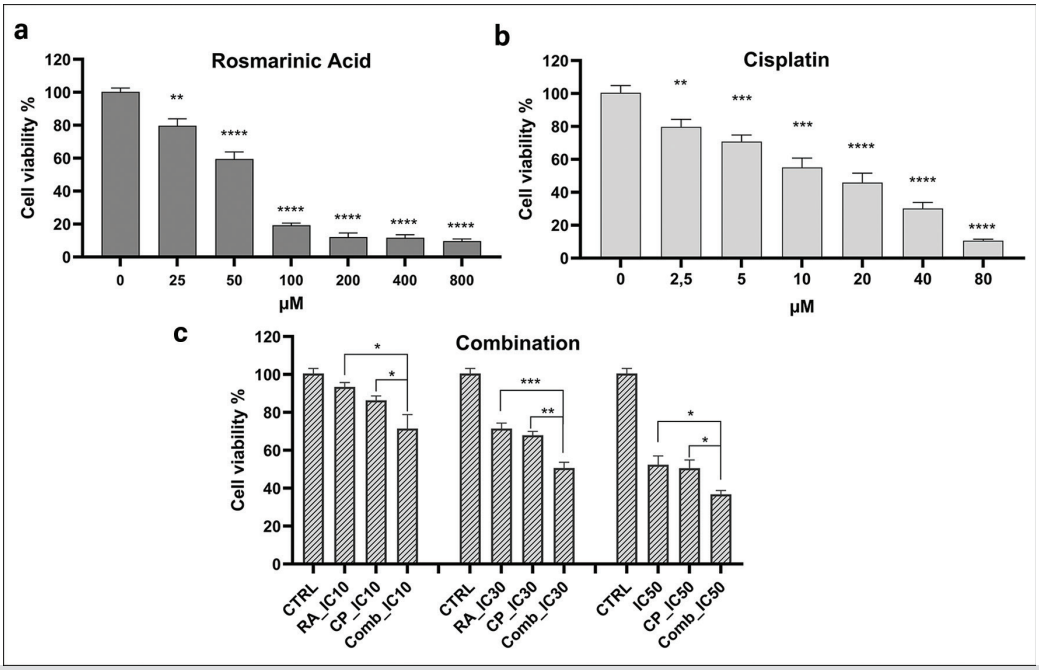

Figure 1. Cytotoxic effects of RA, CP and their combination against HGC-27 cell line. a) RA treatment, b) CP treatment, c) Combination treatment. Statistical analysis was performed using Student's t-test. *p<0.05, **p<0.01, ***p<0.001, ****p<0.0001.

RA: Rosmarinic acid, CP: Cisplatin , HGC-27: Human gastric carcinoma cells

fully covered the scratched area. At IC10 doses of RA and CP, the scratch area showed near-complete closure; at IC30 doses, it was wider. Administration of a single IC10 dose of RA resulted in approximately 85% closure of the scratch area, while a single IC10 dose of CP resulted in 95% closure. Co-administration of IC10 doses of RA and CP resulted in the suppression of cellular motility, leading to a 65% closure of the scratch area. Using an IC30 dose of RA alone resulted in approximately 70% closure of the scratch area, whereas a single IC30 dose of CP resulted in 71% closure. When IC30 doses of RA and CP were combined, cellular motility decreased further, resulting in only 46% of the area being covered by cells. Thus, the scratch areas were found to be wider than those observed with individual treatments (Figure 3).

The Combination of RA and CP Suppressed Tumor Spheroid Growth

A spheroid growth assay was conducted to further investigate the combined effects of RA and CP on tumor growth in a 3D setting. Measurements of spheroid core area from the 3D spheroid growth assay revealed that RA and CP, at IC10 and IC30 doses, significantly reduced spheroid size over time under both individual and combined treatment conditions (Figure 4A-C). On day 3, CP alone exhibited the highest inhibition of spheroid growth (42%), followed by the combination treatment (34%) and RA alone (25.7%) (Figure 4D). Although the combination treatment showed the most statistically significant effect compared with the control group (p<0.0001), this inhibition was not greater than that observed with CP alone. Moreover, no significant difference was observed in spheroid size between the combined and individual treatments (Figure 4D), indicating no additive or synergistic effect between RA and CP. This highlights the need for further optimization of dosing in 3D tumor models.

DISCUSSION

Combination therapies are now widely favored in cancer treatment to increase efficacy and reduce adverse effects. Specifically, combining chemotherapy with natural compounds may improve treatment outcomes while permitting reduced doses. Our study examines the cytotoxic and antiproliferative effects of RA and CP on the HGC-27 gastric cancer cell line, both individually and in combination, to advance this approach.

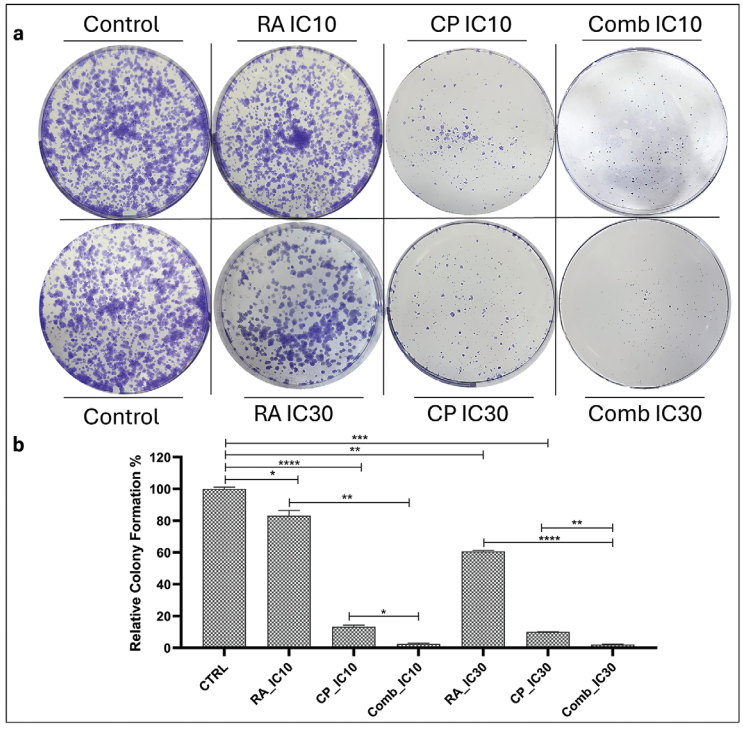

Figure 2. The colony formation of HGC-27 cells following RA, CP and combination treatments. a) Colony formation of HGC-27 cells, b) Statistical analysis (Student's t-test, *p<0.05, **p<0.01, ***p<0.001).

RA: Rosmarinic acid, CP: Cisplatin , HGC-27: Human gastric carcinoma cells

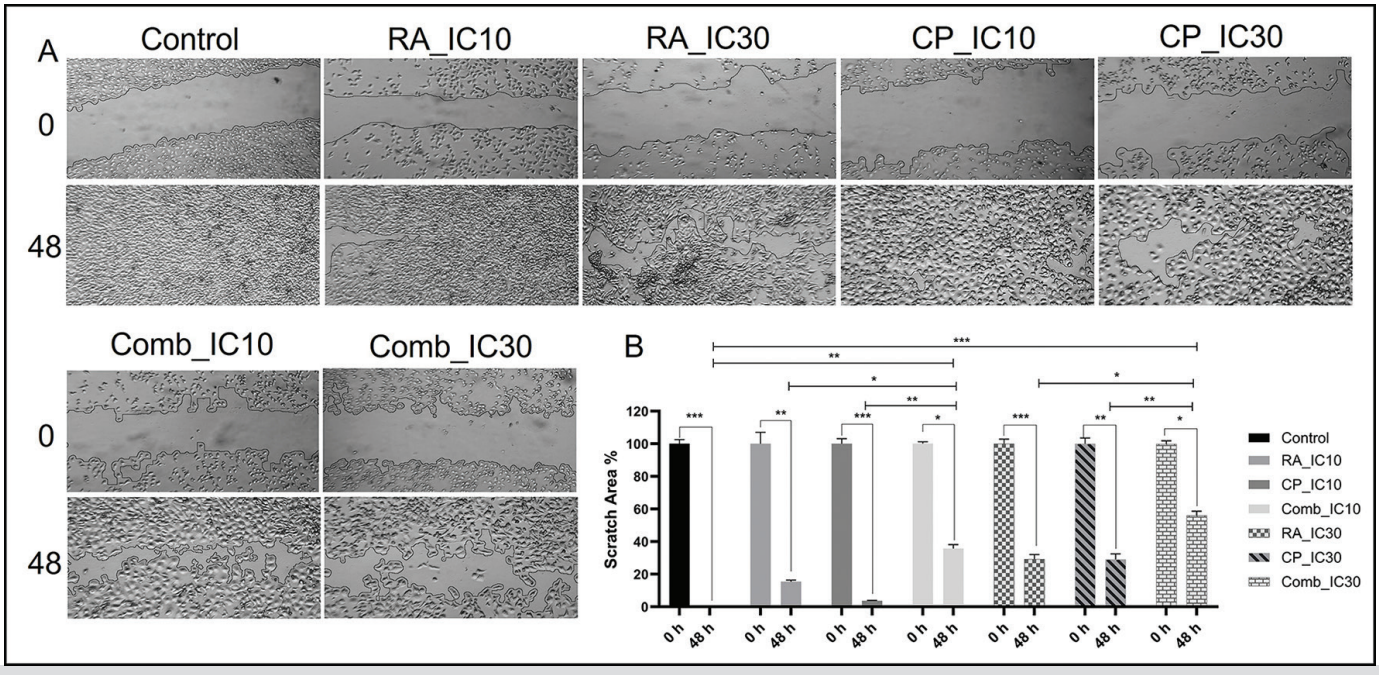

Figure 3. *In vitro* scratch assay of HGC-27 cells following RA, CP and combination treatments. A) Scratched regions of cells, B) Statistical analysis (Student's t-test, *p<0.05, **p<0.01, ***p<0.001).

RA: Rosmarinic acid, CP: Cisplatin , HGC-27: Human gastric carcinoma cells

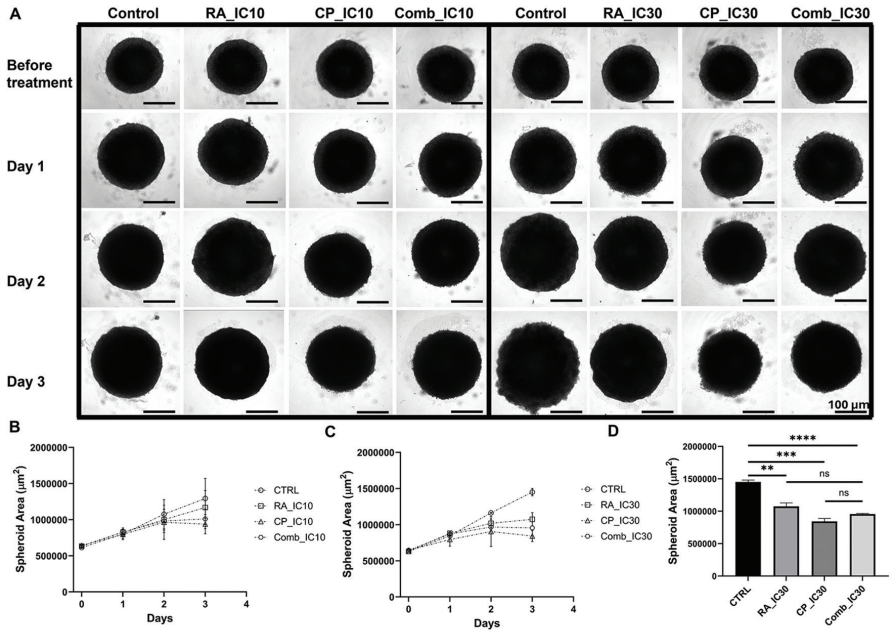

Figure 4. Spheroid growth assay of HGC-27 cells following RA, CP and combination treatments. A) Microscopic images of cells, B) Spheroid core area measurement following IC10 treatments up to day 3, C) Spheroid core area measurement following IC30 treatments up to day 3, D) Spheroid core area measurement on day 3 following IC30 treatments (Student's t-test, **p<0.01, ***p<0.001, ****p<0.0001).

HGC: Human gastric carcinoma, RA: Rosmarinic acid, CP: Cisplatin, IC:Inhibitory concentration

After determining the appropriate IC values for each agent, the combination groups (RA+CP IC10 and RA+CP IC30) exhibited greater cytotoxicity than the groups treated with each agent individually. The results indicate that the combination therapy's impact on cell viability may be additive or synergistic. Prior investigations have documented the synergistic impact of polyphenols in conjunction with chemotherapeutic agents[20]. Analysis across a broader dose range may reveal more significant synergistic effects.

Prior studies have indicated that various polyphenols can inhibit the colony-forming ability of cancer cells [20-22]. Thus, we utilized colony formation assays to assess how RA and CP, alone or in combination, influenced the long-term growth potential of HGC-27 cells. Individual administration of RA and CP significantly inhibited colony formation, although CP exerted a more substantial effect than RA. Nevertheless, the IC10 and IC30 combinations exhibited a marked reduction in colony numbers, suggesting that these combinations possess more potent antiproliferative effects than the individual treatments.

Cellular motility is essential to the pre-metastatic process and poses a major challenge to cancer treatment[23-25]. For this reason, the development of therapeutic strategies that can impact cell motility is of the utmost importance. In addition to affecting cell viability and proliferation, combining polyphenols with chemotherapeutic agents may inhibit cell motility. Our study revealed that after 48 hours of incubation, the scratched region in the control group had completely closed. Although the scratched region was almost closed at IC10 doses, complete closure was not achieved at IC30 doses. At IC10 concentrations, cell motility was largely unaffected, permitting cells to move and close the scratch region. In contrast, following treatment with IC30 doses of both agents, cell motility was considerably reduced, and a larger scratch area remained after 48 hours. These findings align with the dose-dependent inhibitory effects of RA and CP; specifically, higher concentrations demonstrate more pronounced cytotoxic effects, which impede scratch closure. Therefore, the observed "near-complete closure" at IC10 doses appears indicative of preserved basal motility under minimal toxicity, whereas the "larger scratch area" at IC30 doses reflects suppression of cell motility due to cytotoxic stress. The scratched region, however, revealed a significant gap when IC10 and IC30 doses were used in combination. This indicates that the simultaneous administration of RA and CP suppressed cellular migration to a greater extent

than individual treatments. These findings suggest that this combination has the potential to reduce cell motility and indirectly inhibit metastasis.

3D tumor models provide improved tools to more fully recapitulate the complex architecture of tumors and to enhance drug-screening processes, thus facilitating the identification of more effective therapeutic candidates[26-28]. Therefore, to better mimic the tumor microenvironment and to obtain more physiologically relevant drug responses, we employed a 3D spheroid growth assay. Our findings demonstrated that RA and CP, both individually and in combination, significantly inhibited spheroid growth in HGC-27 cells compared with the untreated control group. RA alone reduced spheroid size by 34% and CP reduced it by 42%, whereas the combination treatment reduced size by only 25.7%. Although all treatments significantly suppressed spheroid growth relative to the control, no significant difference was observed between individual treatments and the combined treatment. Interestingly, although our study observed a combinatorial efficacy of RA and CP in 2D cultures, this interaction was not reproduced in the 3D spheroid model. This discrepancy may be attributed to the structural and physiological differences between 2D and 3D culture systems. Unlike 2D cultures, tumor spheroids, with diameters greater than 500 µm, typically develop gradients of oxygen, nutrients, and waste, leading to the formation of hypoxic and necrotic zones that are observed in solid tumors. Furthermore, in 3D cultures, tight cell-cell and cell-matrix interactions, along with diffusion barriers, can limit drug penetration, thereby altering cellular drug responses[28,29]. Consistent with the literature, the spheroids established in our study, each larger than 500 µm, are expected to reflect the architectural complexity of solid tumors. Therefore, the doses that were effective in 2D in our study might not be optimal in the 3D setting. Although no study to date has reported on CA's efficacy in HGC-27-derived spheroids, it has been tested in 3D spheroid models of several cancer types. These studies provide evidence of differences in drug sensitivity between 2D and 3D cell culture systems, indicating that 3D models are more drug-resistant than 2D systems[30-33]. For instance, Baek et al.[30] directly compared CA's cytotoxicity in 2D and 3D models and reported that IC50 values for all tested 3D spheroids were higher than previously reported 2D results in different cancer types. Inducing cytotoxicity in 3D spheroids would require higher concentrations than in 2D systems, suggesting that each system may require different treatment optimization. This emphasizes the importance of using 3D tumor models, which more accurately recapitulate tumor architecture and therapeutic resistance, to evaluate combination strategies.

Study Limitations

This study revealed that the combined use of RA and CP elevated cellular cytotoxicity and limited cell motility in HGC-27 gastric cancer cells. Despite this, the underlying molecular mechanisms of these effects remained unexplored. While reduced cell motility could influence metastatic processes, the underlying mechanisms and metastasis-related parameters (e.g., signaling pathways and gene/protein expression profiles) were not assessed. Thus, the research findings lack full mechanistic support, and *in vitro* outcomes must be validated in 3D and *in vivo* models. To this end, we attempted to establish spheroid cultures to better reflect the tumor microenvironment. However, the effects observed in 2D in vitro assays, particularly those of the combination treatment, were not detected in 3D models. This discrepancy suggests that 3D spheroid models, which better recapitulate the native tumor, may require further dose optimization.

Additional research is necessary to elucidate the molecular processes driving the observed cytotoxicity and motility inhibition, with particular regard to their potential impact on metastasis, and to validate the results in different experimental models. These studies are important for evaluating the clinical significance of the combination strategy and its potential translation into practical therapeutic methodologies.

CONCLUSION

In this study, we demonstrated that both RA and CP exhibit inhibitory effects on the proliferation, colony-forming capacity, and motility of HGC-27 gastric cancer cells. The drug combination showed enhanced efficacy compared with individual treatments in 2D assays, suggesting that combining these agents is a promising approach. However, this additive effect was not observed in our 3D spheroid models, highlighting the need to consider the biological complexity and therapeutic resistance reproduced by 3D tumor models when evaluating drug combination approaches. Ultimately, our study provides insight into the efficacy of the combination of RA and CP in gastric cancer therapy and emphasizes the importance of integrating 3D culture systems into preclinical testing to obtain more physiologically relevant results.

Acknowledgements

We express our appreciation to the team members of the Türkiye Cancer Institute.

Ethics

Ethics Committee Approval: Since this study does not involve human participants, human data, or animal experiments, ethical approval is not required.

Informed Consent: Not appreciable.

Footnotes

Author Contributions

Concept: C.S., C.Sü., S.K.A., B.Y., Design: C.S., C.Sü., S.K.A., B.Y., Data Collection or Processing: C.S., C.Sü., S.K.A., B.Y., Analysis or Interpretation: C.S., C.Sü., Literature Search: C.S., C.Sü., S.K.A., B.Y. Writing: C.S., C.Sü.

Conflict of Interest: The authors declare no conflicts of interest.

Financial Disclosure: The authors declared that this study has received no financial support.

REFERENCES

1. Siegel RL, Giaquinto AN, Jemal A. Cancer statistics, 2024. CA Cancer J Clin. 2024;74:12-49.
2. Cheng XJ, Lin JC, Tu SP. Etiology and prevention of gastric cancer. Gastrointest Tumors. 2016;3:25-36.
3. Petrelli F, Zaniboni A, Coinu A, et al. Cisplatin or not in advanced gastric cancer: a systematic review and meta-analysis. PLoS One. 2013;8:e83022.
4. Li K, Li J, Li Z, Men L, Zuo H, Gong X. Cisplatin-based combination therapies: their efficacy with a focus on ginsenosides co-administration. Pharmacol Res. 2024;203:107175.
5. Blagosklonny MV. Overcoming limitations of natural anticancer drugs by combining with artificial agents. Trends Pharmacol Sci. 2005;26:77-81.
6. Wu J, Li Y, He Q, Yang X. Exploration of the use of natural compounds in combination with chemotherapy drugs for tumor treatment. Molecules. 2023;28:1022.
7. Castañeda AM, Meléndez CM, Uribe D, Pedroza-Díaz J. Synergistic effects of natural compounds and conventional chemotherapeutic agents: recent insights for the development of cancer treatment strategies. Heliyon. 2022;8:e09519.
8. Ijaz S, Iqbal J, Abbasi BA, et al. Rosmarinic acid and its derivatives: current insights on anticancer potential and other biomedical applications. Biomed Pharmacother. 2023;162:114687.
9. Nadeem M, Imran M, Aslam Gondal T, et al. Therapeutic potential of rosmarinic acid: a comprehensive review. Applied Sciences. 2019;9:3139.
10. Liu Y, Xu X, Tang H, Pan Y, Hu B, Huang G. Rosmarinic acid inhibits cell proliferation, migration, and invasion and induces apoptosis in human glioma cells. Int J Mol Med. 2021;47:67.
11. Hossan MS, Rahman S, Bashar A, Jahan , Nahian A, Rahmatullah M. Rosmarinic acid: a review of its anticancer action. World J Pharm Pharm Sci. 2014;3:57-70.
12. Tai J, Cheung S, Wu M, Hasman D. Antiproliferation effect of Rosemary (Rosmarinus officinalis) on human ovarian cancer cells in vitro. Phytomedicine. 2012;19:436-43.
13. Villegas C, Cortez N, Ogundele AV, et al. Therapeutic applications of rosmarinic acid in cancer-chemotherapy-associated resistance and toxicity. Biomolecules. 2024;14:867.
14. Nunes S, Madureira AR, Campos D, et al. Therapeutic and nutraceutical potential of rosmarinic acid-Cytoprotective properties and pharmacokinetic profile. Crit Rev Food Sci Nutr. 2017;57:1799-806.
15. Luo Y, Ma Z, Xu X, Qi H, Cheng Z, Chen L. Anticancer effects of rosmarinic acid in human oral cancer cells is mediated via endoplasmic reticulum stress, apoptosis, G2/M cell cycle arrest and inhibition of cell migration. J BUON. 2020;25:1245-50.
16. Wang, Yan, Wang, Haiyang, Xu, Shun. Natural Bioactive Compounds Promote cell apoptosis in gastric cancer treatment: evidence from network pharmacological study and experimental analysis. Journal of Chemistry. 2023.
17. Liu Y, Liu C, Tan T, Li S, Tang S, Chen X. Sinomenine sensitizes human gastric cancer cells to cisplatin through negative regulation of PI3K/AKT/Wnt signaling pathway. Anticancer Drugs. 2019;30:983-90.
18. Wang J, Zhang X, Li X, et al. Anti-gastric cancer activity in three-dimensional tumor spheroids of bufadienolides. Sci Rep. 2016;6:24772.
19. Franken NA, Rodermond HM, Stap J, Haveman J, van Bree C. Clonogenic assay of cells in vitro. Nat Protoc. 2006;1:2315-9.
20. Singaravelan N, Tollefsbol TO. Polyphenol-based prevention and treatment of cancer through epigenetic and combinatorial mechanisms. Nutrients. 2025;17:616.
21. Chen S, Cooper M, Jones M, et al. Combined activity of oridonin and wogonin in advanced-stage ovarian cancer cells: sensitivity of ovarian cancer cells to phyto-active chemicals. Cell Biol Toxicol. 2011;27:133-47.
22. Huangfu L, Wang X, Tian S, et al. Piceatannol enhances Beclin-1 activity to suppress tumor progression and its combination therapy strategy with everolimus in gastric cancer. Sci China Life Sci. 2023;66:298-312.
23. Wang X, Decker CC, Zechner L, Krstin S, Wink M. In vitro wound healing of tumor cells: inhibition of cell migration by selected cytotoxic alkaloids. BMC Pharmacol Toxicol. 2019;20:4.
24. Li L, He Y, Zhao M, Jiang J. Collective cell migration: implications for wound healing and cancer invasion. Burns Trauma. 2013;1:21-6.
25. Stuelten CH, Parent CA, Montell DJ. Cell motility in cancer invasion and metastasis: insights from simple model organisms. Nat Rev Cancer. 2018;18:296-312.
26. Cordeiro S, Oliveira BB, Valente R, Ferreira D, Luz A, Baptista PV, Fernandes AR. Breaking the mold: 3D cell cultures reshaping the future of cancer research. Front Cell Dev Biol. 2024;12:1507388.
27. Mehta G, Hsiao AY, Ingram M, Luker GD, Takayama S. Opportunities and challenges for use of tumor spheroids as models to test drug delivery and efficacy. J Control Release. 2012;164:192-204.
28. Alzeeb G, Metges JP, Corcos L, Le Jossic-Corcos C. Three-dimensional culture systems in gastric cancer research. Cancers (Basel). 2020;12:2800.

29. Hirschhaeuser F, Menne H, Dittfeld C, West J, Mueller-Klieser W, Kunz-Schughart LA. Multicellular tumor spheroids: an underestimated tool is catching up again. J Biotechnol. 2010;148:3-15.

30. Baek N, Seo OW, Lee J, Hulme J, An SS. Real-time monitoring of cisplatin cytotoxicity on three-dimensional spheroid tumor cells. Drug Des Devel Ther. 2016;10:2155-65.

31. Li M, Lu B, Dong X, et al. Enhancement of cisplatin-induced cytotoxicity against cervical cancer spheroid cells by targeting long non-coding RNAs. Pathol Res Pract. 2019;215:152653.

32. Ward Rashidi MR, Mehta P, Bregenzer M, et al. Engineered 3D model of cancer stem cell enrichment and chemoresistance. Neoplasia. 2019;21:822-36.

33. Mora-Lagos B, Reyes ME, Lobos-Gonzalez L, Del Campo M, Buchegger K, Zanella L, Riquelme I, Ili CG, Brebi P. Maraviroc/cisplatin combination inhibits gastric cancer tumoroid growth and improves mice survival. Biol Res. 2025;58:4.

DOI: 10.4274/MMJ.galenos.2025.44045
Medeni Med J 2025;40:250-261

Original Article

Safety Profile of Roxadustat in Anemic Patients: A Meta-Analysis of 21 RCTs

Anemili Hastalarda Roksadustat'ın Güvenlilik Profili: 21 RCT'nin Meta-Analizi

Lokman Hekim TANRIVERDI[1], Ahmet SARICI[2], Mehmet Ali ERKURT[2], Hacı Bayram BERKTAS[3]

[1]Inonu University Faculty of Medicine, Department of Medical Pharmacology, Malatya, Türkiye
[2]Inonu University Faculty of Medicine, Department of Hematology, Malatya, Türkiye
[3]Inonu University Faculty of Medicine, Department of Nephrology, Malatya, Türkiye

ABSTRACT

Objective: Roxadustat is an oral hypoxia-inducible factor prolyl hydroxylase inhibitor used to treat anemia in patients with chronic kidney disease. We aimed to assess its safety and tolerability profile through a meta-analysis of randomized controlled trials (RCTs).

Methods: A systematic search of the Cochrane CENTRAL, Ovid Medline R, PubMed, and Web of Science databases was conducted up to January 1, 2025 was conducted. RCTs comparing roxadustat with control groups were included. Inverse-variance-weighted random-effects models were used. The primary outcome was the risk of any serious treatment-emergent adverse event (TEAE). Subgroup analyses were based on etiology, comparator, and prior erythropoiesis-stimulating agent (ESA) use.

Results: Twenty-one RCTs involving 11.686 patients were included. Roxadustat was not associated with a higher risk of any serious TEAE compared with placebo [risk ratio (RR) =1.37, 95% confidence interval (CI): 0.79-2.37] or with ESA (RR=1.05, 95% CI: 0.99-1.10). Similarly, cardiac serious adverse events (SAEs) did not differ significantly when compared with ESA (RR=1.11, 95% CI: 0.75-1.12) or placebo (RR=1.11, 95% CI: 0.92-1.35). Hyperkalemia incidence was significantly higher compared with placebo (RR=1.25, 95% CI: 1.02-1.53) but not compared with ESA (RR=1.03, 95% CI: 0.77-1.36). There were also no significant differences in the incidence of serious infections (RR=0.74, 95% CI: 0.21-2.59), azotemia (RR=0.96, 95% CI: 0.46-2.00), hypertension (RR=1.06, 95% CI: 0.93-1.21), or pneumonia (RR=0.96, 95% CI: 0.81-1.14) compared with ESA. Notably, withdrawal due to adverse events (RR=2.11, 95% CI: 1.59-2.79) was significantly higher compared with ESA. TEAEs leading to death were similar compared with ESA (RR=0.98, 95% CI: 0.85-1.13) but were increased compared with placebo (RR=1.21, 95% CI: 1.04-1.42). All-cause mortality was significantly lower than with placebo (RR=0.40, 95% CI: 0.28-0.57) but was similar to ESA (RR=0.89, 95% CI: 0.57-1.37). Subgroup analyses for the primary outcome by etiology and prior ESA use were not consistent with the main findings.

Conclusions: Roxadustat demonstrated a SAE profile generally comparable to that of ESA, with no significant differences in cardiac SAEs, serious infections, azotemia, hypertension, or pneumonia. Hyperkalemia was more frequent compared with placebo, and withdrawals due to adverse events were more frequent compared with ESA. TEAEs leading

ÖZ

Amaç: Roxadustat, kronik böbrek hastalığına bağlı aneminin tedavisinde kullanılan oral bir hipoksi ile indüklenebilir faktör prolil hidroksilaz inhibitörüdür. Bu çalışmada, randomize kontrollü çalışmaların (RKÇ) meta-analizi ile roksadustatın güvenlilik ve tolere edilebilirlik profilini değerlendirmeyi amaçladık.

Yöntemler: Cochrane CENTRAL, Ovid Medline R, PubMed ve Web of Science veri tabanlarında 1 Ocak 2025 tarihine kadar sistematik literatür taraması yapıldı. Roksadustat ile kontrol gruplarını karşılaştıran RKÇ'ler dahil edildi. Ters varyans ağırlıklı rastgele etki modeli kullanıldı. Birincil sonlanım noktası, herhangi bir ciddi tedaviyle ilişkili advers olay (TEAE) riskiydi. Alt grup analizleri etiyoloji, kontrol grubu ve geçmişte eritropoez uyarıcı ajan (ESA) kullanımı temelli yapıldı.

Bulgular: Toplam 11,686 hastayı içeren 21 RKÇ dahil edildi. Roksadustat, plasebo [risk oranı (RR)=1,37, %95 güven aralığı (GA): 0,79-2,37] veya ESA (RR=1,05, %95 GA: 0,99-1,10) ile karşılaştırıldığında herhangi bir ciddi TEAE riskinde artış göstermedi. Benzer şekilde, kardiyak ciddi advers olaylar ESA (RR=1,11, %95 GA: 0,75-1,12) veya plasebo (RR=1,11, %95 GA: 0,92-1,35) ile karşılaştırıldığında anlamlı farklılık göstermedi. Hiperkalemi plaseboya kıyasla anlamlı olarak daha yüksekti (RR=1,25, %95 GA: 1,02-1,53), ancak ESA ile karşılaştırıldığında farklı değildi (RR=1,03, %95 GA: 0,77-1,36). ESA'ya kıyasla ciddi enfeksiyonlar (RR=0,74, %95 GA: 0,21-2,59), azotemi (RR=0,96, %95 GA: 0,46-2,00), hipertansiyon (RR=1,06, %95 GA: 0,93-1,21) veya pnömoni (RR=0,96, %95 GA: 0,81-1,14) açısından anlamlı fark gözlenmedi. Advers olaylara bağlı tedavi kesilmesi ESA'ya göre anlamlı olarak yüksekti (RR=2,11, %95 GA: 1,59-2,79). Ölüme yol açan TEAE'ler ESA ile benzerdi (RR=0,98, %95 GA: 0,85-1,13), ancak plaseboya göre yüksekti (RR=1,21, %95 GA: 1,04-1,42). Tüm nedenlere bağlı mortalite plaseboya (RR=0,40, %95 GA: 0,28-0,57) kıyasla daha düşüktü, ancak ESA (RR=0,89, %95 GA: 0,57-1,37) ile karşılaştırıldığında farklı değildi. Birincil sonlanım noktası, etiyoloji ve geçmişte ESA kullanımına göre alt grup analizleri ile değerlendirildiğinde esas analizden farklılıklar tespit edildi.

Sonuçlar: Roksadustat, ESA ile karşılaştırıldığında genel olarak benzer ciddi advers olay profili göstermiş olup, kardiyak SAEs, ciddi enfeksiyonlar, azotemi, hipertansiyon veya pnömoni açısından anlamlı fark saptanmamıştır. Hiperkalemi plaseboya kıyasla daha yüksek

Address for Correspondence: L.H. Tanrıverdi, Inonu University Faculty of Medicine, Department of Medical Pharmacology, Malatya, Türkiye
E-mail: lokmanhekim.tanriverdi@gmail.com **ORCID ID:** orcid.org/0000-0003-4263-5234

Received: 30.08.2025
Accepted: 25.11.2025
Published: 31.12.2025

Cite as: Tanrıverdi LH, Sarıcı A, Erkurt MA, Berktaş HB. Safety profile of roxadustat in anemic patients: a meta-analysis of 21 RCTs. Medeni Med J. 2025;40:250-261

to death were similar to ESA but higher than with placebo, whereas all-cause mortality was lower than with placebo and comparable to ESA. Taken together, current evidence supports the overall non-inferiority of roxadustat to ESA in terms of safety.

Keywords: Roxadustat, iron deficiency anemia, chronic kidney disease, hiperkalemi, meta-analysis

bulunmuş ve advers olaylara bağlı tedavi kesilmesi ESA'ya kıyasla artmıştır. Ölüme yol açan TEAE'ler ESA ile benzer, plaseboya göre ise daha yüksektir. Tüm nedenlere bağlı mortalite plaseboya göre daha düşük olup ESA'ya benzemektedir. Genel olarak mevcut kanıtlar, güvenlilik açısından roksadustatın ESA'ya karşı non-inferior olduğunu desteklemektedir.

Anahtar kelimeler: Roksadustat, demir eksikliği anemisi, kronik böbrek hastalığı, hiperkalemi, meta-analiz

INTRODUCTION

The World Health Organization defines anemia as a hemoglobin (Hb) level of <13.0 g/dL for adult males and postmenopausal women, and <12.0 g/dL for premenopausal women[1]. Patients with chronic kidney disease (CKD), as a distinct group, will still have anemia even when appropriately treated.

Anemia is a common complication in patients with CKD, with erythropoietin deficiency recognized as one of its principal underlying causes[2]. Iron deficiency constitutes the second most significant contributor to anemia in this population[3]. Current treatment strategies recommend oral iron supplementation as the first-line therapy for iron-deficiency anemia; however, in patients requiring a more rapid and effective correction, intravenous iron formulations are generally preferred[4].

Another therapeutic option for the treatment of anemia is hypoxia-inducible factor prolyl hydroxylase inhibitors (HIF-PHIs). HIF-PHIs stimulate erythropoietin release from the kidneys and liver, thereby increasing endogenous erythropoietin levels[5-7]. Among the HIF-PHIs, vadadustat is approved by the US Food and Drug Administration (FDA) for the treatment of anemia due to CKD in adults receiving hemodialysis for at least 3 months, whereas daprodustat is approved for adults receiving hemodialysis for at least 4 months[8]. It is well established that anemia is associated with increased mortality and reduced quality of life in patients with CKD. The benefit of correcting anemia in this patient group is clear. It is anticipated that HIF-PH inhibitors will improve compliance in clinical practice because of their oral administration[7,9].

Roxadustat is the first orally administered HIF-PHI available for adult patients with anemia associated with CKD in Europe[10]. Beyond the class effects of HIF-PHIs, results on the safety of roxadustat are conflicting. Findings for hyperkalemia, all-cause mortality, and cardiovascular (CV) outcomes were inconsistent across published randomized controlled trials (RCTs).

This study aims to assess the safety and tolerability of roxadustat in anemic patients through a meta-analysis of RCTs, with particular attention to identifying patients at increased risk of adverse outcomes.

MATERIALS and METHODS

Study Design

A systematic review and meta-analysis were conducted to evaluate the safety of roxadustat for the treatment of iron-deficiency anemia in the CKD population, in patients with myelodysplastic syndrome (MDS), and in post-transplantation patients. Approval to conduct the study was obtained from the Malatya Non-Interventional Clinical Research Ethics Committee (approval number: 2025/7455, date: 25.03.2025). As this meta-analysis used only aggregated data from published RCTs, informed consent was not required.

Data Sources and Search Strategy

A comprehensive search of four electronic databases — Cochrane CENTRAL, PubMed, Ovid Medline R, and Web of Science — was performed from inception to January 1, 2025. The search was designed to identify RCTs evaluating the safety profile of roxadustat in anemic patients. Search terms included combinations of "Roxadustat" OR "FG-4592" OR "ASP1517" OR "AZD9941" (Supplementary File 1).

Eligibility Criteria

We included only RCTs that:

- Enrolled adult patients with anemia of any etiology,
- Compared roxadustat with a placebo, standard of care, or erythropoiesis-stimulating agents (ESAs),
- Reported safety outcomes included serious treatment-emergent adverse events (TEAEs), specific adverse events (AEs) (e.g., cardiac events, hypertension), and mortality.

Studies were excluded if they were:

- Non-randomized designs (e.g., observational, experimental studies),
- Focused on pharmacokinetics/pharmacodynamics without clinical endpoints,

- Not reporting original patient-level or aggregate data.

The search was limited to English-language, full-text publications.

Study Selection

Two independent reviewers screened the identified records for inclusion. Disagreements were resolved through discussion. Records that met the eligibility criteria were included.

Data Extraction and Synthesis

Data extraction was independently performed by two reviewers using a standardized form. Extracted data included study design, population characteristics, interventions, comparators, follow-up duration, and safety outcomes. Discrepancies were resolved through discussion or consultation with a third reviewer.

Assessment of Risk of Bias

Risk of bias (RoB) was assessed using the Cochrane Risk of Bias 2.0 tool for RCTs[11]. Domains evaluated included randomization process, deviations from intended interventions, missing outcome data, measurement of outcomes, and selection of reported results.

Statistical Analysis

This meta-analysis was performed using an inverse variance–weighted random-effects approach. The between-study variance (τ^2) was estimated using the Paule-Mandel method. Summary effect estimates were expressed as pooled risk ratios (RRs) with corresponding 95% confidence intervals (CIs). Statistical heterogeneity was evaluated using the I^2 statistic[12] and further examined using Cochran's Q test and I^2 values. I^2 values ranging from 30% to 60% were interpreted as indicating moderate heterogeneity, values exceeding 60% as indicating high heterogeneity, and values above 75% as indicating substantial heterogeneity. All statistical analyses and data synthesis were conducted using R for macOS (www.r-project.org, version 4.4.3; R Foundation for Statistical Computing, Vienna, Austria). Sensitivity analyses were undertaken by removing studies judged to be at high RoB. In addition, subgroup analyses were performed according to anemia etiology (e.g., CKD, MDS), comparator type, and prior use of ESAs. For subgroup comparisons, p for interaction 0.1 was considered statistically significant[13].

RESULTS

This systematic review and meta-analysis was reported in accordance with the Preferred Reporting Items for Systematic Reviews and Meta-Analyses (PRISMA) 2020 guidelines[14].

Study Selection

The initial database search yielded a total of 2.044 records, including 230 from Cochrane CENTRAL, 504 from PubMed, 497 from Ovid MEDLINE, and 812 from Web of Science. After removing 1.056 duplicate records, 980 unique records remained for title and abstract screening. Of these, 916 records were excluded based on irrelevance to the study objective.

The full texts of 64 reports were sought. However, eleven reports were not included: two were post-hoc analyses and nine were secondary data analyses. Thus, 53 reports were assessed for full eligibility. Following full-text review, 15 reports were excluded: 4 due to inappropriate comparator groups and 11 due to ineligible study designs.

A total of 38 reports, representing 21 RCTs, met all inclusion criteria and were included in the qualitative and quantitative synthesis. The complete study selection process is illustrated in the PRISMA 2020 flow diagram (Figure 1).

Study Characteristics

This systematic review and meta-analysis included 21 RCTs[15-34] comprising a total of 11.686 adult patients with anemia regardless of etiology. Studies published between 2015 and 2024 were conducted in diverse international settings, including Asia[15-17,21-23,28,32,34], North America[19,20,29], and Europe[18,25,31]. The study populations included dialysis-dependent (DD-CKD) patients[17,20,21,23,25,26,29,30,32,34], non-dialysis-dependent (NDD-CKD) patients[15,16,18,19,22-24,31,33], patients with MDS[27], and patients with posttransplant anemia[28].

The sample sizes across trials ranged from 91 to 2.761 participants. Follow-up durations ranged from 4 to 208 weeks. All included trials investigated roxadustat, an oral HIF-PHI, administered either at fixed doses or at doses titrated based on Hb response. The Comparator was ESAs[16-18,20,21,23,25,26,29,30,32,34] or placebo[15,19,22-24,27,31,33] in the vast majority of the included trials, whereas oral iron[28] was used in post-transplant anemia.

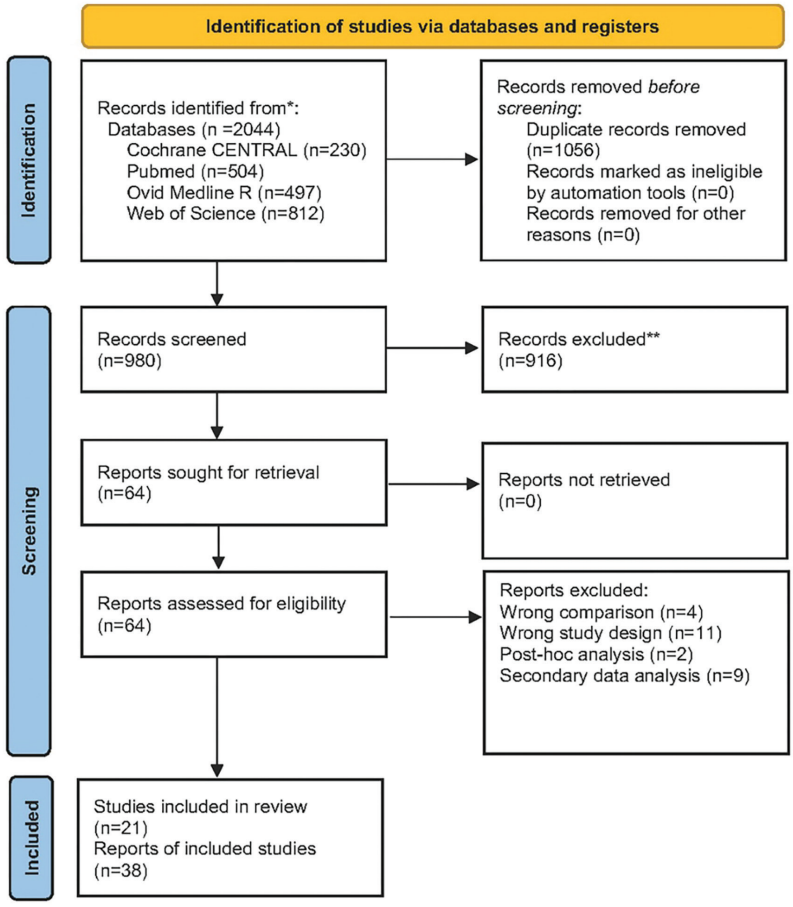

Figure 1. PRISMA flow diagram. PRISMA: Preferred Reporting Items for Systematic Reviews and Meta-Analyses

Primary safety outcomes reported included TEAEs, serious adverse events (SAEs), and AEs leading to withdrawal or death. Many studies reported specific AEs of interest, including hypertension, hyperkalemia, infections, and CV events. A minority of studies[18,25,31] also reported quality of life and functional status, although these were not the focus of this study.

A detailed summary of each study's design, population characteristics, and follow-up duration is provided in Table 1.

Risk of Bias Assessment

The Cochrane Collaboration's RoB 2 tool was used to evaluate the RoB in the included RCTs, focusing on the primary safety outcome. Overall, the quality of most studies was acceptable, with the vast majority of the trials judged to be at low RoB for the randomization process, missing outcome data, and selective reporting (Figure 2). However, the majority of trials were rated as having "some concerns" in at least one domain, most often due to the use of "as-treated" or "safety analysis set" population analyses instead of strict intention-to-treat (ITT), and to the prevalence of open-label designs. Open-label designs, used in most trials, introduce concerns regarding deviations from intended interventions and potential measurement bias in subjective safety outcomes. Two studies, including three trials[23,30], were judged to be at high RoB overall, primarily because of open-label designs, non-ITT safety analyses and potential co-intervention differences (i.e., oral iron), which increased the RoB.

Primary Outcome and Subgroup Analysis

A total of 13 RCTs involving 9.386 patients contributed data on the primary outcome of any serious TEAE[15-18,21,25-27,29-31,33,34]. In the pooled analysis, roxadustat was not associated with a significant increase in the risk of any serious TEAE compared with the ESA (RR=1.05, 95% CI: 0.99 to 1.10; I^2=59%) or with placebo (RR=1.37, 95% CI: 0.79 to 2.37; I^2=51%) (Figure 3). The absolute risk difference was 2.9 percentage points (95% CI: 0.5 to 5.2), corresponding to more events in the roxadustat group (absolute risks: 50.5% vs. 47.6% in the control group).

Table 1. Study characteristics of included trials.

First author, year	Country (ies)	Blinding status	Population	Sample size	Intervention	Control	Male (%)	Follow-up (weeks)
Besarab 2015	United States	Blinded	NDD-CKD	116	Roxadustat	Placebo	49	4
Provenzano 2016	United States	Open-label	DD-CKD	144	Roxadustat	Epoetin-alfa	66	19
Chen 2017[c]	China	Blinded	NDD-CKD	91	Roxadustat	Placebo	28.6	8
Chen 2017[d]	China	Open-label	DD-CKD	96	Roxadustat	Epoetin-alfa	60.4	6
Akizawa 2019	Japan	Blinded	NDD-CKD	107	Roxadustat	Placebo	46.7	24
Chen 2019[a]	China	Blinded	NDD-CKD	152	Roxadustat	Placebo	54.9	8
Chen 2019[b]	China	Open-label	DD-CKD	304	Roxadustat	Epoetin-alfa	60.5	26
Akizawa 2020	Japan	Blinded	DD-CKD	302	Roxadustat	Darbepoetin-alfa	69.1	24
Akizawa 2021	Japan	Open-label	NDD-CKD	262	Roxadustat	Darbepoetin-alfa	58.1	52
Barratt 2021	International (primarily European)	Open-label	NDD-CKD	616	Roxadustat	Darbepoetin-alfa	44.5	104
Charytan 2021	United States	Open-label	DD-CKD	740	Roxadustat	Epoetin-alfa	54.2	52
Coyne 2021	United States, South America, Australia, New Zealand, and Asia.	Blinded	NDD-CKD	916	Roxadustat	Placebo	39.6	52
Csiky 2021	International (primarily European)	Open-label	DD-CKD	834	Roxadustat	Epoetin-alfa, darbepoetin-alfa	57.6	52
Fishbane 2021	Multinational (Americas, Europe, and Asia)	Blinded	NDD-CKD	2761	Roxadustat	Placebo	42.3	164
Henry 2021	Multinational (North America, Europe, Asia, and Australia)	Open-label	MDS	140	Roxadustat	Placebo	50	52
Hou 2021	China	Open-label	DD-CKD	129	Roxadustat	ESAs	55.8	24
Provenzano 2021	Multinational (North America, South America, Europe, and Asia)	Open-label	DD-CKD	1039	Roxadustat	Epoetin-alfa	59	52
Shutov 2021	Multinational (Europe, South America, Central America, and Africa)	Blinded	NDD-CKD	594	Roxadustat	Placebo	45.1	104
Fishbane 2022	Multinational (North America, Europe, Asia, South America, and Australia)	Open-label	DD-CKD	2101	Roxadustat	Epoetin-alfa	59.4	208
Kong 2024	China	Open-label	PTA	128	Roxadustat	Oral iron	21	12
Tan 2024	China	Open-label	DD-CKD	114	Roxadustat	Epoetin-alfa	53.5	52

CKD: Chronic kidney disease, DD-CKD: Dialysis dependent CKD, NDD-CKD: Non-dialysis dependent CKD, MDS: Myelodysplastic syndrome, PTA: Posttransplant anemia, ESAs: Erythropoiesis-stimulating agents, [a, b]: Distinct study populations (NDD-CKD and DD-CKD, respectively) derived from the same trial. [c, d]: correspond to different independent studies.

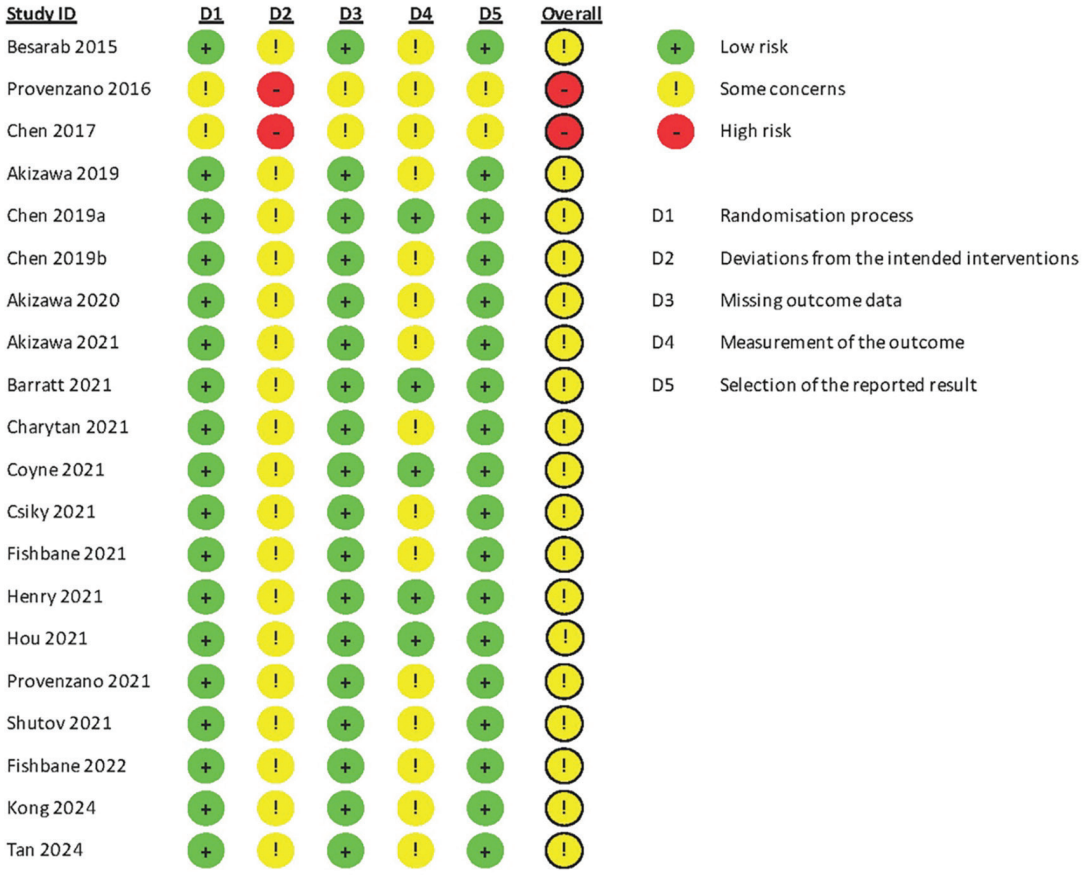

Figure 2. Risk of bias assessments of the included studies.

Prespecified subgroup analyses were conducted based on the dialysis status (DD-CKD vs. NDD-CKD), prior use of ESAs (ESA-naive vs. ESA-used), and comparators (placebo, ESA, or oral iron).

By Dialysis Status: In patients with DD-CKD, roxadustat did not significantly increase the risk of any serious TEAEs compared to control (RR=1.04, 95% CI: 0.98 to 1.10; I^2=0%). In contrast, among patients with NDD-CKD, a higher but not statistically significant risk was observed (RR=1.18, 95% CI: 0.85 to 1.63; I^2=29.1%). The test for subgroup interaction was not statistically significant (p=0.3884) (Figure S1).

Subgroup analysis by ESA status revealed an inconsistency. The RR for serious TEAEs in ESA-mixed patients was 1.04 (95% CI: 1.00 to 1.09); in ESA-experienced patients it was 1.10 (95% CI: 1.01 to 1.21); and in ESA-naive patients it was 5.50 (95% CI: 1.26 to 24.03, 1 RCT), with overlapping 95% CIs. The interaction test did not show significant subgroup differences (p=0.42; Figure S2).

According to the RoB assessment, only one study[29] that reported any serious TEAE; it had a high RoB (Figure S3). The RoB study assessed as "some concerns" reported an RR of 1.06 (95% CI: 1.01 to 1.11), whereas the high-RoB study showed an RR of 1.41 (95% CI: 0.65 to 3.23). Studies with some concerns about RoB remained consistent with the main analysis. Therefore, no definitive conclusion can be drawn regarding the influence of RoB on the treatment effect.

Secondary Outcomes

Cardiac Safety Outcomes: Six outcomes were analyzed to evaluate the cardiac safety of roxadustat: any cardiac AEs, any serious cardiac AEs, any TEAEs, hyperkalemia, hypertension, and peripheral edema (Table 2). The pooled analysis revealed comparable risks between roxadustat and control groups for any cardiac AEs (RR=0.93, 95% CI: 0.76 to 1.13; I^2=39.3%), any serious cardiac AEs (RR=1.01, 95% CI: 0.88 to 1.16; I^2=0%), any TEAE (RR=1.03, 95% CI: 0.97 to 1.09; I^2=21% vs. ESA, RR=0.79, 95% CI: 0.37 to 1.71; I^2=0% vs. oral iron and RR=1.02, 95% CI: 0.97 to 1.06; I^2=2%

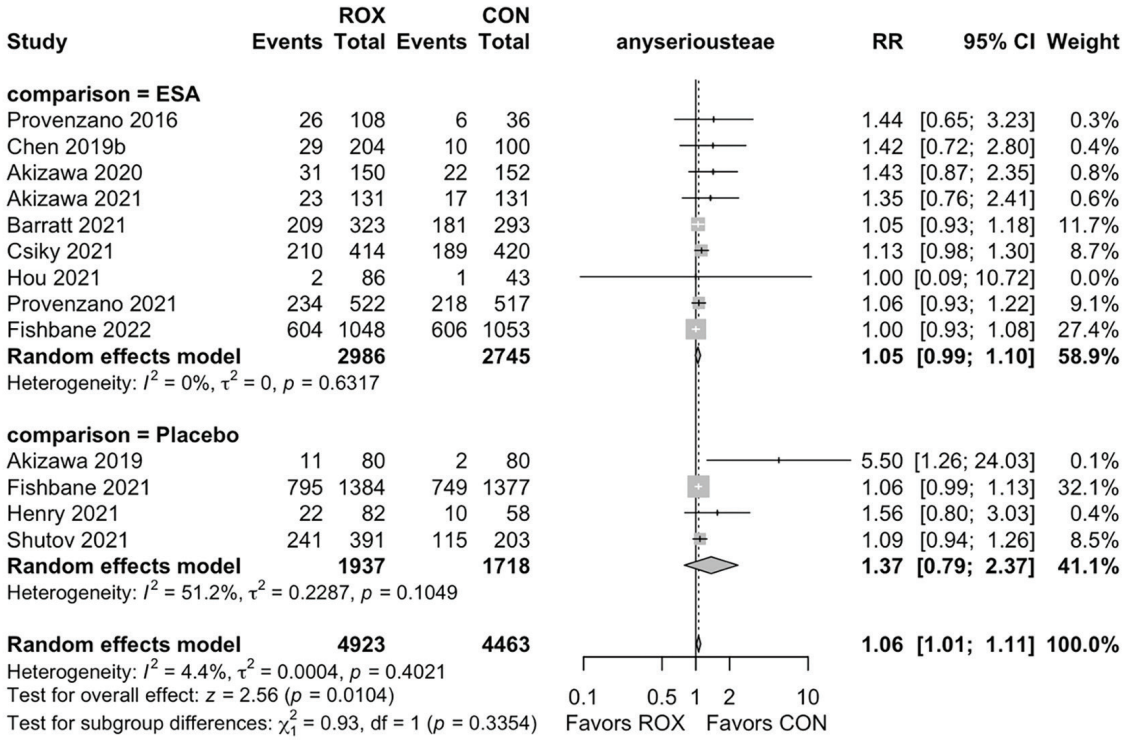

Figure 3. Effect of roxadustat on any serious TEAE by comparator ROX: Roxadustat, CON: Control, RR: Risk ratio, CI: Confidence interval, ESA: Erythropoiesis-stimulating agent, TEAE: Treatment-emergent adverse event

Table 2. Effects of roxadustat on cardiac safety outcomes.

Outcomes	Number of RCTs	Number of patients	Overall efect estimate RR (95% CI)	p-value	I-square (%)
Any cardiac AEs	7	5990	0.93 (0.76-1.13)	0.44	39
Any serious cardiac AEs	5	6020	1.01 (0.88-1.16)	0.8	0
Hyperkalemia	17	10315	1.12 (0.97-1.30)	0.10	0
Hypertension	16	10865	1.13 (1.01-1.26)	0.03	0
Pulmonary edema	8	5703	1.25 (0.98-1.60)	0.07	19

AEs: Adverse events, RCT: Randomized controlled trials, RR: Risk ratio, CI: Confidence interval

vs. placebo; Figure S4) and hyperkalemia (RR=1.03, 95% CI: 0.77 to 1.36; I^2=15% vs. ESA). Furthermore, roxadustat was associated with a 25% increased risk of hyperkalemia compared with placebo (RR=1.25, 95% CI: 1.02 to 1.53; I^2=0%) (Figure 4). Similarly, hypertension was significantly more frequent in patients treated with roxadustat compared with placebo (RR=1.31, 95% CI: 1.08 to 1.60; I^2=0%), but not when compared with ESA (RR=1.06, 95% CI: 0.93 to 1.21; I^2=0%) (Figure S5). Roxadustat was associated with a non-significant increase in the risk of peripheral edema (RR=1.25, 95% CI: 0.98 to 1.60; I^2=19.1%).

Mortality and Tolerability Outcomes: We examined how well patients tolerated roxadustat (Table 3). Patients receiving roxadustat were more likely to discontinue treatment because of AEs, with the risk of withdrawal nearly doubling compared with ESA (RR=2.11, 95% CI: 1.59 to 2.79; I^2=0%), but not compared with placebo (RR=1.57, 95% CI: 0.79 to 3.13; I^2=0%) (Figure S6). Importantly, roxadustat did not increase the risk of TEAEs leading to death (RR=1.07, 95% CI: 0.95-1.21; I^2=29.5%). Accordingly, we observed a notable reduction in all-cause mortality among those receiving roxadustat compared to placebo (RR=0.40, 95% CI: 0.28 to 0.57; I^2=13%), but not compared

to ESA (RR=0.89, 95% CI: 0.57 to 1.37; I²=0%) or to oral iron (RR=1.00, 95% CI: 0.01 to 71.75) (Figure S7). A sensitivity analysis excluding two trials that assessed posttransplant anemia or MDS did not change the direction of the effect estimate (Figure S8).

Infection-related Outcomes: We also examined whether roxadustat influenced the risk of infection (Table 4). The risk of experiencing any infection was similar between the roxadustat and control groups (RR=1.01, 95% CI: 0.68 to 1.49; I²=26.9%). When we focused on more severe events, such as infections (e.g., pneumonia), the results remained consistent. Serious infections occurred at similar rates (RR=1.05, 95% CI: 0.69 to 1.60; I²=0%) (Figure S9), and the risk of pneumonia showed no significant increase (RR=1.04, 95% CI: 0.91 to 1.19; I²=10.3%) (Figure S10). Again, when examining specific types of infections, such as urinary tract infections (UTIs) and upper respiratory tract infections, no notable differences were observed. Overall, these results suggest that roxadustat does not increase the likelihood of infectious complications.

Kidney-related Outcomes: We assessed several kidney-specific outcomes to explore whether roxadustat might adversely affect renal function (Table 5). The risk of any kidney-related AEs was similar among groups (RR=1.09, 95% CI: 0.88 to 1.36; I²=0%) (Figure S11). Similarly, the risks of azotemia (RR=1.00, 95% CI: 0.77 to 1.30; I²=0%), worsening CKD, and progression to end-stage kidney disease (ESKD) were comparable (Figures S12-S14).

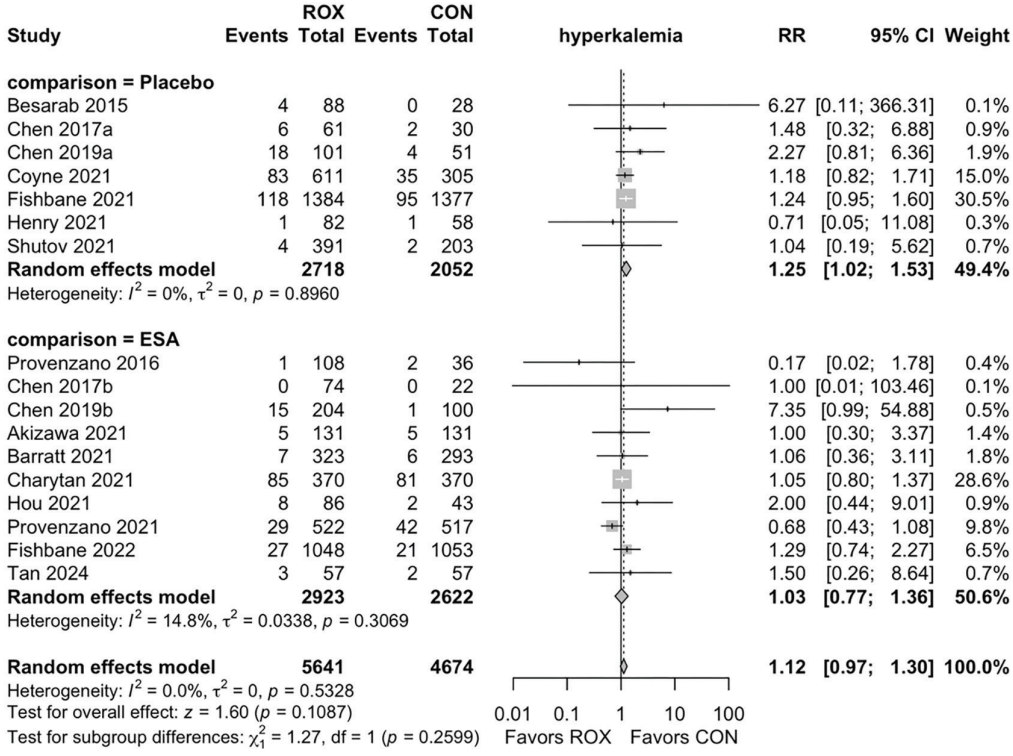

Figure 4. Effect of roxadustat on hyperkalemia by comparator ROX: Roxadustat, CON: Control, RR: Risk ratio, CI: Confidence interval, ESA: Erythropoiesis-stimulating agent

Table 3. Effects of roxadustat on mortality and tolerability outcomes.

Outcomes	Number of RCTs	Number of patients	Overall effect estimate RR (95% CI)	p-value	I-square (%)
All cause mortality	18	10510	0.56 (0.41-0.75)	0.0001	32
Withdrawal due to AE	7	4816	2.02 (1.56-2.62)	<0.0001	0
TEAE leading to death	6	7945	1.07 (0.95-1.21)	0.26	29
Any TEAE	15	8664	1.01 (0.99-1.04)	0.25	5

AE: Adverse event, RCT: Randomized controlled trials, TEAE: Treatment emergent adverse events, RR: Risk ratio, CI: Confidence interval

Table 4. Effects of roxadustat on infection-related outcomes.					
Outcomes	**Number of RCTs**	**Number of patients**	**Overall effect estimate RR (95% CI)**	**p-value**	**I-square (%)**
Any infections	4	669	1.01 (0.68-1.49)	0.97	27
Any serious infections	3	1027	1.05 (0.69-1.60)	0.81	0
Pneumonia	12	10299	1.04 (0.91-1.19)	0.58	10
Upper respiratory tract infection	15	8425	1.02 (0.85- 1.23)	0.79	29
Urinary tract infection	10	8993	1.03 (0.72-1.47)	0.88	58
RCT: Randomized controlled trials, RR: Risk ratio, CI: Confidence interval					

Table 5. Effects of roxadustat on kidney-related outcomes.					
Outcomes	**Number of RCTs**	**Number of patients**	**Overall Effect Estimate RR (95% CI)**	**p-value**	**I-square (%)**
Any kidney-related AEs	5	1383	1.09 (0.88-1.36)	0.41	0
Azotemia	7	7402	1.00 (0.77-1.30)	0.99	0
CKD worsening	5	1585	0.97 (0.64-1.46)	0.88	0
End-stage kidney disease	4	4423	1.06 (0.94-1.19)	0.37	0
AEs: Adverse events, CKD: Chronic kidney disease, RCT: Randomized controlled trials, RR: Risk ratio, CI: Confidence interval					

Stratified Analysis by Blinding Status: We stratified the included trials by blinding status to evaluate the potential influence of study design on key safety outcomes. For several outcomes—including pneumonia, hypertension, TEAEs leading to death, and all-cause mortality—the pooled effect estimates were consistent between blinded and open-label trials, with no statistically significant interaction observed (p for interaction >0.1 for all outcomes). Detailed results of these stratified analyses have been presented in Supplementary Figures S15-S[22].

DISCUSSION

We included nine trials on NDD-CKD, ten on DD-CKD, one on MDS, and one on post-transplant anemia. Data on kidney transplant recipients and children were scarce. In sum, our analysis revealed that roxadustat has uncertain effects on any TEAE, TEAEs leading to death, and CV AEs (e.g., hyperkalemia and pulmonary edema), but is associated with a mild increase in hypertension risk and a significant decrease in all-cause mortality. Comparable risks were also observed for infection-related parameters (any serious infections, pneumonia, UTIs etc.) and for kidney-related outcomes (azotemia, progression of CKD, ESKD, etc.) compared with placebo or ESA. However, we found that withdrawals due to AEs were 102% higher with roxadustat than with placebo or ESA.

The FDA did not approve the use of roxadustat for the treatment of anaemia in people with CKD, including those requiring dialysis, because HIF stabilisers were associated with a higher risk of thrombosis than placebo or ESA[35]. However, Roxadustat is currently approved for both indications in the European Union, China, Japan, Chile, South Korea, and Türkiye[36].

There were inconsistencies in adverse effects reported among published clinical trials, particularly regarding SAEs such as hyperkalemia, all-cause mortality, and serious infections. Several meta-analyses that assess the safety of roxadustat in specific populations or physiological systems, such as CV and renal systems employing different inclusion criteria and methodologies.

The Cochrane systematic review by Natale et al.[6] comprehensively evaluated the safety and efficacy of HIF-PHIs as a class effect in CKD. Across the class, HIF-PHIs were generally comparable to ESAs in achieving target Hb levels, with little or no difference in all-cause mortality (RR=0.98, 95% CI: 0.91 to 1.06; I^2=0%), myocardial infarction (RR=0.91, 95% CI: 0.76 to 1.10; I^2=0%), and hyperkalemia (RR=0.92, 95% CI: 0.82 to 1.04; I^2=10%) when compared with ESAs; however, roxadustat may be associated with an increased risk compared with placebo (RR= 1.29, 95% CI: 1.01 to 1.64; I^2=18%). However, subgroup analysis based on specific agents was not applied in the study.

In a meta-analysis conducted by Zhou et al.[37] to assess the safety of roxadustat in patients with DD-CKD — which included 10 RCTs (published in 9 studies) and 5698 patients —the risk of any TEAE (RR=1.02, 95%CI: 1.00-1.05, p=0.11), any serious TEAE (RR=1.05, 95%CI: 0.99-1.12, p=0.11), and major CV events (RR=1.04, 95% CI: 0.85-1.28, p=0.70) was found to be comparable to ESAs. The main difference between our study and others is that ours included studies regardless of etiology or comparator (21 RCTs involving 11,546 patients). Furthermore, we found a mild but statistically significant increase in the risk of any serious TEAE with roxadustat (RR=1.06, 95% CI: 1.01-1.11, p=0.0104). In addition, Zhou et al.[37] used the Mantel-Haenszel (M-H) fixed-effect weighting model for any serious TEAE. This is problematic because, when data are sparse—either due to low event risks or small study sizes— the estimates of the standard errors of the effect estimates used in inverse-variance methods may be poor[38]. M-H has been recommended by the Cochrane Collaboration as having better statistical properties when there are few events[39]. Also, the authors[37] used Cochrane RoB v1 for assessing RoB, which was updated to the Cochrane RoB2 tool that we used. These methodological differences were the main causes of our results.

In the meta-analysis conducted by Tian et al.[40], data from 18 studies with a total of 8.806 CKD patients were included. Serious cardiac-related AEs were not significantly increased in the roxadustat group, regardless of dialysis status[40]. However, we found that roxadustat notably increased the incidence of hypertension (RR=1.13; 95% CI: 1.01-1.26; p=0.03). Our finding overlapped with that of this study, highlighting an increased incidence of hypertension, particularly in NDD-CKD populations, compared to placebo[40]. Also, both studies found that the risk of hypertension was comparable among DD-CKD patients. Furthermore, that study[40] evaluated the risk of hypertension using a meta-regression analysis by continent (US, Asia, and Europe), but no significant differences were found.

Hou et al.[41] also evaluated the safety profile of roxadustat in patients with CKD. They reported that the incidence of AEs and SAEs was significantly higher in the roxadustat group than in the control group[41]. In another study, Zhang et al.[42] reported no differences in any TEAEs and any serious AEs between roxadustat and placebo or ESA groups in the same population; however, hyperkalemia and withdrawal due to AEs were more common in the roxadustat group than in the control group[42]. Our findings align with the study by Zhang et al.[42] but not with Hou et al.[41], as roxadustat was associated with a significantly higher risk of any serious TEAE, and withdrawals due to AEs were significantly increased in the roxadustat group compared with the control group. As M-H methods are fixed-effect meta-analysis methods using different weighting schemes[39], Zhang et al.[42] used M-H random effects, which resulted in differences in pooled effect sizes. Also, one of the major strengths of our study is the inclusion of 21 RCTs (published in 20 studies) with detailed subgroup analyses based on comparator, ESA status, and etiology of the anemia.

Our findings for all-cause mortality (RR=0.56, 95% CI: 0.41-0.75; p=0.0001) and hyperkalemia (RR=1.12, 95% CI: 0.97-1.30; p=0.11) were notable. There was inconsistency between these two outcomes in the published literature. Several meta-analysis found an increase in risk of hyperkalemia[40,42,43] but some not[6,37,44]. Similarly, some meta-analyses showed a comparable risk of all-cause mortality associated with roxadustat. Lei et al.[43] (included 16 RCTs, 6518 patients) and Tian et al.[40] reported that roxadustat treatment increased the risk of hyperkalemia by 36% in NDD-CKD and by 41% regardless of dialysis status, respectively. However, Zhou et al.[37] (2023) (10 RCTs, 5698 DD-CKD) reported no increased risk of hyperkalemia (RR=1.07; 95% CI: 0.70-1.64; p=0.75).

The study by Li et al.[45] aimed to compare the CV safety of roxadustat and ESAs in patients with CKD-related anemia, using a combination of meta-analysis and bioinformatics approaches. While the authors reported that their pooled analysis included data on 143,065 patients from 15 articles, this study is poorly substantiated[45]. Only three of the included RCTs (20, 26, 30) in study[45] actually assessed the safety of roxadustat, whereas the remaining trials primarily evaluated the safety profiles of ESAs. The authors applied an indirect comparison between the two groups; however, no justification was provided for excluding other eligible roxadustat trials. This lack of transparency in trial selection raises concerns regarding selection bias. Given the small number of roxadustat-specific RCTs and the predominance of ESA studies, pooled estimates for roxadustat[45] may be disproportionately influenced by indirect evidence, thereby posing a high risk of selection bias[46] and reducing the reliability of the conclusions.

Study Limitations

This meta-analysis has several limitations. First, although we included 21 RCTs, heterogeneity in study design, patient populations, follow-up durations, and comparator arms may have influenced the pooled estimates. Second, most trials were open-label and assessed safety outcomes using "as-treated" or "safety analysis set" populations rather than strict ITT, which may introduce bias. Third, missing outcome data and selective reporting of AEs, combined with variability in outcome definitions across trials, may further bias results.

CONCLUSION

Roxadustat was associated with a mildly increased risk of hypertension and a markedly higher rate of withdrawal from treatment due to AEs, while risks of serious cardiac AEs, serious infections, and kidney-related outcomes remained comparable to controls. Notably, all-cause mortality was significantly lower in the roxadustat group. Across 21 trials involving NDD-CKD, DD-CKD, MDS, and posttransplant anemia, evidence for kidney transplant recipients and children was scarce. Overall, roxadustat showed uncertain effects on the occurrence of any TEAEs, any serious TEAEs, and CV events such as hyperkalemia and pulmonary edema, but demonstrated a consistent mortality benefit. Future studies should address the use of roxadustat in specific populations (e.g., children and patients with post-transplant anemia), switching from ESAs, cost-effectiveness, important outcomes such as health-related quality of life and patient-reported measures.

In this meta-analysis of 21 RCTs including 11.686 patients, roxadustat demonstrated an overall safety profile comparable to that of ESAs. Rates of SAEs, including cardiac events, serious infections, azotemia, hypertension, and pneumonia, did not differ significantly between roxadustat and ESA. Hyperkalemia occurred more frequently than with placebo, and treatment withdrawal due to AEs was more frequent than with ESA. While all-cause mortality was reduced compared with placebo and was similar to that with ESA, treatment-emergent events leading to death were increased compared with placebo but not with ESA. Notably, stratified analyses by blinding status did not materially alter the direction or significance of key outcomes, supporting the robustness of the primary findings. Overall, current evidence indicates that roxadustat is non-inferior to ESA with respect to safety.

Ethics

Ethics Committee Approval: Approval to conduct the study was obtained from the Malatya Non-Interventional Clinical Research Ethics Committee (approval number: 2025/7455, date: 25.03.2025).

Informed Consent: As this meta-analysis used only aggregated data from published RCTs, informed consent was not required.

Footnotes

Author Contributions

Concept: L.H.T., A.S., M.A.E., H.B.B., Design: L.H.T., M.A.E., H., Data Collection and/or Processing: L.H.T., A.S., H.B.B., Analysis or Interpretation: L.H.T., M.A.E., H.B.B., Literature Search: L.H.T., A.S., H.B.B., Writing: L.H.T., A.S., M.A.E., H.B.B.

Conflict of Interest: The authors have no conflict of interest to declare.

Financial Disclosure: The authors declared that this study has received no financial support.

REFERENCES

1. Lopez A, Cacoub P, Macdougall IC, Peyrin-Biroulet L. Iron deficiency anaemia. Lancet. 2016;387:907-16.
2. Fishbane S, Spinowitz B. Update on anemia in ESRD and earlier stages of CKD: Core Curriculum 2018. Am J Kidney Dis. 2018;71:423-35.
3. Gafter-Gvili A, Schechter A, Rozen-Zvi B. Iron deficiency anemia in chronic kidney disease. Acta Haematol. 2019;142:44-50.
4. Bhandari S, Spencer S, Oliveira B, et al. UK kidney association clinical practice guideline: update of anaemia of chronic kidney disease. BMC Nephrol. 2025;26:193.
5. Tanriverdi LH, Tay M, Sarici A. Efficacy and safety of molidustat for the anemia of chronic kidney disease: a systematic review and meta-analysis of randomized controlled trials. Annals of Medical Research. 2024;31:177-84.
6. Natale P, Palmer SC, Jaure A, et al. Hypoxia-inducible factor stabilisers for the anaemia of chronic kidney disease. Cochrane Database Syst Rev. 2022;8:CD013751.
7. Odawara M, Nishi H, Nangaku M. A spotlight on using HIF-PH inhibitors in renal anemia. Expert Opin Pharmacother. 2024;25:1291-9.
8. Gul MH, Waheed A, Jha M, Wardak AB, Ilma B, Khan U. Revolutionizing anemia management in dialysis: unveiling the potential of FDA-approved Vadadustat for chronic kidney disease (CKD) patients. Ann Med Surg (Lond). 2025;87:1094-6.
9. Wang Y, Yu X. Stabilizing hypoxia-inducible factor to manage anemia in chronic kidney disease: from basic theory to clinical study. Kidney Dis (Basel). 2024;10:132-42.
10. Macdougall IC. Hypoxia-inducible factor prolyl hydroxylase enzyme inhibitors: ready for primetime? Curr Opin Nephrol Hypertens. 2022;31:399-405.
11. Sterne JAC, Savović J, Page MJ, et al. RoB 2: a revised tool for assessing risk of bias in randomised trials. BMJ. 2019;366:l4898.
12. Higgins JP, Thompson SG. Quantifying heterogeneity in a meta-analysis. Stat Med. 2002;21:1539-58.
13. Richardson M, Garner P, Donegan S. Interpretation of subgroup analyses in systematic reviews: a tutorial. Clinical Epidemiology and Global Health. 2019;7:192-8.
14. Page MJ, McKenzie JE, Bossuyt PM, et al. Updating guidance for reporting systematic reviews: development of the PRISMA 2020 statement. J Clin Epidemiol. 2021;134:103-12.
15. Akizawa T, Iwasaki M, Otsuka T, Reusch M, Misumi T. Roxadustat treatment of chronic kidney disease-associated anemia in japanese patients not on dialysis: a phase 2, randomized, double-blind, placebo-controlled trial. Adv Ther. 2019;36:1438-54.
16. Akizawa T, Iwasaki M, Otsuka T, Yamaguchi Y, Reusch M. Phase 3 study of roxadustat to treat anemia in non-dialysis-dependant CKD. Kidney Int Rep. 2021;6:1810-28.
17. Akizawa T, Iwasaki M, Yamaguchi Y, Majikawa Y, Reusch M. Phase 3, Randomized, Double-Blind, Active-Comparator (Darbepoetin

Alfa) Study of Oral Roxadustat in CKD Patients with Anemia on Hemodialysis in Japan. J Am Soc Nephrol. 2020;31:1628-39.

18. Barratt J, Andric B, Tataradze A, et al. Roxadustat for the treatment of anaemia in chronic kidney disease patients not on dialysis: a Phase 3, randomized, open-label, active-controlled study (DOLOMITES). Nephrol Dial Transplant. 2021;36:1616-28.
19. Besarab A, Provenzano R, Hertel J, et al. Randomized placebo-controlled dose-ranging and pharmacodynamics study of roxadustat (FG-4592) to treat anemia in nondialysis-dependent chronic kidney disease (NDD-CKD) patients. Nephrol Dial Transplant. 2015;30:1665-73.
20. Charytan C, Manllo-Karim R, Martin ER, et al. A randomized trial of roxadustat in anemia of kidney failure: SIERRAS study. Kidney Int Rep. 2021;6:1829-39.
21. Chen N, Hao C, Liu BC, et al. Roxadustat treatment for anemia in patients undergoing long-term dialysis. N Engl J Med. 2019;381:1011-22.
22. Chen N, Hao C, Peng X, et al. Roxadustat for anemia in patients with kidney disease not receiving dialysis. N Engl J Med. 2019;381:1001-10.
23. Chen N, Qian J, Chen J, et al. Phase 2 studies of oral hypoxia-inducible factor prolyl hydroxylase inhibitor FG-4592 for treatment of anemia in China. Nephrol Dial Transplant. 2017;32:1373-86.
24. Coyne DW, Roger SD, Shin SK, et al. Roxadustat for CKD-related anemia in non-dialysis patients. Kidney Int Rep. 2020;6:624-35.
25. Csiky B, Schömig M, Esposito C, et al. Roxadustat for the maintenance treatment of anemia in patients with end-stage kidney disease on stabledialysis: a european phase 3, randomized, open-label,active-controlled study (PYRENEES). Adv Ther. 2021;38:5361-80.
26. Fishbane S, Pollock CA, El-Shahawy M, et al. Roxadustat versus epoetin alfa for treating anemia in patients with chronic kidney disease on dialysis: results from the randomized phase 3 ROCKIES study. J Am Soc Nephrol. 2022;33:850-66.
27. Henry DH, Glaspy J, Harrup R, et al. Roxadustat for the treatment of anemia in patients with lower-risk myelodysplastic syndrome: Open-label, dose-selection, lead-in stage of a phase 3 study. Am J Hematol. 2022;97:174-84.
28. Kong W, Wu X, Shen Z, et al. The efficacy and safety of roxadustat for the treatment of posttransplantation anemia: a randomized study. Kidney Int Rep. 2024;9:1705-17.
29. versus epoetin alfa for anemia in patients receiving maintenance hemodialysis: a phase 2, randomized, 6- to 19-week, open- label, active-comparator,dose-ranging, safety and exploratory efficacy study. Am J Kidney Dis. 2016;67:912-24.
30. Provenzano R, Shutov E, Eremeeva L, et al. Roxadustat for anemia in patients with end-stage renal disease incident to dialysis. Nephrol Dial Transplant. 2021;36:1717-30.
31. Shutov E, Sułowicz W, Esposito C, et al. Roxadustat for the treatment of anemia in chronic kidney disease patients not on dialysis: a phase 3, randomized, double-blind, placebo-controlled study (ALPS). Nephrol Dial Transplant. 2021;36:1629-39.
32. Tan W, Wang X, Sun Y, et al. Roxadustat reduces left ventricular mass index compared to rHuEPO in haemodialysis patients in a randomized controlled trial. J Intern Med. 2024;295:620-33.
33. Fishbane S, El-Shahawy MA, Pecoits-Filho R, et al. Roxadustat for treating anemia in patients with CKD not on dialysis: results from a randomized phase 3 study. J Am Soc Nephrol. 2021;32:737-55.
34. Hou YP, Mao XY, Wang C, et al. Roxadustat treatment for anemia in peritoneal dialysis patients: a randomized controlled trial. J Formos Med Assoc. 2022;121:529-38.
35. US Food & Drug Administration. Cardiovascular and Renal Drugs Advisory Committee. [Jul; 2021]; https://www.fda.gov/advisory-committees/human-drug-advisory-committees/cardiovascular-and-renal-drugs-advisory-committee URL: https://www.fda.gov/media/150728/download.; 2021.
36. Locatelli F, Ravera M, Esposito C, Grandaliano G, Gesualdo L, Minutolo R. A novel scenario in the therapeutic management of anemia of chronic kidney disease: placement and use of roxadustat. J Nephrol. 2024;37:1107-19.
37. Zhou Q, Mao M, Li J, Deng F. The efficacy and safety of roxadustat for anemia in patients with dialysis-dependent chronic kidney disease: a systematic review and meta-analysis. Ren Fail. 2023;45:2195011.
38. Mantel N, Haenszel W. Statistical aspects of the analysis of data from retrospective studies of disease. J Natl Cancer Inst. 1959;22:719-48.
39. Higgins J, Thomas J, Chandler J, Cumpston M, Li T, Page M. Cochrane Handbok for Systematic Reviews of Interventions. Version 6.4 (Updated August 2023). Cochrane, 2023. 2024.
40. Tian L, Wang M, Liu M, et al. Cardiovascular and renal safety outcomes of hypoxia-inducible factor prolyl-hydroxylase inhibitor roxadustat for anemia patients with chronic kidney disease: a systematic review and meta-analysis. Ren Fail. 2024;46:2313864.
41. Hou YP, Wang C, Mao XY, Zhang MZ, Li B. Roxadustat regulates iron metabolism in dialysis-dependent and non-dialysis-dependent chronic kidney disease patients: a meta-analysis. J Formos Med Assoc. 2022;121:2288-99.
42. Zhang L, Hou J, Li J, Su SS, Xue S. Roxadustat for the treatment of anemia in patients with chronic kidney diseases: a meta-analysis. Aging (Albany NY). 2021;13:17914-29.
43. Lei J, Li H, Wang S. Efficacy and safety of roxadustat in patients with chronic kidney disease: an updated meta-analysis of randomized controlled trials including 6,518 patients. Biomed Res Int. 2022;2022:2413176.
44. Liu J, Zhang A, Hayden JC, et al. Roxadustat (FG-4592) treatment for anemia in dialysis-dependent (DD) and not dialysis-dependent (NDD) chronic kidney disease patients: a systematic review and meta-analysis. Pharmacol Res. 2020;155:104747.
45. Li X, Jiang S, Gu X, et al. Assessment of the safety of Roxadustat for cardiovascular events in chronic kidney disease-related anemia using meta-analysis and bioinformatics. Front Pharmacol. 2024;15:1380326.
46. Egger M, Smith GD. Bias in location and selection of studies. BMJ. 1998;316:61-6.

Supplementary Figures: https://d2v96fxpocvxx.cloudfront.net/07d42497-fb2b-47e0-be2f-8805fa940376/content-images/a2f75693-b42d-42a0-af5b-3e0c997cce26.pdf

DOI: 10.4274/MMJ.galenos.2025.15043
Medeni Med J 2025;40:262-268

Original Article

Serum Podocalyxin Level as a Potential Biomarker for Diagnosis of Nephrotic Syndrome and Prediction of Steroid Response

Nefrotik Sendromun Tanısı ve Steroid Yanıtının Tahmininde Potansiyel Biyobelirteç Olarak Serum Podokaliksin Düzeyi

Emre LEVENTOGLU[1], Mustafa SORAN[1], Ummugulsum CAN[2]

[1]Konya City Hospital, Clinic of Pediatric Nephrology, Konya, Türkiye
[2]Konya City Hospital, Clinic of Medical Biochemistry, Konya, Türkiye

ABSTRACT

Objective: Idiopathic nephrotic syndrome (NS) is a common pediatric glomerular disorder. Podocyte damage constitutes a central mechanism in its pathophysiology. Podocalyxin, a major sialoglycoprotein expressed on podocytes, has been found to be elevated in urine samples from patients with glomerular diseases. However, its potential role in serum and its association with steroid responsiveness in NS remain unexplored.

Methods: This observational study included 17 children diagnosed with NS and age-matched controls without kidney pathology. Serum podocalyxin levels were measured at diagnosis using enzyme-linked immunosorbent assay. Patients received standard corticosteroid therapy at a dose of 2 mg/kg/day for four weeks, followed by a gradual taper. Based on clinical response, patients were classified as steroid-sensitive or steroid-dependent NS (SDNS). Serum podocalyxin levels were compared between patients and controls, and among subgroups based on treatment response.

Results: Serum podocalyxin levels were significantly higher in NS than in the control group [1.87 ng/dL [interquartile range (IQR: 0.87)] vs. 1.54 ng/dL (IQR: 0.29), p=0.031]. All patients initially achieved remission with corticosteroids; however, six patients subsequently developed SDNS. Among these, 4 responded to calcineurin inhibitors, while 2 required rituximab to achieve remission. Current results indicate that serum podocalyxin levels do not provide sufficient predictive value for estimating steroid response or disease course. No significant correlations were found between podocalyxin levels and other laboratory parameters.

Conclusions: Serum podocalyxin levels are elevated in pediatric NS and may reflect the degree of podocyte injury. However, current findings indicate that serum podocalyxin levels are insufficient for predicting disease severity or steroid response. Additional studies involving larger patient cohorts are needed to further substantiate findings.

Keywords: Children, nephrotic syndrome, podocalyxin, steroid response

ÖZ

Amaç: İdiyopatik nefrotik sendrom (NS), yaygın bir pediatrik glomerüler bozukluktur. Podosit hasarı, patofizyolojisinde önemli bir rol oynar. Podositlerde eksprese edilen başlıca sialoglikoprotein olan podokalsin, glomerüler hastalıkları olan hastaların idrar örneklerinde yüksek seviyelerde bulunmuştur. Ancak, serumdaki potansiyel rolü ve NS'de steroid yanıtıyla ilişkisi henüz araştırılmamıştır.

Yöntemler: Bu gözlemsel çalışmaya, NS tanısı konmuş 17 çocuk ve böbrek patolojisi olmayan yaşıtları kontrol grubu olarak dahil edilmiştir. Serum podokalsin düzeyleri, tanı sırasında enzim bağlantılı immünosorbent analiz kullanılarak ölçülmüştür. Hastalar standart kortikosteroid tedavisi (4 hafta boyunca 2 mg/kg/gün) almış, ardından doz kademeli olarak azaltılmıştır. Klinik yanıtlara göre, hastalar steroid duyarlı veya steroid bağımlı NS (SDNS) olarak sınıflandırılmıştır. Serum podokalsin düzeyleri, hastalar ve kontrol grubu arasında ve tedavi yanıtına göre alt gruplar arasında karşılaştırıldı.

Bulgular: Sonuçlar, NS'de kontrol grubuna kıyasla serum podokalsin düzeylerinin anlamlı olarak daha yüksek olduğunu ortaya koydu [1,87 ng/dL çeyrekler arası aralık (IQR: 0,87) vs. 1,54 ng/dL (IQR: 0,29), p=0,031]. Tüm hastalar başlangıçta kortikosteroidlerle remisyon elde etmişlerdir; ancak 6'sı (%35,2) SDNS geliştirmiştir. Bunların 4'ü kalsinörin inhibitörlerine yanıt verirken, 2'si remisyon elde etmek için rituksimaba ihtiyaç duymuştur. Mevcut sonuçlar serum podokaliksin seviyesinin steroid yanıtını veya hastalık seyrini tahmin etmek için yeterli öngörüye sahip olmadığını göstermiştir. Ayrıca, podokalsin düzeyleri ile diğer laboratuvar parametreleri arasında anlamlı bir korelasyon bulunmamaktadır.

Sonuçlar: Serum podokalsin düzeyleri pediatrik NS'de yüksektir ve podosit hasarının derecesini yansıtabilir. Ancak, mevcut bulgular serum podokaliksin düzeylerinin hastalığın ciddiyetini veya steroid yanıtını tahmin etmek için yetersiz olduğunu göstermektedir. Daha büyük kohortlarla daha fazla çalışma yapılması gerekmektedir.

Anahtar kelimeler: Çocuklar, nefrotik sendrom, podokalsin, steroid yanıtı

A preliminary version of this study was previously presented as a poster at the 57th Annual Meeting of the European Society for Paediatric Nephrology (ESPN) in Athens, Greece. The abstract of this presentation was published in the congress abstract book.*

Address for Correspondence: E. Leventoglu, Konya City Hospital, Clinic of Pediatric Nephrology, Konya, Türkiye
E-mail: dremrelevent@gmail.com **ORCID ID:** orcid.org/0000-0002-0504-7911

Cite as: Leventoglu E, Soran M, Can U. Serum podocalyxin level as a potential biomarker for diagnosis of nephrotic syndrome and prediction of steroid response. Medeni Med J. 2025;40:262-268

Received: 07.08.2025
Accepted: 26.11.2025
Published: 31.12.2025

INTRODUCTION

Idiopathic nephrotic syndrome (NS) is a clinical entity characterized by heavy proteinuria, hypoalbuminemia, edema, and hyperlipidemia. Light microscopy typically demonstrates minimal structural alterations; however, electron microscopy reveals substantial glomerular podocyte injury characterized by diffuse foot-process effacement and disruption of the slit diaphragm[1]. The integrity of foot processes and the slit diaphragm is crucially maintained by the specialized protein complexes. Any abnormalities of these molecules result in severe proteinuria[2].

Podocalyxin is a sialoglycoprotein that constitutes a major structural component of the podocyte glycocalyx[3]. It interacts with the actin cytoskeleton of the podocytes, facilitating the normal formation of the negatively charged surface of the foot processes[4]. Its expression was universally reduced in patients with podocytopathies such as minimal change disease, focal segmental glomerulosclerosis, membranous nephropathy, and lupus nephritis[5,6]. Although podocalyxin expression is reduced, urinary podocalyxin levels are markedly elevated in patients with NS[7]. Elevated urinary podocalyxin levels have also been observed in patients with immunoglobulin A (IgA) nephropathy, IgA vasculitis-associated nephritis, and diabetic nephropathy[8,9]. In addition to podocytes, podocalyxin is expressed on the surface of vascular endothelial cells in several organs, such as the heart, lungs, and kidneys. It contributes to the maintenance of vascular integrity by modulating interactions with the extracellular matrix and basement membranes[10]. In preeclamptic women with endothelial damage, serum and urinary podocalyxin levels increase[11].

Serum podocalyxin levels have not previously been assessed in NS. The objectives of this study were to investigate the diagnostic utility of serum podocalyxin levels in pediatric NS and to assess their ability to predict response to steroid therapy.

MATERIALS and METHODS

Selection of Study Subjects and Definitions

This observational study was conducted in children with NS who had regular-follow-up at the tertiary pediatric nephrology clinic of a single hospital. Fifty-one age- and sex-matched children without tubular and/or glomerular pathology were used as the control group. Patients with known cardiovascular disease were excluded. All participants enrolled in the study were between 2 and 18 years of age. Written informed consent was obtained from all participants and their parents before enrollment.

The NS was identified by massive proteinuria (spot urine protein:creatinine ratio (UPCR) >2.0 mg/mg or proteinuria >40 mg/m^2/hour), hypoalbuminemia (<2.5 g/dL), and edema[1]. The standard treatment for idiopathic NS is prednisolone administered orally at 2 mg/kg per day (maximum 60 mg per day) for 4 weeks. Patients in complete remission who had trace or negative protein on urinalysis for three consecutive days were considered to have steroid-sensitive NS. In these patients, steroid therapy was continued on alternate days for another 4 weeks. Afterwards, the daily dose is usually tapered over 2-4 months and then discontinued. Relapse was defined by the presence of 2+ protein on the urinary albumin dipstick on three consecutive days after complete remission. In the event of a relapse, steroid treatment is resumed. Steroid-dependent NS (SDNS) was diagnosed when two consecutive relapses occurred during tapering of prednisone or prednisolone, or within 15 days of steroid withdrawal[12,13].

Data Collection and Assessment of Laboratory Parameters

Participants' actual age, sex, weight, height, and blood pressure were recorded. Weight gain was calculated for patients whose weight had been recorded before the onset of NS. Patients with a history of upper respiratory tract infection (URTI) were identified. Z-scores for height and weight were derived from the reference standards reported by Neyzi et al.[14] Blood pressure was assessed using a manual auscultatory method. Hypertension was identified in accordance with the 2017 "Clinical Practice Guideline for Screening and Management of High BP in Children and Adolescents"[15].

Laboratory results for participants at their initial presentation were recorded. Biochemical tests, including serum creatinine, albumin, electrolytes, urinalysis, and UPCR, were recorded. In addition to routine tests, serum podocalyxin levels were measured using a competitive enzyme-linked immunosorbent assay. The assay plate supplied with the kit was pre-coated with an antibody directed against human podocalyxin. Samples or standards were added to the wells, where they bound to the specific antibody. Next, a biotinylated detection antibody specific for human podocalyxin and an avidin-horseradish peroxidase (HRP) conjugate were added sequentially to each well and then incubated. Unbound components were removed by washing. A substrate solution was then added to each well. Only wells containing human podocalyxin, the biotinylated

detection antibody, and the avidin-HRP conjugate would develop a blue color. The enzymatic reaction was terminated by the addition of a stop solution, resulting in a color change to yellow. Absorbance was subsequently measured at 450 nm using a spectrophotometer and found to be proportional to the human podocalyxin concentration. Sample concentrations were calculated by comparison with a standard calibration curve.

Patients were started on treatment according to the Kidney Disease: Improving Global Outcomes 2021 Glomerular Disease Management Guidelines[12]. At week 4 of treatment, patients were divided into subgroups based on steroid response. Whether serum podocalyxin levels at diagnosis differed between patient and control groups and by steroid response was evaluated.

The authors confirm that all procedures performed in this study were conducted in accordance with national ethical guidelines for human research and the Declaration of Helsinki. The study was approved by the KTO Karatay University Medical Ethics Committee with decision no.:2024/257, date:18.12.2024.

Statistical Analysis

Data normality was evaluated using the Shapiro-Wilk test. Non-normally distributed continuous variables were summarized using the median and interquartile range (IQR), while categorical data were reported as numbers and percentages. Comparisons between two independent groups were performed using the Mann-Whitney U test for non-normally distributed data. The relationships between serum podocalyxin levels and other clinical or laboratory parameters were assessed using simple linear regression. Regression equations, adjusted R^2 values, and p-values were presented. Categorical variables were compared using Fisher's exact test and the chi-square test. A p-value <0.05> was considered statistically significant. All statistical analyses were performed using IBM SPSS Statistics, version 22.

RESULTS

General Study Population

A total of 17 patients diagnosed with idiopathic NS were included in the study. The median age was 5.9 years (IQR: 5.6), with a male-to-female ratio of 2.4. All patients were diagnosed on presentation with edema; 7 patients (41.1%) developed edema following a non-specific URTI. None of the patients had symptoms or findings such as fever, rash, arthralgia, or myalgia.

At admission, the median height standard deviation score (SDS) and weight SDS were -0.23 (IQR: 1.49) and 0.01 (IQR: 1.31), respectively. In patients with a known previous weight (n=13), the median weight gain at the time of admission was 2.20 kg (IQR: 2.85 kg). All patients were normotensive. Laboratory examination showed a median serum creatinine level of 0.21 mg/dL (IQR: 0.14) and a median serum albumin level of 1.95 g/dL (IQR: 0.50). The UPCR was 6.21 mg/mg (IQR: 2.78). Median erythrocyte count in urine was 4/high-power field (IQR: 17); 3 (17.6%) patients had microscopic hematuria. No bacterial growth was detected in urine cultures. Viral markers were negative. Immunologic assessment revealed negative results for antinuclear antibodies, anti-neutrophil cytoplasmic antibodies, and anti–double-stranded DNA antibodies. The median complement C3 level was 86.5 mg/dL (IQR, 19.6 mg/dL; normal range, 80-178 mg/dL).

All patients received oral prednisolone at a dose of 2 mg/kg per day (maximum 60 mg/day). After four weeks of treatment, remission was achieved in all of them. However, SDNS was observed in six (35.2%) patients during prednisone tapering. Complete remission was achieved in 4 (66.6%) of these patients after a calcineurin inhibitor (CNI) was added to the treatment. In the remaining two (33.3%) patients, relapses continued despite CNI during steroid tapering. In these patients, remission was achieved with rituximab.

The clinical and laboratory features of the participants are summarized in Table 1.

Assessments of Podocalyxin Levels in Predicting Steroid Response

At initial presentation, the median serum podocalyxin level in patients was higher than that in the control group [1.87 ng/dL (IQR: 0.87) vs. 1.54 ng/dL (IQR: 0.29); p=0.031] (Figure 1). Also, its median level at diagnosis was numerically higher in patients who developed SDNS than in patients who never relapsed; however, this difference did not reach statistical significance [1.95 ng/dL (IQR: 1.17) vs. 1.65 ng/dL (IQR: 0.92), p=0.148]. Evaluations of podocalyxin levels in relation to clinical characteristics and steroid response are shown in Table 2.

In the linear regression analysis, no significant relationship was found between serum podocalyxin levels and other laboratory data (Table 3).

Table 1. Clinical and laboratory characteristics of the patients.			
	General study group		
Initial Features	**n (%)**	**Median (IQR)**	**Min-max**
Age (years)		5.9 (5.6)	1.9-15.6
Sex			
Male	12 (70.5)		
Female	5 (29.5)		
History of URTI	7 (41.1)		
Anthropometric measures			
Height (SDS)		-0.23 (1.49)	-2.11-1.09
Weight (SDS)		0.01 (1.31)	-1.55-0.97
Weight gain (kg) (n=13)		2.20 (2.85)	1.5-5.4
Blood pressure measurements			
SBP (SDS)		-0.22 (1.12)	-0.66-0.99
DBP (SDS)		0.44 (0.85)	-0.08-1.48
Hypertension	0 (0)		
Blood			
Hemoglobin (g/dL)		13.1 (1.6)	11.5-16.3
Hematocrit (%)		41.7 (5.4)	34.7-51.5
Platelets (/μL)		379000 (164500)	199000-562000
White blood cell (/μL)		10035 (6415)	6150-18150
Creatinine (mg/dL)		0.21 (0.14)	0.17-0.75
BUN (mg/dL)		11 (10)	5-43
Uric acid (mg/dL)		4.1 (1.9)	2.4 -7.2
Albumin (g/L)		1.95 (0.5)	1.4-2.4
Protein (g/L)		4.0 (0.5)	3.2-4.5
Ca (mg/dL)		7.60 (0.8)	6.8-8.6
P (mg/dL)		4.65 (0.6)	3.6-6.8
Na (mmol/L)		135.5 (4.0)	126-141
K (mmol/L)		4.45 (0.4)	4-5.9
Cl (mmol/L)		105 (8)	92-112
Urine			
Gravity		1034 (19)	1002-1045
pH		6.5 (0.5)	5.5-7.5
Erythrocyte (/HPF)		3 (9)	0-27
Microscobic hematuria	3 (17.6)		
UPCR (mg/mg)		6.21 (2.78)	1.9-15.2
4th week results	**n (%)**	**Mean ± SD**	**Min-max**
Blood			
Creatinine (mg/dL)		0.28 (0.2)	0.2-0.5
Albumin (g/L)		4.2 (0.6)	3.6-4.7
Urine			
UPCR (mg/mg)		0.15 (0.05)	0.11-0.22
Steroid response	n (%)		
SSNS (no relapse)	11 (64.8)		
SDNS	6 (35.2)		
CNIs	4 (66.6)		
Rituximab	2 (33.3)		

URTI: Upper respiratory tract infection, SBP: Systolic blood pressure, DBP: Diastolic blood pressure, BUN: Blood urea nitrogen, UPCR: Spot urine protein:creatinine ratio, SRNS: Steroid resistant nephrotic syndrome, SSNS: Steroid sensitive nephrotic syndrome, SDNS: Steroid dependent nephrotic syndrome

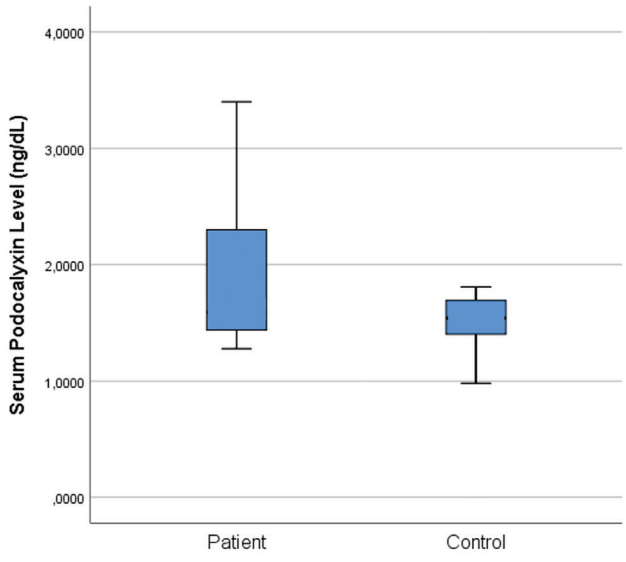

Figure 1. Comparison of serum podocalyxin levels between children with idiopathic nephrotic syndrome and healthy controls.

The median serum podocalyxin level in patients was higher compared to control group [1.87 ng/dL (IQR: 0.87) vs. 1.54 ng/dL (IQR: 0.29), p=0.031].

IQR: Interquartile range

DISCUSSION

This study investigated the clinical features and therapeutic responses of children with idiopathic NS, with particular emphasis on the utility of serum podocalyxin levels for predicting steroid responsiveness. All participants achieved remission following initial corticosteroid therapy; however, more than one-third (35.2%) developed SDNS during tapering. Among these patients, a subset required escalation to CNI, while two achieved remission only after rituximab therapy, indicating variability in treatment response. Notably, serum podocalyxin levels at diagnosis were markedly elevated in NS compared with controls and showed a nonsignificant trend toward higher values in those who progressed to SDNS and required more intensive treatment. These results indicate that podocalyxin may serve as a biomarker for the diagnosis of NS.

Podocytes, situated in the outer layer of the glomerular filtration barrier, play an essential role in the pathogenesis of glomerular diseases. Their detachment from the glomerular basement membrane reflects severe kidney injury. Healthy individuals have significantly lower urinary podocyte counts than patients with glomerular diseases. Therefore, quantifying podocytes in urine can be used to assess and monitor glomerular diseases. However, the determination of the podocyte-associated

Table 2. Evaluations of podocalyxin levels in clinical characteristics and steroid response.

	Serum podocalyxin level		
Initial features	**Median (IQR)**	**Min-max**	**p-value**
Control group (n=51)	1.54 (0.29)	0.61-3.18	0.031
Patients (n=17)	1.87 (0.87)	1.27-3.59	
Steroid response			
SSNS (no relapse)	1.65 (0.92)	1.27-3.40	0.148
SDNS	1.95 (1.17)	1.42-3.59	

IQR: Interquartile range, SSNS: Steroid sensitive nephrotic syndrome, FRNS: Frequently relapsing nephrotic syndrome, SDNS: Steroid dependent nephrotic syndrome

Table 3. Evaluation of the relationship between podocalyxin level and other parameters.

Dependent variables	Independent variables	Equation	Adjusted R^2	p-value
Podocalyxin level at initial diagnosis (ng/dL)	Age (years)	2.134 - 0.023 x age	0.111	0.690
	Weight gain (kg)	1.945 + 0.041 x weight gain	0.060	0.838
	Serum albumin (g/dL)	1.202 - 0.036 x serum albumin level	0.028	0.522
	UPCR (mg/mg)	2.423 - 0.076 x UPCR	0.164	0.107

UPCR: Spot urine protein:creatinine ratio

protein podocalyxin, rather than podocyte quantification, is increasingly used in clinical practice as a simpler method to assess kidney disease and to predict its prognosis[7]. A recent review evaluated new biomarkers that could be used in the early assessment and longitudinal monitoring of kidney diseases, emphasizing that podocalyxin could serve as a diagnostic marker for early podocyte damage. The integration of this new biomarker into routine clinical practice is expected to contribute to the early diagnosis and personalized treatment of kidney diseases[16]. In a study by Giannou et al.[17], urinary podocalyxin levels were evaluated in patients with various types of glomerulonephritis, and significant associations were found with serum creatinine and histological features of chronicity. The findings support the view that urinary podocalyxin levels may indicate podocyte injury and kidney dysfunction[17]. In another study, a sensitive liquid chromatography–tandem mass spectrometry assay was established to measure urinary podocalyxin for the early detection of chronic kidney disease; baseline levels were determined in 60 healthy controls and 20 patients. These results suggest that urinary podocalyxin levels could serve as a non-invasive biomarker of glomerular damage[18]. Podocalyxin levels in urine have also been shown to be a potential non-invasive biomarker for detecting the early stages of diabetic nephropathy, and these urinary levels increase even in the normoalbuminuric stage[19]. Additionally, podocalyxin levels in urine are significantly elevated in patients with lupus nephritis, and these levels have been found to correlate strongly with proteinuria, disease activity scores, and kidney biopsy findings. These results suggest that urinary podocalyxin may serve as non-invasive marker of renal involvement in systemic lupus erythematosus[20]. As seen in previous studies, podocalyxin levels were mostly assessed by measuring urinary excretion[7-9,16-20]. However, because of podocyte injury in NS, we can assume that podocalyxin enters the circulation and is excreted in the urine. Therefore, we measured serum podocalyxin levels in the present study. The reasons for choosing this approach include the possibility that urinary podocalcin levels may be affected by factors such as proteinuria intensity, urine concentration, and sample processing, which may limit its reliability. A study by Khalid and Ali[21] found a negative correlation between serum podocalyxin levels and glomerular filtration rate, suggesting that podocyte injury may increase as kidney damage progresses, leading to increased serum podocalyxin levels. In our study, serum podocalyxin levels at initial presentation of NS were significantly higher than those in healthy controls. This confirms that there may be some degree of podocyte injury in patients with NS.

The NS is one of the most extensively researched glomerular conditions in children, and its prognosis has significantly improved over time. The goal in treating idiopathic NS is to achieve remission as quickly as possible and to prevent relapses. Corticosteroids have been used in the treatment since the 1960s[13]. Because steroids are the first-line drugs of choice cumulative steroid dose can reach 187.3 mg/kg even in patients with a single episode of NS; it increases to 375.7 mg/kg in patients who develop steroid resistance or experience relapses[22]. Glucocorticoids exert biological effects on multiple cells and systems, affecting carbohydrate metabolism, blood pressure, vascular integrity, mood and behavior, musculoskeletal and skin health, body weight, immune function, and bone growth and mineralization[13,23]. Therefore, predicting the response of NS to steroids and using steroid-sparing agents or other immunosuppressive agents at an early stage in patients predicted to develop relapses will be valuable for protecting against steroid side effects. Although serum podocalyxin levels were elevated in children with NS in our study, current findings indicate that their levels are insufficient to predict disease severity or steroid response. Considering that initial serum podocalyxin levels are numerically higher in patients who were subsequently diagnosed with SDNS, we believe that this limitation can be addressed by multicenter studies with longer follow-up and larger sample sizes.

Study Limitations

The primary limitation of this study is the relatively small sample size. Although NS is a common glomerular pathology in children, we could not enroll more newly diagnosed NS cases at a single center during the relatively short study period. We believe that more statistically robust results could be obtained in a longer, multicenter study. In a study with longer follow-up, it may be possible to examine whether serum podocalyxin levels and other characteristics affect long-term prognosis. Another limitation is that the histopathological characteristics of the patients are unknown. Although kidney biopsy is not routinely indicated in children with NS, the absence of histopathological confirmation prevents us from definitively establishing the relationship between serum podocalyxin levels and podocyte injury. Also, podocalyxin is found in endothelial cells, suggesting that the results may be affected by endothelial damage. Clarifying this finding using additional markers of endothelial damage in the initial evaluation would increase the study's value.

CONCLUSION

This study suggests that serum podocalyxin levels at diagnosis may have utility as a biomarker in children

with idiopathic NS. Although remission was achieved in all patients with initial steroid therapy, a significant proportion required additional immunosuppressive agents, highlighting the importance of early risk stratification. However, current findings indicate that serum podocalyxin levels are insufficient for predicting disease severity or steroid response. Additional studies involving larger patient cohorts are needed to further substantiate findings.

Ethics

Ethics Committee Approval: The study was approved by the KTO Karatay University Medical Ethics Committee with decision no.:2024/257, date:18.12.2024.

Informed Consent: Written informed consent was obtained from all participants and their parents before enrollment.

Footnotes

Author Contributions

Surgical and Medical Practices: E.L., M.S., Concept: E.L., U.C., Design: E.L., U.C., Data Collection or Processing: E.L., M.S., U.C., Analysis or Interpretation: E.L., M.S., U.C., Literature Search: E.L., M.S., U.C., Writing: E.L., M.S., U.C.

Conflict of Interest: The authors have no conflict of interest to declare.

Financial Disclosure: The authors declared that this study has received no financial support.

REFERENCES

1. Vivarelli M, Massella L, Ruggiero B, Emma F. Minimal change disease. Clin J Am Soc Nephrol. 2017;12:332-45.
2. Grahammer F, Schell C, Huber TB. The podocyte slit diaphragm--from a thin grey line to a complex signalling hub. Nat Rev Nephrol. 2013;9:587-98.
3. Nielsen JS, Graves ML, Chelliah S, Vogl AW, Roskelley CD, McNagny KM. The CD34-related molecule podocalyxin is a potent inducer of microvillus formation. PLoS One. 2007;2:e237.
4. Orlando RA, Takeda T, Zak B, et al. The glomerular epithelial cell anti-adhesin podocalyxin associates with the actin cytoskeleton through interactions with ezrin. J Am Soc Nephrol. 2001;12:1589-98.
5. Kavoura E, Gakiopoulou H, Paraskevakou H, et al. Immunohistochemical evaluation of podocalyxin expression in glomerulopathies associated with nephrotic syndrome. Hum Pathol. 2011;42:227-35.
6. Nawata A, Hisano S, Shimajiri S, Wang KY, Tanaka Y, Nakayama T. Podocyte and endothelial cell injury lead to nephrotic syndrome in proliferative lupus nephritis. Histopathology. 2018;72:1084-92.
7. Karatoy Erdem B, Özcan M, Yılmaz VT, et al. A UFLC-MS/MS method for the simultaneous analysis of urinary podocin and podocalyxin in patients with nephrotic syndrome. Lab Med. 2022;53:246-54.
8. Hara M, Yanagihara T, Kihara I. Cumulative excretion of urinary podocytes reflects disease progression in IgA nephropathy and Schönlein-Henoch purpura nephritis. Clin J Am Soc Nephrol. 2007;2:231-8.
9. Tanal Şambel I, Eren E, Bozyigit C, Sarandöl E. Serum Mindin, Nephrin and Podocalyxin Levels in Patients with Type 1 Diabetes: are these new markers to detect the development of nephropathy? J Curr Pediatr. 2022;20:147-54.
10. Sassetti C, Tangemann K, Singer MS, Kershaw DB, Rosen SD. Identification of podocalyxin-like protein as a high endothelial venule ligand for L-selectin: parallels to CD34. J Exp Med. 1998;187:1965-75.
11. Chen Q, Wang Y, Li Y, Zhao M, Nie G. Serum podocalyxin is significantly increased in early-onset preeclampsia and may represent a novel marker of maternal endothelial cell dysfunction. J Hypertens. 2017;35:2287-94.
12. Rovin BH, Adler SG, Barratt J, et al. Executive summary of the KDIGO 2021 Guideline for the Management of Glomerular Diseases. Kidney Int. 2021;100:753-79.
13. Khullar S, Banh T, Vasilevska-Ristovska J, et al. Impact of steroids and steroid-sparing agents on quality of life in children with nephrotic syndrome. Pediatr Nephrol. 2021;36:93-102.
14. Neyzi O, Saka HN, Kurtoğlu S. Anthropometric studies on the Turkish population--a historical review. J Clin Res Pediatr Endocrinol. 2013;5:1-12.
15. Flynn JT, Kaelber DC, Baker-Smith CM, et al. Clinical practice guideline for screening and management of high blood pressure in children and adolescents. Pediatrics. 2017;140:e20171904.
16. Choudhary BB, Puri B, Gaikwad AB. Novel molecular biomarkers in kidney diseases: bridging the gap between early detection and clinical implementation. J Pharm Pharmacol. 2025:rgaf096.
17. Giannou P, Gakiopoulou H, Stambolliu E, et al. Urine nephrin and podocalyxin reflecting podocyte damage and severity of kidney disease in various glomerular diseases-a cross-sectional study. J Clin Med. 2024;13:3432.
18. Morales-Betanzos CA, Berasi SP, Federspiel JD, Neubert H, Fernandez Ocana M. Development of a multiplexed LC-MS/MS assay for the quantitation of podocyte injury biomarkers nephrin, podocalyxin, and podocin in human urine. J Proteome Res. 2025;24:282-8.
19. Ye H, Bai X, Gao H, et al. Urinary podocalyxin positive-element occurs in the early stage of diabetic nephropathy and is correlated with a clinical diagnosis of diabetic nephropathy. J Diabetes Complications. 2014;28:96-100.
20. Fayed A, Elnokeety MM, Elyamny M, Hammad H, Soliman DHA, Ahmed RA. Urinary podocalyxin: Is it a real index of disease activity in egyptian patients lupus nephritis? Saudi J Kidney Dis Transpl. 2020;31:1198-205.
21. Khalid Z, Ali A. Assessment of serum podocalyxin as a biomarker for diabetic nephropathy in type 2 diabetes patients in duhok city. J Life Bio Sci Res. 2022;3:71-75.
22. Leventoğlu E, Kavgacı A, İncedere F, Tokgöz S, Büyükkaragöz B. Arterial stiffness and cardiac functions in children with idiopathic nephrotic syndrome. Indian J Pediatr. 2023;90:413.
23. Croitoru A, Balgradean M. Treatment-associated side effects in patients with steroid-dependent nephrotic syndrome. Maedica (Bucur). 2022;17:285-90.

DOI: 10.4274/MMJ.galenos.2025.66664
Medeni Med J 2025;40:269-277

Original Article

The Effect of Flow-Controlled Ventilation on Mechanical Power in Laparoscopic Surgeries: A Comparative Analysis with Pressure Controlled Volume Guaranteed and Volume Controlled Ventilation

Laparoskopik Cerrahilerde Akış Kontrollü Ventilasyonun Mekanik Güç Üzerindeki Etkisi: Basınç Kontrollü Hacim Garantili ve Hacim Kontrollü Ventilasyon ile Karşılaştırmalı Bir Analiz

Ayse SENCAN, Nurseda DUNDAR, Bedirhan GUNEL, Ahmet YUKSEK

University of Health Sciene Türkiye, Kocaeli City Hospital, Clinic of Anaesthesiology and Reanimation, Kocaeli, Türkiye

ABSTRACT

Objective: To compare mechanical power (MP) levels among flow-controlled ventilation (FCV), volume-controlled ventilation (VCV), and pressure-controlled volume-guaranteed ventilation (PCV-VG) during laparoscopic surgery and to test the hypothesis that the stable flow dynamics of FCV would reduce MP.

Methods: Patients were divided into three groups according to the mechanical ventilation modes applied during laparoscopic surgery: PCV-VG (n=15), VCV (n=14), and FCV (n=15). MP was calculated at four timepoints: baseline (T1), post-induction (T2), during CO_2 insufflation (T3), and post-insufflation (T4). The primary outcome of the study was the comparison of MP in the FCV mode with MP in the other groups during insufflation. Driving pressure (DP), plateau pressure, and peak airway pressure were also analyzed.

Results: Baseline MP was highest in PCV-VG (6.9 J/min vs. 5.0 J/min in VCV and 5.1 J/min in FCV; p=0.002). During insufflation (T3), MP increased to a similar extent across groups (PCV-VG: 9.4 J/min, VCV: 8.7 J/min, FCV: 8.6 J/min), with PCV-VG showing the smallest relative rise (p<0.001). DP and plateau pressures increased during pneumoperitoneum, but Bonferroni-adjusted comparisons revealed that these were not statistically significant. PCV-VG maintained higher positive end-expiratory pressure (5 vs. 4 cmH_2O, p<0.001); however, it did not significantly affect peak pressures.

Conclusions: Contrary to our hypothesis, FCV did not reduce MP more effectively than either VCV or PCV-VG. However, PCV-VG demonstrated better mitigation of insufflation-induced increases in MP, suggesting potential advantages for lung protection during laparoscopy. Further prospective studies are needed to assess clinical outcomes.

Keywords: Respiratory mechanics, mechanical ventilation, laparoscopy, ventilator-induced lung injury

ÖZ

Amaç: Bu çalışmanın amacı, laparoskopik cerrahi sırasında akış kontrollü ventilasyon (FCV), volüm kontrollü ventilasyon (VCV) ve basınç kontrollü volüm garantili ventilasyon (PCV-VG) modları arasındaki mekanik güç (MP) düzeylerini karşılaştırmak ve FCV'nin stabil akış dinamiğinin MP'yi azaltacağı hipotezini test etmektir.

Yöntemler: Laparoskopik cerrahi geçiren 44 hasta uygulanan mekanik ventilasyon modlarına göre üç gruba ayrıldı: PCV-VG (n=15), VCV (n=14) ve FCV (n=15). MP dört zaman noktasında hesaplandı: başlangıç (T1), indüksiyon sonrası (T2), CO_2 insüflasyonu sırasında (T3) ve insüflasyon sonrası (T4). Çalışmanın birincil sonucu, insüflasyon sırasında FCV modundaki MP'nin diğer gruplarla karşılaştırılmasıydı. Sürücü basınç (DP), plato basıncı ve pik hava yolu basınçları da analiz edildi.

Bulgular: Başlangıç MP değeri PCV-VG grubunda en yüksekti (6,9 J/dk vs. VCV: 5.0, FCV: 5.1 J/dk, p=0,002). İnsüflasyon sırasında (T3), MP tüm gruplarda benzer şekilde arttı (PCV-VG: 9,4, VCV: 8,7, FCV: 8,6 J/dk), ancak PCV-VG en düşük relatif artışı gösterdi (p<0,001). DP ve plato basınçları pnömoperitoneum sırasında arttı, ancak Bonferroni düzeltmesi sonrası gruplar arası fark anlamlı değildi. PCV-VG daha yüksek PEEP seviyeleri sağladı (5 vs. 4 cmH_2O, p<0,001), ancak pik basınçları etkilemedi.

Sonuçlar: Hipotezimizin aksine, FCV MP'yi VCV veya PCV-VG'ye göre daha etkili şekilde azaltmadı. Bununla birlikte, PCV-VG'nin insüflasyon kaynaklı MP artışını daha iyi sınırladığı ve laparoskopide akciğer korunumuna katkı sağlayabileceği görüldü. Klinik sonuçları değerlendirmek için ileri prospektif çalışmalara ihtiyaç vardır.

Anahtar kelimeler: Solunum mekanikleri, mekanik ventilasyon, laparoskopi, ventilatör ilişkili akciğer hasarı

Address for Correspondence: A. Şencan, University of Health Sciene Türkiye, Kocaeli City Hospital, Clinic of Anaesthesiology and Reanimation Kocaeli, Türkiye
E-mail: draysesencan@gmail.com **ORCID ID:** orcid.org/0000-0003-2225-5269

Cite as: Sencan A, Dundar N, Gunel B, Yuksek A. The effect of flow-controlled ventilation on mechanical power in laparoscopic surgeries: a comparative analysis with pressure controlled volume guaranteed and volume controlled ventilation. Medeni Med J. 2025;40:269-277

Received: 17.08.2025
Accepted: 28.11.2025
Published: 31.12.2025

INTRODUCTION

The primary aims of mechanical ventilation are lung protection, maintenance of adequate gas exchange, and prevention of ventilator-induced lung injury (VILI) caused by barotrauma, volutrauma, atelectrauma, and biotrauma[1]. Significant efforts have been made to identify and minimize factors contributing to VILI[2]. Key triggers include barotrauma (associated with high plateau pressures), volutrauma [related to high tidal volumes (Vt)], and atelectrauma (resulting from cyclic alveolar collapse and reopening)[2]. A novel approach to VILI focuses on the energy dissipated in lung tissue during respiratory cycles as a fundamental mechanism of injury[3]. The energy transferred from the ventilator to the respiratory system appears to be directly related to VILI, and reducing mechanical energy may decrease lung damage[3].

In laparoscopic surgery, pneumoperitoneum increases intra-abdominal pressure (IAP). Cranial displacement of the diaphragm elevates intrathoracic pressure, reduces lung compliance, promotes atelectasis, and impairs gas exchange[4]. To prevent atelectasis and maintain adequate ventilation in the presence of elevated airway pressures, mechanical ventilators must deliver higher energy[4]. Therefore, ventilation modes associated with lower mechanical power (MP) may facilitate lung-protective strategies during laparoscopic procedures[4].

During mechanical ventilation, electrical energy is converted to kinetic and thermal energy to generate pressure for Vt delivery. The energy transferred per breath is termed mechanical energy, while the energy transferred per unit time is defined as MP[5]. Gattinoni et al.[6] developed the formula for calculating MP using ventilator parameters in 2016. Becher et al.[7] later simplified this formula by eliminating the need to measure compliance, resistance, and elastance. The simplified calculation incorporates peak pressure (Ppeak), Vt, and respiratory rate (RR)[7]. Thus, MP serves as a comprehensive variable representing ventilator-induced damaging factors[7]. The relationship between MP and VILI was first demonstrated in a porcine model, establishing 12.1 J/min as the threshold for VILI development[8]. Subsequent animal and human studies have further investigated the role of MP in VILI across various patient populations and procedures[5].

Flow-controlled ventilation (FCV), an innovative strategy developed in 2010, delivers a constant linear flow during both inspiratory and expiratory phases[9]. When implemented via the Evone ventilator (Ventinova Medical BV, Eindhoven, Netherlands), this method minimizes airway resistance through active expiration and reduces intratracheal pressure fluctuations[2]. FCV dynamically optimizes Vt and RR based on preset pressure-flow parameters and demonstrates particular efficacy in high-risk populations (patients with morbid obesity and those undergoing laparoscopic surgery) by reducing atelectasis, hypercapnia, and pressure-related injuries[10]. However, FCV's impact on MP remains insufficiently explored compared to volume-controlled (VCV) and pressure-controlled volume-guaranteed (PCV-VG) modes.

Primary objective: This study compared FCV's MP-reducing efficacy with that of VCV and PCV-VG during laparoscopic surgery to test our hypothesis that FCV's low Vt and stable pressure dynamics would significantly reduce MP. Our primary endpoint was the intermodal MP difference under CO_2 insufflation.

MATERIALS and METHODS

Study Design

The current study was conducted in a tertiary care hospital. Ethical protocol number 2025-79 was received from the University of Health Sciene Türkiye, Kocaeli City Hospital Scientific Research Ethics Committee with protocol no.: 2025-79, date: 10.07.2025. The study was conducted in accordance with the Declaration of Helsinki. VCV and PCV-VG are the ventilation modes most frequently used for laparoscopic procedures in our clinical practice. During the study period (November 2024-February 2025), when FCV was implemented at our institution, we enrolled 44 patients, assigned to three study groups who underwent laparoscopic surgery and had complete intraoperative ventilation data recorded under the three distinct ventilation modalities. Due to the retrospective design, individual patient consent was not obtained.

Patients were divided into three groups according to the applied ventilation modes:

- Group 1: PCV-VG (n=15)

- Group 2: VCV (n=14)

- Group 3: FCV (n=15)

Data Collection and Variables

Information regarding patients' ages, gender, American Society of Anesthesiologists (ASA) scores, height, weight, heart rate (HR), systolic blood pressure, diastolic blood pressure, mean blood pressure, peripheral oxygen saturation (SpO_2), type of surgery, duration of surgery, duration of anesthesia, CO_2 insufflation time, and ventilation mode was recorded. The parameters analyzed

according to ventilation mode included Vt, RR, end-tidal carbon dioxide pressure ($EtCO_2$), positive end-expiratory pressure (PEEP), peak airway pressure (Ppeak), driving pressure (DP), and plateau pressure. MP was calculated from simplified formulas defined in the literature, using these parameters:

Group 1: Pressure-controlled-volume-guaranteed ventilation (PCV-VG) (n=15)

For pressure-controlled ventilation: MP (J/min) = 0.098 × RR (1/min) × Vt (L) × (Peak inspiratory pressure change (ΔPinsp) + PEEP] (cmH_2O)[6,7].

Group 2: VCV (n=14)

For VCV: MP (J/min) =0.098 × RR (1/min) × VT (L) × [ΔPinsp - ½ (Plateau Pressure - PEEP)] (cmH_2O)[11]. Group 3: FCV (n=15)

For FCV, MP (J/min) =0.098 × RR (1/min) × VT (L) × ½ × (Plateau Pressure - PEEP) (cmH_2O)[6,11].

Inclusion criteria were adults (≥18 years of age) undergoing elective laparoscopic surgery under general anesthesia and ventilated in continuous mode for at least 15 minutes.

Exclusion criteria included conversion to open surgery, intraoperative ventilation mode changes due to hemodynamic instability or hypoxemia, missing ventilation data, emergency surgical interventions, and pregnant women. Additionally, patients with preoperative pulmonary diseases (chronic obstructive pulmonary disease, interstitial lung disease) or severe cardiovascular pathologies (ejection fraction <30%, pulmonary hypertension) were excluded from the study.

The study screened a total of 80 patients; 28 had incomplete data and 8 were excluded due to conversion to open surgery. As a result, data from 44 patients were analyzed. These strict exclusion criteria ensured the comparability of ventilation parameters between study groups and maintained data homogeneity.

To compare variables, four different time periods were determined during the mechanical ventilation process:

T1: The point at which mechanical ventilation was initiated after anesthesia induction

T2: 15 minutes of mechanical ventilation after anesthesia induction

T3: 15 minutes of CO_2 insufflation

T4: 15 minutes after CO_2 insufflation was discontinued

Primary and Secondary Outcome Measure

The primary endpoint of the study was the difference in MP between ventilation modes during CO_2 insufflation. The secondary outcomes were comparisons of MP values measured during the anaesthesia induction phase of mechanical ventilation in the perioperative period, at the 15th minute of mechanical ventilation prior to pneumoperitoneum, and at the 15th minute after completion of pneumoperitoneum.

Statistical Analysis

Statistical analyses were performed using IBM SPSS Statistics version 27.0. Descriptive statistics were presented as median (minimum-maximum) or mean ± standard deviation for continuous variables, and as frequency and percentage (n, %) for categorical variables. The distribution of numerical variables was assessed using the Shapiro-Wilk test. For independent numerical variables that were not normally distributed, the Kruskal-Wallis test was used, and results were expressed as median (minimum-maximum). For normally distributed variables, one-way analysis of variance was applied, and values were presented as mean ± standard deviation. To assess the independence of categorical variables, Fisher's exact test was used. A p-value <0.05 was considered statistically significant.

For within-group comparisons across multiple time points, the Friedman test was used. If a significant difference was found, Dunn's test was performed for post-hoc multiple comparisons. For between-group comparisons at each time point, the Kruskal-Wallis test was applied, followed by Dunn's post-hoc test when appropriate.

To control for type I error, Bonferroni correction was applied. For variables measured at four time points, a significance threshold of p<0.007 was used; for those measured at five time points, a significance threshold of p<0.006 was used.

RESULTS

During the study period, a total of 80 patients underwent laparoscopic procedures. After applying the exclusion criteria —28 patients with missing data and 8 patients who converted to open procedures — data from 44 patients who met the study criteria were included in the analysis. According to our patient data, no perioperative mortality or intraoperative complications were reported.

The perioperative mechanical ventilation targets were similar for all patients in terms of saturation, $EtCO_2$, and Ppeak. Any ad hoc adjustments to mechanical ventilation made during surgery were excluded from the analysis. Instead, MP values were calculated based on data from specified time intervals.

Evaluation of the demographic data of the study patients revealed no difference between the groups in gender distribution (p=1.000). The PCV-VG, VCV, and FCV groups included 11 (73.4%), 11 (78.6%), and 12 (80.0%) female patients, respectively. The mean age in the PCV-VG group was significantly higher (61.9±10.7 years; p=0.039). The mean ages in the VCV and FCV groups were 49.4±17.4 years and 48.7±16.8 years, respectively. No significant differences were observed between the groups with respect to height and weight (Table 1).

A significant difference in ASA scores among the groups was observed (p=0.003). In the PCV-VG group, no patients were classified as ASA I, while 53.3% were ASA II and 46.7% were ASA III. In the VCV group, 14.3% of patients were ASA I, 78.7% were ASA II, and 7.1% were ASA III. In the FCV group, 13.3% were ASA I and 86.7% were ASA II, with no ASA III patients (Table 1).

The median anesthesia durations were 150 minutes (range, 60-400) in the PCV-VG group, 122.5 minutes (range, 70-300) in the VCV group, and 125 minutes (range, 90-310) in the FCV group (p=0.672). Surgical durations were 120 (50-375), 102.5 (45-280), and 105 (50-300) minutes, respectively (p=0.837). CO_2 insufflation times were also similar across groups: 75 (15-300) minutes in PCV-VG, 75 (30-240) minutes in VCV, and 85 (40-255) minutes in FCV (p=0.976). The insufflation pressure showed comparable median values of 13 mmHg across all groups (p=0.934). No statistically significant differences were observed among the three ventilation modes regarding anesthesia duration, surgical duration, CO_2 insufflation time, or insufflation pressure at the 15-minute mark (Table 2).

MP Values: In our study, baseline (T1) MP was significantly higher in the PCV-VG group [6.9 (4.8-11.3) J/min] compared with VCV [5.0 (4.2-8.1) J/min] and FCV [5.1 (3.5-9.4) J/min] (p=0.002). However, this difference diminished over time. At 15 minutes post-CO_2 insufflation (T3), MP increased in all groups: PCV-VG [9.4 (6.0-13.1)], VCV [8.7 (4.6-13.6)], and FCV [8.6 (0.8-13.6)]. Following insufflation termination (T4), MP returned to baseline levels in all groups. In the VCV and FCV groups, the rise in MP at T2 and T3 time points was statistically significant (p<0.001), whereas in PCV-VG the T3 increase was also statistically significant (p=0.008) (Table 3).

DP and plateau pressure dynamics; All ventilation modes demonstrated significant increases in DP during

Table 1. Patients' demographic and clinical characteristics.

	PCV-VG	VCV	FCV	p-value*
Sex				
Female	11 (73.4)	11 (78.6)	12 (80)	1.000[a]
Male	4 (26.7)	3 (21.4)	3 (20)	
Age (years)	61.9±10.7[a]	49.4±17.4[b]	48.7±16.8[c]	**0.039[a]***
Height (cm)	161.7±8.2	163.5±6.5	163.5±6.2	0.712[a]
Weight (kg)	81.5±11.9	74.8±9.9	73.9±9.3	0.110[a]
ASA score				
ASA I	0 (0)	2 (14.3)	2 (13.3)	**0.003*[z]**
ASA II	8 (53.3)	11 (78.7)	13 (86.7)	
ASA III	7 (46.7)	1 (7.1)	0 (0)	
Type of surgery				
Laparoscopic hysterectomy	8 (53.3)	8 (57.1)	7 (46.7)	0.114[z]
Ovarian cyst	0 (0)	1 (7.1)	5 (33.3)	
Laparoscopic colon tumor	3 (20)	3 (21.4)	0 (0)	
Other	4 (26.7)	2 (14.3)	3 (20)	

Data are presented as number (%) or mean ± standard deviation. [a-c]: Groups with different letters are statistically significantly different.

[a]: One-way ANOVA test; [z]: Fisher's exact test. p*<0.05 was considered statistically significant, PCV-VG: pressure-controlled volume-guaranteed ventilation, VCV: volume-controlled ventilation, FCV: Flow-controlled ventilation, ASA: American Society of Anesthesiologists

Table 2. Operative time parameters and insufflation pressure data across groups.				
	PCV-VG	**VCV**	**FCV**	**p-value**
Anesthesia duration (minute)	150 (60-400)	122.5 (70-300)	125 (90-310)	0.672[1]
Surgical duration (minute)	120 (50-375)	102.5 (45-280)	105 (50-300)	0.837[1]
CO_2 insufflation duration (minute)	75 (15-300)	75 (30-240)	85 (40-255)	0.976[1]
Insufflation pressure at 15th minute	13 (8-15)	13 (7-18)	13 (7-15)	0.934[1]
Data are presented as median (minimum-maximum). 1Kruskal Wallis test. PCV-VG: Pressure-controlled volume-guaranteed ventilation, VCV: Volume-controlled ventilation, FCV: Flow-controlled ventilation				

pneumoperitoneum at T3 (p<0.001). The PCV-VG group exhibited the most pronounced elevation, with DP rising from 14 (6-26) cmH_2O at baseline (T1) to 22 (13-29) cmH_2O during insufflation. The VCV and FCV groups showed more moderate increases, to 17.5 (13-26) and 16 (13-26) cmH_2O, respectively. Plateau pressure followed a similar trend, with PCV-VG reaching significantly higher values [26 (17-33) cmH_2O] than VCV [20.5 (17-29) cmH_2O) and FCV [19 (17-30) cmH_2O]. While initial analysis suggested intergroup differences at T3 (p=0.034), Bonferroni-adjusted comparisons revealed that these differences were not statistically significant (adjusted p>0.007), indicating that the observed variations may reflect physiological variability rather than mode-dependent effects (Table 3).

Ventilatory Pressure Characteristics; The PCV-VG strategy consistently maintained higher PEEP levels [5 (4-6) cmH_2O] throughout the procedure compared with VCV and FCV [4 (3-5) cmH_2O, p<0.001], reflecting its distinct algorithmic approach to lung protection. Ppeak during pneumoperitoneum showed mode-dependent variation, with PCV-VG generating the highest pressures [27 (18-34) cmH_2O], followed by VCV [21.5 (18-30) cmH_2O] and FCV [20 (18-31) cmH_2O] (Table 3).

Haemodynamic data; Significant decreases in mean arterial pressure (MAP) (p*<0.001) and HR (p*=0.001) were observed in the PCV group. In the VCV and FCV groups, however, changes in MAP and HR were not found to be significant (p*=0.035 and 0.048 for MAP, and p*=0.009 and 0.006 for HR; values correspond to VCV and FCV, respectively). Although SpO_2 increased in all groups, this change was not statistically significant (p>0.006). Intergroup comparisons revealed differences only in measurements of MAP-2, MAP-3, and MAP-4 (p<0.006) (Table 4).

DISCUSSION

This study compared the effects of PCV-VG, VCV, and FCV ventilation modes on MP during laparoscopic surgery. The mechanical ventilation process was evaluated at four distinct time points, analyzing both within-group changes and between-group differences. Our findings show that, contrary to our hypothesis, FCV yields MP values similar to those of PCV-VG and VCV during CO_2 insufflation for laparoscopic surgery. The most notable finding of the study is that the PCV-VG mode limits the increase in MP during laparoscopy more effectively than other ventilation modes.

The concept of MP, defined by Gattinoni et al.[6], is a critical parameter in the pathogenesis of VILI. Essentially, it is the time-normalized expression of the energy transmitted to the lung parenchyma and is calculated by the following formula: MP=0.098× RR (1/min) × VT (L) × (ΔPinsp + PEEP) (cmH_2O)[6]. In our study, the initially observed high MP values in the PCV-VG group (T1) may be associated with this mode's requirement for higher PEEP and higher plateau pressure. However, the significantly lower rate of MP increase after CO_2 insufflation (T3) compared with other groups suggests physiological advantages of PCV-VG. Specifically, the adaptive flow profile (initially high and gradually decreasing) may optimize gas distribution under conditions of increased IAP, thereby ensuring a more homogeneous distribution of mechanical stresses. Additionally, its autoregulatory capacity, which dynamically adjusts pressure limits while maintaining Vt, enhances this adaptation[12].

Laparoscopic surgery is widely preferred because it is minimally invasive, results in shorter hospital stays, and yields favorable cosmetic outcomes[13]. However, pneumoperitoneum and the Trendelenburg position increase IAP, restrict diaphragmatic movement, elevate mechanical stress in the lungs, and raise the risk of atelectasis[13]. Pozzi et al.[14] reported that MP increased across different PEEP levels during pneumoperitoneum. Consistent with Pozzi[14]'s findings, our study also observed increased MP values during insufflation, independent of ventilation mode. Similar MP values were observed across all three ventilation modes during insufflation; however, the PCV-VG mode significantly attenuated the increase

Table 3. Mechanical ventilation values of the groups in the T1, T2, T3, T4 time periods.					
Groups	**MP-1**	**MP-2**	**MP-3**	**MP-4**	**p*-value***
PCV-VG	6.9 (4.8-11.3)^{A}	7.1 (4.5-10.4)	9.4 (6-13.1)	7.5 (4.7-9.5)	0.008[1]
VCV	5 (4.2-8.1)^{Ba}	8 (4.9-11.9)^{b}	8.7 (4.6-13.6)^{b}	6.5 (3.4-11.2)^{a}	**<0.001[1]***
FCV	5.1 (3.5-9.4)^{Ba}	7.9 (5.1-12.3)^{b}	8.6 (0.8-13.6)^{b}	6.4 (3-10)^{a}	**<0.001[1]***
p-value*	**0.002[2]***	**0.109[2]**	**0.976[2]**	**0.415[2]**	
Groups	**DP-1**	**DP-2**	**DP-3**	**DP-4**	**p*-value**
PCV-VG	14 (6-26)^{a}	13 (7-26)^{b}	22 (13-29)^{b}	13 (9-20)^{a}	<0.001[1]*
VCV	10.5 (5-25)^{a}	15.5 (11-27)^{b}	17.5 (13-26)^{b}	12 (3-16)^{a}	<0.001[1]*
FCV	11 (5-9)^{a}	14 (12-27)^{b}	16 (13-26)^{b}	12 (3-22)^{a}	<0.001[1]*
p-value*	0.2042	0.0602	0.9702	0.1712	
Groups	**PEEP-1**	**PEEP-2**	**PEEP-3**	**PEEP-4**	**p*-value**
PCV-VG	5 (4-6)^{A}	5 (5-5)^{A}	5 (5-7)^{A}	5 (5-7)^{A}	0.112[1]
VCV	4 (3-5)^{B}	4 (3-5)^{B}	4 (4-5)^{B}	4.5 (3-5)^{B}	0.466[1]
FCV	4 (3-5)^{B}	4 (3-5)^{B}	4 (4-5)^{B}	5 (3-5)^{B}	0.091[1]
p-value*	**0.002[2]***	**<0.001[2]***	**<0.001[2]***	**<0.001[2]***	
Groups	**PLATO-1**	**PLATO-2**	**PLATO-3**	**PLATO-4**	**p*-value**
PCV-VG	18 (11-30)^{a}	17 (11-30)^{a}	26 (17-33)^{b}	17 (13-26)^{a}	<0.001[1]*
VCV	13 (9-27)^{a}	19 (14-30)^{b}	20.5 (17-29)^{b}	15.5 (6-19)^{a}	<0.001[1]*
FCV	15 (7-23)^{a}	18 (14-30)^{b}	19 (17-30)^{b}	16 (6-25)^{a}	<0.001[1]*
p-value	**0.082[2]**	**0.244[2]**	**0.034[2]**	**0.083[2]**	
Groups	**PEAK-1**	**PEAK-2**	**PEAK-3**	**PEAK-4**	**p-value***
PCV-VG	19 (12-31)^{a}	18 (12-31)^{a}	27 (18-34)^{b}	18 (14-27)^{a}	**<0.001[1]***
VCV	14 (10-28)^{a}	20 (15-31)^{b}	21.5 (18-30)^{b}	16.5 (7-20)^{a}	**<0.001[1]***
FCV	16 (8-24)^{a}	19 (15-31)^{b}	20 (18-31)^{b}	17 (7-26)^{a}	**<0.001[1]***
p-value	**0.082[2]**	**0.244[2]**	**0.034[2]**	**0.083[2]**	
Groups	**RR-1**	**RR-2**	**RR-3**	**RR-4**	**p-value***
PCV-VG	12 (10-14)	12 (10-20)^{A}	12 (10-16)^{A}	12 (10-16)	0.408[1]
VCV	12 (10-14)^{b}	18 (13-30)^{Ba}	17 (13-28)^{Ba}	14 (9-24)^{ab}	<0.001[f]*
FCV	12 (10-14)^{c}	17 (13-30)^{Bb}	17 (13-28)^{Bb}	13 (10-20)^{a}	<0.001[f]*
p-value*	**0.996[2]**	**<0.001[2]***	**<0.001[2]***	**0.148[2]**	
Groups	**VT-1**	**VT-2**	**VT-3**	**VT-4**	**p-value***
PCV-VG	0.5 (0.4-0.6)	0.5 (0.4-0.5)^{A}	0.5 (0.4-0.6)^{A}	0.5 (0.4-0.6)	0.197[1]
VCV	0.5 (0.4-0.5)^{b}	0.4 (0.2-0.5)^{Ba}	0.4 (0.3-0.5)^{Ba}	0.5 (0.4-0.5)^{ab}	0.001[1]*
FCV	0.5 (0.4-0.5)^{b}	0.4 (0.2-0.5)^{Bab}	0.4 (0-0.5)^{Ba}	0.4 (0.4-0.5)^{ab}	0.007[1]*
p-value*	**0.033[2]**	**<0.001[2]***	**0.006[2]***	**0.450[2]**	
Groups	**$ETCO_2$-1**	**$ETCO_2$-2**	**$ETCO_2$-3**	**$ETCO_2$-4**	**p-value***
PCV-VG	14 (26-30.5)	14 (27-34)^{A}	14 (30-35.5)	14 (29-33)	0.780[1]
VCV	15 (32-26)^{b}	15 (28-35)^{Ba}	15 (30-37)^{a}	15 (29-35)^{ab}	**0.002[1]***
FCV	44 (23-30.5)^{b}	44 (27-32.5)^{Bab}	44 (24-34)^{a}	44 (27-33)^{ab}	**0.002[1]***
p-value*	**0.507[2]**	**0.0072***	**0.094[2]**	**0.033[2]**	

Data are presented as median (minimum-maximum) *p<0.007 was considered statistically significant. [1]Friedman test, [2]Kruskal Wallis test. $^{A-C}$: For each parameter within columns, groups sharing the same letter are not significantly different (Dunn's test). $^{a-c}$: For each parameter within rows, groups sharing the same letter are not significantly different (Dunn's test).

MP: Mechanical power (cmH_2O l/min), DP: Driving pressure (cmH_2O), PEEP: Positive end-expiratory pressure (cmH_2O), PLATO: Plateau pressure (cmH_2O), PEAK: Peak inspiratory pressure (cmH_2O), RR: Respiratory rate (breaths per minute), Vt: Tidal volume (L), $ETCO_2$: End-tidal carbon dioxide (mmHg)

Table 4. Comparisons of MAP, SPO_2, and HR across groups at different time periods.

Groups	MAP-0	MAP-1	MAP-2	MAP-3	MAP-4	p*-value
PCV	98 (81-123)^{b}	67 (57-93)^{a}	68 (58-92)^{Aa}	82 (65-111)^{Aab}	76 (59-103)^{Aa}	**<0.001[1]***
VCV	99.8 (75.3-114.7)	85.8 (57.3-106.7)	103.3 (83.3-116)^{B}	96.2 (67.7-177)^{B}	97.2 (69.7-121.3)^{B}	0.035[1]
FCV	99.7 (82.3-119)	87 (60.7-114.3)	104.3 (79-125.3)^{B}	99.3 (76.7-114.7)^{B}	94 (81-131.3)^{B}	0.048[1]
p*-value	0.907[2]	0.026[2]	**<0.001[2]***	**0.006[2]***	**0.001[2]***	
Groups	**SPO_2-0**	**SPO_2-1**	**SPO_2-2**	**SPO_2-3**	**SPO_2-4**	**p*-value**
PCV	98 (96-100)	100 (98-100)	99 (97-100)	99 (96-100)	100 (95-100)	0.0120[1]
VCV	98 (95-100)^{b}	99.5 (98-100)^{ab}	99.5 (97-100)^{ab}	100 (98-100)^{ab}	100 (99-100)^{a}	**<0.001[1]***
FCV	98 (95-100)^{b}	100 (98-100)^{ab}	100 (96-100)^{ab}	100 (98-100)^{ab}	100 (99-100)^{a}	**<0.001[1]***
p-value	0.8062	0.4452	0.1002	0.2552	0.0682	
Groups	**HR-0**	**HR-1**	**HR-2**	**HR-3**	**HR-4**	**p*-value**
PCV	80 (55-115)^{b}	79 (54-91)^{b}	72 (53-117)^{ab}	64 (53-87)^{a}	67 (54-91)^{ab}	**0.001[1]***
VCV	79.5 (47-96)	74 (54-111)	67 (51-94)	71 (57-89)	68.5 (49-95)	0.009[1]
FCV	79 (47-104)^{b}	70 (54-111)^{ab}	68 (50-103)^{b}	70 (57-89)^{ab}	73 (53-95)^{ab}	**0.006[1]***
p-value	0.812[2]	0.991[2]	0.765[2]	0.168[2]	0.727[2]	

Data are presented as median (minimum-maximum). [1]Friedman test, [2]Kruskal Wallis test. p*<0.006 was considered statistically significant. $^{A-C}$: For each parameter within columns, groups sharing the same letter are not significantly different (Dunn's test). $^{a-c}$: For each parameter within rows, groups sharing the same letter are not significantly different (Dunn's test).

MAP: Mean arterial pressure (mmHg), SpO_2: Peripheral capillary oxygen saturation (%), HR: Heart rate (beats per minute, bpm), FCV: Flow-controlled ventilation, PCV: Pressure-controlled volume

in MP. Accordingly, PCV-VG's variable flow profile and dynamic pressure regulation allow better adaptation to increased IAP. Additionally, the lower rate of MP increase observed in the PCV-VG group between T1 and T3 may offer clinically significant advantages. First, a smaller increase in MP in the early stages of surgery may reduce the cumulative mechanical energy load transmitted to the lungs throughout the procedure, thus minimizing the risk of VILI during prolonged surgeries. Second, PCV-VG's more effective prevention of alveolar distortion in the pre-insufflation phase may enhance lung compensation during surgical stress, preserve pulmonary reserve, and increase the patient's tolerance to surgical stress. Therefore, although the final MP values were similar, this dynamic adaptation provided by PCV-VG may offer a clinically meaningful advantage, particularly in high-risk patients who have limited pulmonary reserve, who are obese, or who are undergoing prolonged surgery. However, prospective studies evaluating postoperative pulmonary complications and long-term outcomes are needed to confirm this hypothesis.

FCV is a strategy that controls gas flow during both inspiration and expiration, and it has been shown to be a safe ventilation method in various experimental and clinical studies[15]. In FCV, MP is a parameter comprising pressure, volume, and frequency components that are transmitted to the lungs. For MP calculation, integration of the pressure-volume curve is considered the gold standard[16]. Since inspiratory and expiratory flows are constant, the pressure waveform approximates a triangular profile. In a triangular pressure profile, the pressure-volume integral is approximately halved; thus, MP can be calculated using a simplified formula with a conversion factor of 0.49 instead of 0.98. This approach can be particularly useful for the rapid estimation of MP during FCV in clinical practice[6,11]. In our study, the integral method was not used for MP calculation during FCV; instead, MP was calculated using the formula advocated by Giosa et al.[11] A modified VCV formula was used for this calculation, as there is no universally accepted formula for FCV in the literature. Wittenstein et al.[17] reported, in a porcine model, that FCV reduced MP compared with VCV during one-lung ventilation. Abram et al.[18] reported, in human studies, that FCV reduced MP compared to PCV and improved oxygenation. Weber et al.[10] demonstrated in morbidly obese patients that, compared with VCV, FCV reduced the risk of atelectasis by minimizing lung collapse during expiration. Bialka et al.[2], in their literature review on FCV, suggested that FCV may be beneficial for patient groups at increased risk of compression atelectasis, such as those undergoing laparoscopy or surgery in the Trendelenburg position.

Although MP measured during CO_2 insufflation in the FCV group was lower than in other groups in our study (8.6 J/min; PCV-VG: 9.4 J/min, VCV: 8.7 J/min), the difference was not statistically significant. Additionally, insufflation led to a noticeable increase in MP compared with baseline. These findings suggest that FCV does not provide a significant advantage in laparoscopic surgeries; however, because data in the literature are limited, no definitive conclusion can be drawn.

The main limitation of our study is the small sample size. This is perhaps an inevitable issue of a cross-sectional retrospective analysis. Since FCV cannot be performed with standard anesthesia machines and requires additional equipment, its routine use in clinical practice is limited. This may explain the small sample sizes observed both in our study and in the existing literature. Nevertheless, we believe that our study contributes to the development of new strategies aimed at reducing the MP associated with mechanical ventilation during laparoscopic surgery. Another limitation is that postoperative outcomes associated with the ventilation modes were not assessed because our current dataset was not suitable for analyzing this relationship. The lack of adequate follow-up and postoperative data makes it difficult to objectively track postoperative complications based on retrospective records. Numerous confounding factors —such as the definition of postoperative pulmonary complications and the timing of their assessment— render the acquisition and interpretation of these parameters challenging. We believe that prospective studies with larger sample sizes focusing specifically on postoperative clinical outcomes are necessary to evaluate this issue. An additional limitation is that MP was calculated using simplified formulas because of the study's retrospective design. Although the accuracy of these formulas has been demonstrated in previous studies, the simplified formula has not been sufficiently or specifically tested for FCV. This may represent both a limitation of our study and a contribution to the literature. Our hypothesis was that FCV might be associated with lower MP during insufflation in laparoscopic surgery. However, FCV produced MP values similar to those of other modes. Therefore, we were not able to confirm our hypothesis. Nonetheless, new prospective randomized studies may help further develop this hypothesis. Moreover, no ventilation mode has yet been identified in either adult or pediatric laparoscopic surgery that has been proven to reduce complications or to be superior in terms of MP[19]. For this reason, we believe that our study will also contribute to the development of mechanical ventilation strategies in laparoscopic procedures.

CONCLUSION

This study demonstrates that PCV-VG, VCV, and FCV modes achieve similar MP levels during laparoscopic surgery; however, PCV-VG more effectively limits insufflation-induced increases in MP than the other modes. This feature may be clinically significant, particularly in high-risk patients with limited pulmonary reserve, with obesity, or scheduled for prolonged surgery. Our findings may contribute to clinical decisions regarding the optimization of ventilation strategies. However, prospective studies with larger sample sizes, including postoperative outcome assessments, are needed.

Ethics

Ethics Committee Approval: Ethical approval was received from the Scientific Research Ethics Committee of University of Health Sciene Türkiye, Kocaeli City Hospital Scientific Research Ethics Committee with protocol no: 2025-79, date: 10.07.2025.

Informed Consent: Due to the retrospective design individual patient consent waived.

Footnotes

Author Contributions

Surgical and Medical Practices: A.S., N.D., B.G., A.Y., Concept: A.S., N.D., A.Y., Design: A.S., N.D., A.Y., Data Collection and/or Processing: A.S., N.D., A.Y., Analysis or Interpretation:B.G., A.Y., Literature Search: A.S., A.Y., Writing: A.S., N.D., B.G., A.Y.

Conflict of Interest: The authors have no conflict of interest to declare.

Financial Disclosure: The authors declared that this study has received no financial support.

REFERENCES

1. Şenay H, Sıvacı R, Kokulu S, Koca B, Bakı ED, Ela Y. The effect of pressure-controlled ventilation and volume-controlled ventilation in prone position on pulmonary mechanics and inflammatory markers. Inflammation. 2016;39:1469-74.
2. Bialka S, Palaczynski P, Szuldrzynski K, et al. Flow-controlled ventilation -a new and promising method of ventilation presented with a review of the literature. Anaesthesiol Intensive Ther. 2022;54:62-70.
3. Beitler JR, Malhotra A, Thompson BT. Ventilator-induced lung Injury. Clin Chest Med. 2016;37:633-46.
4. Shaji U, Jain G, Tripathy DK, Kumar N, Chowdhury N. Influence of intra-abdominal pressure on ventilatory mechanical power delivery and respiratory driving pressure during laparoscopic cholecystectomy: a prospective cohort study. J Anaesthesiol Clin Pharmacol. 2024;40:516-22.

5. Paudel R, Trinkle CA, Waters CM, et al. Mechanical power: a new concept in mechanical ventilation. Am J Med Sci. 2021;362:537-45.
6. Gattinoni L, Tonetti T, Cressoni M, et al. Ventilator-related causes of lung injury: the mechanical power. Intensive Care Med. 2016;42:1567-75.
7. Becher T, van der Staay M, Schädler D, Frerichs I, Weiler N. Calculation of mechanical power for pressure-controlled ventilation. Intensive Care Med. 2019;45:1321-3.
8. Cressoni M, Gotti M, Chiurazzi C, et al. Mechanical power and development of ventilator-induced lung injury. Anesthesiology. 2016;124:1100-8.
9. Hamaekers AE, Götz T, Borg PA, Enk D. Achieving an adequate minute volume through a 2 mm transtracheal catheter in simulated upper airway obstruction using a modified industrial ejector. Br J Anaesth. 2010;104:382-6.
10. Weber J, Straka L, Borgmann S, Schmidt J, Wirth S, Schumann S. Flow-controlled ventilation (FCV) improves regional ventilation in obese patients - a randomized controlled crossover trial. BMC Anesthesiol. 2020;20:24.
11. Giosa L, Busana M, Pasticci I, et al. Mechanical power at a glance: a simple surrogate for volume-controlled ventilation. Intensive Care Med Exp. 2019;7:61.
12. Kothari A, Baskaran D. Pressure-controlled volume guaranteed mode improves respiratory dynamics during laparoscopic cholecystectomy: a comparison with conventional modes. Anesth Essays Res. 2018;12:206-12.
13. Nguyen TK, Nguyen VL, Nguyen TG, et al. Lung-protective mechanical ventilation for patients undergoing abdominal laparoscopic surgeries: a randomized controlled trial. BMC Anesthesiol. 2021;21:95.
14. Pozzi T, Coppola S, Catozzi G, et al. Mechanical power during robotic-assisted laparoscopic prostatectomy: an observational study. J Clin Monit Comput. 2024;38:1135-43.
15. Spraider P, Abram J, Martini J, et al. Flow-controlled versus pressure-controlled ventilation in cardiac surgery with cardiopulmonary bypass - a single-center, prospective, randomized, controlled trial. J Clin Anesth. 2023;91:111279.
16. Van Oosten JP, Francovich JE, Somhorst P, et al. Flow-controlled ventilation decreases mechanical power in postoperative ICU patients. Intensive Care Med Exp. 2024;12:30.
17. Wittenstein J, Scharffenberg M, Ran X, et al. Comparative effects of flow vs. volume-controlled one-lung ventilation on gas exchange and respiratory system mechanics in pigs. Intensive Care Med Exp. 2020;8:24.
18. Abram J, Spraider P, Martini J, et al. Flow-controlled versus pressure-controlled ventilation in thoracic surgery with one-lung ventilation - a randomized controlled trial. J Clin Anesth. 2025;103:111785.
19. Yuksek A, Miniksar OH, Yardimci C, Cikrikci AP. Can mechanical power be used as a safety precaution in pediatric patients? JARSS. 2022;30:232-9.

DOI: 10.4274/MMJ.galenos.2025.89021
Medeni Med J 2025;40:278-279

Letter to the Editor

Right Coronary Artery Perforation with Subsequent Graft Stent Embolization to the Left Main Coronary Artery: It Never Rains but It Pours!

Sağ Koroner Arter Perforasyonunu Takiben Sol Ana Koroner Artere Greft Stent Embolizasyonu: Yağmur Yağmaz ama Yağınca Sağanak Yağar!

Efe YILMAZ, Furkan KARAHAN, Çağlar KAYA, Kenan YALTA

Trakya University Faculty of Medicine, Department of Cardiology, Edirne, Türkiye
*This study was presented as a poster at the 2024 National Cardiology Congress.

Keywords: Coronary perforation, percutaneous coronary intervention, stent embolization
Anahtar kelimeler: Koroner perforasyon, perkütan koroner girişim, stent embolizasyonu

Dear Editor,

A 72-year-old female patient was hospitalized with acute coronary syndrome. Coronary angiogram (CAG) demonstrated a critical stenosis in the distal right coronary artery (RCA) [posterior descending artery, (PDA)]; the artery was severely tortuous and calcified. The Amplatz 1 guiding catheter was engaged into the RCA. The PDA and posterolateral artery branches were pruned The culprit lesion in the PDA was then predilated with 1.5×12-mm and 2.0×10-mm compliant balloons, respectively. Finally, a 2.5×23-mm DES was implanted in the predilated stenotic segment. However, repeat images demonstrated an Ellis type 3 coronary rupture distal to the PDA at the level of distal bifurcation point. Subsequently, coronary obstruction was induced using a 2.75×10 mm non-compliant (NC) balloon for 3 minutes. Because the perforation persisted on repeat CAG images, coronary occlusion was performed using 2.0 × 6-mm NC and 2.5×10-mm NC balloons, inflated three consecutive times, each for more than 10 minutes. Thereafter, the extra-stiff guidewire was exchanged for a floppy guidewire over a microcatheter to prevent further guidewire-induced perforation. Intravenous protamine was also administered. Due to the failue of all the above-mentioned attempts, we decided to implant a graft stent in the PDA at the level of bifurcation point. However, the stent graft could not be advanced beyond the mid-RCA. We retrieved the balloon-stent system, however, we were not able to discern any stent material over the balloon. Thereafter, we inflated a 1.0×10 mm compliant balloon distal to the system and pulled the system back. However, the stent material remained loose. To our consternation, we were able to identify the stent material in the left main coronary artery (LMCA) CAG images. The patient was transferred for emergency surgery due to persistent coronary perforation and dislodged stent material in the LMCA.

The primary focus of this report is the sequential occurrence of two severe coronary complications in a single patient. This report also underscores that a timely surgical backup is essential during PCI. Although coronary perforations and stent dislodgement are quite

Address for Correspondence: E. Yilmaz, Trakya University Faculty of Medicine, Department of Cardiology, Edirne, Türkiye
E-mail: drefeyilmaz@gmail.com **ORCID ID:** orcid.org/0000-0003-2976-3063

Received: 27.10.2025
Accepted: 31.10.2025
Published: 31.12.2025

Cite as: Yilmaz E, Karahan F, Kaya C, Yalta K. Right coronary artery perforation with subsequent graft stent embolization to the left main coronary artery: it never rains but it pours! Medeni Med J. 2025;40:278-279

rare during coronary interventions, they appear to be associated with mortality and poor prognosis. Patients with risk factors for coronary perforation (as mentioned in the Introduction) should be managed carefully. In this context, mitigation of risk factors is imperative. For instance, aggressive guidewire manipulation and oversized balloons should be avoided, particularly in the context of high-risk vessel features (tortuosity, calcification, etc.). On the other hand, hydrophilic and stiff wires should be used only when necessary. Particular care should be taken when handling atherectomy devices or cutting balloons[1,2]. In the case of a coronary perforation, pericardiocentesis (where necessary) and mechanical occlusion with a balloon (inflated at 2-6 ATM for 10-15 minutes) should be performed, followed by preparation of a stent graft with the assistance of a new guiding catheter introduced from the contralateral artery. Anticoagulant therapy should be discontinued in all patients. Emergency surgery should be considered when percutaneous interventions fail[3].

We performed all of the above steps. However, the graft stent was found to have embolized into the LMCA during its advancement through the RCA lumen. Embolized stents can be retrieved with snare catheters, or by advancing a smaller balloon and inflating it within the dislodged stent, or by looping two guidewires through the stent struts and withdrawing them. Capturing devices, such as forceps or a bioptome, can also be used to retrieve embolized stents from coronary arteries. Another plausible option is to embed the dislodged stent into the coronary artery wall in an inappropriate location. However, this method is not recommended. This technique has been found to increase the incidence of myocardial infarction, mortality, and the need for emergency surgery during the procedure[4]. In this case, no further intervention was undertaken to retrieve the embolized graft stent. This was because the patient had an active perforation in the RCA and the embolized stent was in the LMCA. Further attempts to remove the embolized stent material would have delayed either the management of the perforation or the retrieval of the embolized material, thereby increasing the risk of LMCA thrombosis over time. The combination of the two complications and ongoing bleeding from the perforated site led us to consider emergency surgery. Emergency surgery was considered the best option for this patient because percutaneous interventions had failed and two precarious conditions coexisted.

Footnotes

Author Contributions

Surgical and Medical Practices: E.Y., F.K., Concept: E.Y., Ç.K., Design: E.Y., Ç.K., Data Collection and/or Processing: F.K., Analysis and/or Interpretation: E.Y., K.Y., Literature Search: E.Y., F.K., Writing: E.Y., Ç.K.

Conflict of Interest: The authors have no conflict of interest to declare.

Financial Disclosure: The authors declared that this study has received no financial support.

REFERENCES

1. Ellis SG, Ajluni S, Arnold AZ, et al. Increased coronary perforation in the new device era. Incidence, classification, management, and outcome. Circulation. 1994;90:2725-30.
2. Ramana RK, Arab D, Joyal D, et al. Coronary artery perforation during percutaneous coronary intervention: incidence and outcomes in the new interventional era. J Invasive Cardiol. 2005;17:603-5.
3. Fassa AA, Roffi M. "Complications of PCI: stent loss, coronary perforation, and aortic dissection." Cardiovascular Catheterization and Intervention. CRC Press, 2017. 593-606.
4. Bolte J, Neumann U, Pfafferott C, et al. Incidence, management, and outcome of stent loss during intracoronary stenting. Am J Cardiol. 2001;88:565-7.

2025 Referee Index - 2025 Hakem Dizini

Abdullah Özkök
Abdullah Şişik
Adem Atıcı
Ahmet Ahmet Sarıcı
Ahmet Emre Eşkazan
Akif Güneş
Ali Erdoğan
Ali Karakuş
Ali Zeybek
Asiye Kanbay
Aslı Görek Dilektaşlı
Aslıhan Kiraz
Aslıhan Yılmaz Çebi
Ayhan Akbulut
Ayhan Kamanlı
Aylin Kılınç Uğurlu
Aynur Görmez
Ayse Selcan Koç
Ayşe Seval Özgü Erdinç
Aytekin Oğuz
Başak Mutlu
Begüm Bektaş
Belgin Erhan
Beray Selver Eklioğlu
Bilge Çağlar
Burak Mergen
Burcu Arpınar Yiğitbaş
Burcu Yücel
Bülent Erol
Cagatay Barut
Cansu Yüksel Elgin
Ceren Sarı
Ceren Sümer
Cihangir Ergün
Çiçek Hocaoğlu
Deniz Gezgin Yıldırım
Ebuzer Aydın
Ekrem Ünal
Elif Oğuz
Elif Yilmaz Güleç
Eren Öğüt
Erhan Okay
Erkan Çakır
Erman Öztürk
Esen Kasapoğlu
Esra Ertan Yazar
F. Ümit Malya
Fatma Ceyhan
Fatma Özgüç Çömlek
Filiz Demirdağ
Füsun Fakılı
Gözde Bacık Yaman
Gülden Yorgancıoğlu Budak
Güler Öztürk
Gülhan Örekici Temel
Hakan Parlakpınar
Hamdi Cihan Emeksiz
Handan Ankaralı
Hasan Doğan
Hasan Güçlü
Hülya Sungurtekin
İrfan Esenkaya
Mahmet Ali Erdoğan
Mahmut Gümüş
Mehmet Buğrahan Duz
Mehmet Çağlar Çakıcı
Mehmet Tokdemir
Melda Sarıman
Melike Emiroğlu
Meltem Pusuroğlu
Meryem Hocaoğlu
Mirac Vural Keskinler
Murat Aşık
Murat Beyhan
Mustafa Duran
Nadir Adnan Hacım
Nihal Şahin
Nilüfer Göknar
Oğuz Karabay
Ömer Faruk Ünal
Özgür Efiloglu
Rümeysa Yeni Elbay
Saniye Koç Ada
Seda Banu Banu Akıncı
Seda Kaynak
Selçuk Çetin
Serdar Balsak
Süleyman Can Öztürk
Ş. Kerem Özel
Şükrü Sadık Öner
Tammam Sipahi
Teoman Soysal
Tutku Soyer
Ümit Yaşar Güleser
Ünal Uslu
Yasemin Çağ
Yasemin Gökdemir
Yener Aydın
Yusuf Yılmaz
Zehra Zengin Erkol
Ziya Cibali Açıkgöz
Zülküf Akdağ